UNIVERSITÀ DEGLI STUDI DI MILANO

DIPARTIMENTO DI MATEMATICA

Scuola di Dottorato in Scienze Matematiche

Dottorato di Ricerca in Matematica e Statistica per le Scienze Computazionali

XXVII Ciclo

DIFFERENT SCALE MODELING FOR CROWD DYNAMICS AND MULTI-TEMPERATURE GAS MIXTURES

SSD MAT/07 – MAT/08

Coordinatore:

Chiar.mo Prof. Giovanni Naldi

Tutor:

Chiar.mo Prof. Giovanni Naldi

Chiar.mo Prof. Marzia Bisi

Dottorando: *Giorgio Martalò*

A.A. 2014

UNIVERSITÀ DEGLI STUDI DI MILANO

DIPARTIMENTO DI MATEMATICA

Scuola di Dottorato in Scienze Matematiche

Dottorato di Ricerca in Matematica e Statistica per le Scienze Computazionali

XXVII Ciclo

DIFFERENT SCALE MODELING FOR CROWD DYNAMICS AND MULTI-TEMPERATURE GAS MIXTURES

SSD MAT/07 – MAT/08

Coordinatore:

Chiar.mo Prof. Giovanni Naldi

Tutor:

Chiar.mo Prof. Giovanni Naldi

Chiar.mo Prof. Marzia Bisi

Dottorando: *Giorgio Martalò*

A.A. 2014

To my parents

Contents

List of Figures

Introduction

Mathematical models for multi-agent systems have attracted a lot of attention in recent years and many papers in this framework have been published.
It is clear that one of the most interesting aspects regards the possible applications to several fields and the beneficial outcomes in every day life. For example, a good mathematical treatment of vehicular flows and crowd dynamics can have some positive effects, respectively, on the sustainability of traffic and evacuation problems. Other significant features of collective motion [1] can be reproduced and analyzed, such as swarming, flocking and synchronization, and models in different research fields, like biology [2] and economy [3], can be proposed.
All these phenomena and scenarios can be modeled at different levels depending on the number of agents in the group. Microscopic discrete descriptions following the evolution of each agent are used when the number of agents is small. Mesoscopic and macroscopic models seem more appropriate when the number increases and the collection is more comparable to gases, fluids and granular media.
Mesoscopic approach is based on the study of the distribution function of agents (probability density in the phase space) whose evolution is governed by an integro-differential equation of Boltzmann type. Hydrodynamic equations for major macroscopic fields (for instance number density and mean velocity of the crowd) may be consistently deduced from kinetic equations by suitable asymptotic limits.
Such different levels of description have been originally devised for ideal gases, where the particles play the same role of agents in the previous case. One can follow a more classical approach which analyzes a gas as a continuum and just involves the

macroscopic global quantities. Otherwise, a different strategy at the mesoscopic level, typical of kinetic theory, can be adopted [4]. In this last case one can bear in mind the particle dynamics and this approach can combine the positive aspects of microscopic and macroscopic levels. These tools may be generalized to mixtures of different gas species (possibly undergoing also chemical reactions) [5, 6] and here these different approaches will be proposed to analyze the so-called multi-temperature models. It is indeed well-known that in thermally non-equilibrium conditions a single-temperature model is not efficient to describe several physical situations in which a wide spectrum of temperatures appears in a natural way. A multi-temperature description arises spontaneously when component masses are very disparate, for example in physics of plasmas at high temperature [7] and for hypersonic vehicles at high altitude [8].
These arguments will be developed in this thesis which can be seen divided in two parts: some results about collective dynamics will be discussed in the first part (chapters 1–2) while multi-temperature descriptions for gas mixtures will be presented in the second one (chapters 3–4).

- **PART I - CROWD DYNAMICS**

We are interested to propose a model able to correctly reproduce the dynamics of a crowd in bounded domains (for example rooms and corridors) and in presence of obstacles, and also to discuss the emergence of some behaviors induced by panic.
Starting from some models developed in last years ([9, 10]), we propose a very simple description of the evolution of a small crowd of N agents governed by a set of ordinary differential equations

$$\begin{cases} \dot{\mathbf{x}}_i = \mathbf{v}_i \\ \\ \mathbf{v}_i = \dfrac{v_i^0 \mathbf{e}_i^0 - \mathbf{v}_i}{\tau} + \dfrac{1}{N} \displaystyle\sum_{j \neq i} \nabla U \left(\left\| \mathbf{x}_i - \mathbf{x}_j \right\| \right) \qquad i = 1, \ldots, N \end{cases} \tag{1}$$

where $(\mathbf{x}_i, \mathbf{v}_i)$ denote position and velocity of the $i-$th agent, $v_i^0 \mathbf{e}_i^0$ is the velocity which the $i-$th agent tends to, while the sum takes account of the interactions between agents by means of the generalized Morse potential U.

In chapter 1 we show how the set of preferential directions $\{\mathbf{e}_i^0\}$ can be determined a priori by using the strategy proposed in [11]; more precisely, by a suitable Poisson problem (with Dirichlet and Neumann boundary conditions) one can take account of the geometric restrictions of the domain: walls and exits as well as the presence of obstacles in the walking area. This problem is solved by a standard finite element technique in finite spaces of B-spline functions.
In addition, a modification of the production terms is proposed to model the emergence of panic and some distinctive features, like delay in evacuation dynamics, are discussed.
In chapter 2, we concentrate on scenarios involving a larger number of agents. The first step is the presentation of a mesoscopic model deduced as suitable (mean field or grazing collision) limit of the previous microscopic one [1]. The evolution of the distribution function f in the phase space is described by a Boltzmann-like integro-differential equation

$$\frac{\partial f}{\partial t} + \mathbf{v} \cdot \nabla_{\mathbf{x}} f = Q(f, f) \tag{2}$$

where Q is the collision integral operator. Numerical results can be obtained by using Monte Carlo methods [12] which are really useful to reduce the required computational resources. As usual in kinetic theory problems, this approach is based on a suitable splitting of the problem in transport and collision steps.
Finally, a tentative macroscopic extension, in which crowd can be seen as a continuum, is proposed. The most natural way is to obtain it by considering the weak formulation of the kinetic equation introduced before and using suitable approximations to get a closed set of balance laws. Some numerical results are proposed in a one-dimensional space.

- **PART II - MULTI-TEMPERATURE GAS MIXTURES**

Some multi-temperature models have been presented in recent literature in different frameworks such as rational thermodynamics. In several papers by Ruggeri et al. [13, 14] the starting point to deduce this kind of descriptions is the assumption according to which, in homogeneous mixtures, each constituent obeys the same balance laws as a single fluid. By means of standard tools of kinetic theory we are able

to justify this assumption recovering multi-temperature descriptions as hydrodynamic limits of Boltzmann equations.

In this regard, we propose [15] to model a mixture of Q monoatomic gases in presence of a two scale collision process; the set of Boltzmann-type kinetic equations describing the evolution of the distribution functions f_i in phase space is scaled as

$$\frac{\partial f_i}{\partial t} + \mathbf{v} \cdot \nabla_{\mathbf{x}} f_i = \frac{1}{\varepsilon} I_{ii}[f_i, f_i] + I_{ij}[f_i, f_j] \qquad , \qquad i = 1, \ldots, Q \tag{3}$$

where ε is a small parameter (Knudsen number) and I_{ij} is the integral collision operator for collisions between particles of species i and j. The factor $1/\varepsilon$ amplifies the effect of this part of the collision operator and hence interactions within each component are made dominant.

In chapter 3, starting from this model we aim to include some essential ingredients like chemical reactions (in particular we concentrate on bimolecular reversible ones: $(1,2) \rightleftharpoons (3,4)$) and internal structure for molecules to take non-translational degrees of freedom into account. We show a possible extension of the previous model to these inelastic phenomena and their limitations [16].

A set of macroscopic equations at Euler level is deduced by a consistent hydrodynamic limit and suitable approximations. The resulting (multi-velocity and) multi-temperature models are commented on and some robustness tests, like entropy dissipation and relaxation to equilibrium, are discussed.

In chapter 4 the proposed hyperbolic systems of balance laws for reactive and inert mixtures [17, 18] are used for the analysis of the classical problem of the shock wave structure. Occurrence of smooth solutions and the presence of discontinuities (so-called subshocks) is discussed for varying parameters. In spite of the different approach, our results are in agreement with those presented in extended thermodynamics [19]. The most attractive aspect of this work concerns the possibility to obtain, in particular regimes, weak shock profiles undergoing more than one jump discontinuity and to build up them via suitable numerical techniques.

Chapter 1

Microscopic discrete description for crowd dynamics

1.1 Introduction

The study of mathematical models for multi-agent systems is of great theoretical and practical interest and many papers in this framework have been published to describe the emergence of significant collective behaviors like swarming, flocking and synchronization. Many applications have been proposed in several fields like biology [2, 20], economy [3], opinion formation [21, 22, 23], traffic problems [24, 25] and social sciences [26, 27]. We refer to [1] and to [28] for a review of some of the mathematical approaches and applications presented in last years.

One of the most interesting aspects in collective human dynamics is the practical utility of these models to prevent some disastrous phenomena like stampede induced by panic which can lead to the death of people who are crushed or trampled down by others. In particular, an efficient way to deal with obstacles has a crucial role in evacuation dynamics. In fact, empirical data, although rare, show that in these situations the presence of obstacles can generate a spontaneous self-organization of people and hence a faster and more organized escape.

In addition to panic situations, other behaviors have been addressed mathematically;

for example, pedestrians moving in opposite directions form lanes, as it happens in shopping centers, or flow is slower when a bottleneck occurs.
All these phenomena can be studied at different levels and several approaches can be introduced.
In presence of a small number of agents a microscopic description has to be preferred and agents dynamics can be studied one by one at each time. This is not possibile as the number of agents increases both from a theoretical point of view - the crowd is more comparable to gases and fluids than to a discrete collection of agents - and from a practical one - limited computational resources.
For these reasons mesoscopic and macroscopic models have been proposed; in the first case evolution is described by a suitable distribution function in phase space while in the second one crowd is modeled as a continuum.
In this work, we shall propose a simple microscopic model which takes account of the geometric configuration of the environment (walls, obstacles, exits) and of the interactions between agents. Starting from it, a mesoscopic description can be deduced as a suitable (mean field) limit of the previous microscopic equations. The evolution can be governed by a Boltzmann-type equation whose integral collision operator takes an appropriate interaction rule into account. Finally, using the weak formulations of the last kinetic model, a set of macroscopic balance laws can be obtained for the evolution of density and mean velocity of the crowd.
At each level some test cases and relevant results will be presented.
We shall consider classical Runge-Kutta methods to simulate the evolution of the dynamical system for the microscopic description while at mesoscopic and macroscopic level splitting techniques will be needed. In these last cases we have to split the problem and to solve two different sub-problems: transport and collision steps. Monte Carlo methods will be useful for the mesoscopic description while numerical tools for hyperbolic systems, like Lax-Friedrichs method, will be adopted for the system of macroscopic equations.
Before starting the analysis of the model we shall propose in next sections, it is important to justify the assumptions we shall do later. The basic idea is to combine the positive aspects of the microscopic models proposed in [9] and in [10]. Let us show

pros and cons of these descriptions.
In [9] the motion of N agents is described by the following set of ordinary differential equations

$$\begin{cases} \dot{\mathbf{x}}_i = \mathbf{v}_i \\ \\ m_i \dot{\mathbf{v}}_i = (\alpha - \beta \|\mathbf{v}_i\|) \mathbf{v}_i - \nabla U(\mathbf{x}_i) \end{cases} \tag{1.1}$$

for $i = 1, \ldots, N$, with the generalized Morse potential

$$U(\mathbf{x}_i) = \sum_{j \neq i} \left\{ C_r \exp\left[-\frac{\|\mathbf{x}_i - \mathbf{x}_j\|}{\ell_r} \right] - C_a \exp\left[-\frac{\|\mathbf{x}_i - \mathbf{x}_j\|}{\ell_a} \right] \right\} \tag{1.2}$$

where ℓ_a and ℓ_r represent the attractive and repulsive potential ranges and C_a and C_r the respective amplitudes.
From the physical point of view, when two agents are too close they aim to repulse each other; on the other hand, when agents are quite spread in the whole space they tend to bring themselves closer to others and to go on together (see for instance bird swarms). Hence we would like to reproduce short range repulsion and long range attraction, and to this aim in the Morse potential it is necessary to consider

$$C := \frac{C_r}{C_a} > 1 \qquad \text{and} \qquad \ell := \frac{\ell_r}{\ell_a} < 1. \tag{1.3}$$

Different scenarios correspond to different choices of these ratios and a detailed analysis has been presented in [9].
According to us, this mean of repulsive and attractive effects seems a good way to approximate interactions between humans: especially in panic situations, people tends to move together avoiding to crush or trample down the others.
The term $(\alpha - \beta |\mathbf{v}_i|) \mathbf{v}_i$ represents the tendency of agents to move along a desired direction with a desired velocity. In [9] the quantities α and β have been considered constant but this choice is unrealistic in situations involving walls or obstacles. Therefore, if one is interested in practical applications, a modification is required.
In this respect, one can follow the approach proposed in [10] where equations for

velocities are replaced as follows

$$m_i \dot{\mathbf{v}}_i = m_i \frac{v_i^0(t)\,\mathbf{e}_i^0(t) - \mathbf{v}_i}{\tau_i} + \sum_{j \neq i} f_{ij} + \sum_w f_{iw} \tag{1.4}$$

In addition to interaction forces f_{ij} between agents, the authors introduce a set of functions f_{iw} which treat the interactions with the walls . Moreover, the desired velocities can be considered as suitable functions of time, both in magnitude and direction. This approach can reproduce correctly a wide range of behaviors but it requires also many computational resources; in fact, at each time, one has to evaluate the position of every single agent with respect to the others and with respect to walls and he has to compute both tangential and normal components in the interaction forces.
In order to reduce the computational cost and to simplify the model, we propose the following dynamical system

$$\begin{cases} \dot{\mathbf{x}}_i = \mathbf{v}_i \\ \\ \dot{\mathbf{v}}_i = \dfrac{v_i^0 \mathbf{e}_i^0(\mathbf{x}_i) - \mathbf{v}_i}{\tau_i} - \nabla U(\mathbf{x}_i) \end{cases} \tag{1.5}$$

where the set of directions $\left\{\mathbf{e}_i^0\right\}_{i=1}^N$ can be determined a priori and it takes account of the geometrical domain, while term U is the previous Morse potential.

1.2 Construction of the desired directions

As proposed in [11], the desired velocity field $\left\{\mathbf{e}_i^0\right\}_i$can be obtained as gradient of a suitable scalar potential u which identifies attractive and repulsive zones. This potential, denoted by u, has to satisfy the Poisson problem

$$\Delta u = 0 \quad + \quad \text{Boundary conditions} \tag{1.6}$$

In the applications we shall see later, the more appropriate conditions seem to be

- constant positive Dirichlet boundary conditions in correspondence of exits (attractive zones)

- homogenous Neumann boundary conditions along the walls (repulsive zones)

In particular, the last one is useful to control the normal component of the desired velocity when agents are close to the walls.
Here, for sake of simplicity, we confine ourselves to analyze the case of a geometric domain without obstacles. The occurrence of them will be discussed later.
Therefore, the problem we have to solve is

$$\begin{cases} \Delta u = 0 \quad \text{in } \Omega \\ \\ u = g = 1 \quad \text{on } \Gamma_D \quad \text{and} \quad \dfrac{\partial u}{\partial n} = 0 \quad \text{on } \Gamma_N \end{cases} \tag{1.7}$$

where Ω is a bounded domain, Γ_D and Γ_N denote, respectively, Dirichlet and Neumann boundaries, with $\bar{\Gamma}_D \cup \bar{\Gamma}_N = \Gamma = \partial\Omega$ and g is the assigned Dirichlet datum (in this case the unit function).
Supposing the existence of a function $\mathscr{R}g$, called extension of g over Γ, such that $\mathscr{R}g_{|\Gamma_D} = g$ (and for convenience we suppose also $\dfrac{\partial \mathscr{R}g}{\partial n} = 0$) and introducing the new variable $\tilde{u} = u - \mathscr{R}g$, one can write the problem in the easier way

$$\begin{cases} \Delta \tilde{u} = -\Delta \mathscr{R}g \quad \text{in } \Omega \\ \\ \tilde{u} = 0 \quad \text{on } \Gamma_D \quad \text{and} \quad \dfrac{\partial \tilde{u}}{\partial n} = 0 \quad \text{on } \Gamma_N \end{cases} \tag{1.8}$$

At this point, we can solve numerically the Poisson problem by a Faedo-Galerkin technique [29] based on the weak formulation of the previous equation and on the approximation of it in suitable finite dimension spaces.
We have to introduce a test function space $V = H^1_{\Gamma_D}$ and hence, using integration by parts and boundary conditions, the weak problem reads as

$$\int_\Omega \nabla \tilde{u} \cdot \nabla v d\Omega = -\int_\Omega \nabla \mathscr{R}g \cdot \nabla v d\Omega \qquad v \in V. \tag{1.9}$$

From now on, an accurate choice of the finite space which approximates V will have a crucial role.

It is important to choose the test functions in such a way that the corresponding discrete problem has a simpler form and the approximate solution can be managed easily. In our cases, it is necessary to compute a $\mathscr{C}^1$ solution u because the velocity field is obtained as gradient of it; moreover, choosing functions with compact support, the matrix in the discrete problem will present many zero entries.
For these reasons, we concentrate on the basis of B-splines whose restrictions are polynomial of degree 2. In 1-D case B-spline functions can be introduced by a recursion formula; starting from the piecewise constant functions

$$B_{j,1}(x) = \begin{cases} 1 \text{ if } x_j \leq x < x_{j+1} \\ \\ 0 \text{ otherwise} \end{cases} \tag{1.10}$$

one can define

$$B_{j,k}(x) = \frac{x - x_j}{x_{j+k-1} - x_j} B_{j,k-1}(x) + \frac{x_{j+k} - x}{x_{j+k} - x_{j+1}} B_{j+1,k-1}(x) \tag{1.11}$$

where $\{x_j\}$ denotes a suitable decomposition of the domain. We are interested in 2-D problems and a basis in the bidimensional space can be computed by products of elements of 1-D case.
Let us denote with $\{\varphi_k(x,y)\}$ the basis of B-spline functions whose restriction on Γ_D is zero and hence the approximate solution we are looking for reads as

$$\tilde{u}_h(x,y) = \sum_k c_k \varphi_k(x,y) \qquad \text{where} \qquad \varphi_k(x,y) = \varphi_{i_k}(x)\,\varphi_{j_k}(y) \tag{1.12}$$

The approximate solution must satisfy the discrete problem

$$\int_\Omega \nabla \tilde{u}_h \cdot \nabla v_h d\Omega = -\int_\Omega \nabla \mathscr{R} g \cdot \nabla v_h d\Omega \qquad \forall v_h \in V_h \tag{1.13}$$

where $V_h \subset V$ is the space determined by $\{\varphi_k\}$ and $\{V_h\}_h$ constitute a cover of V. Testing the previous equation with the elements of the basis of V_h, one can deduce the following linear system

$$\mathbf{A} \cdot \mathbf{c} = \mathbf{b} \tag{1.14}$$

where

$$A_{kh} = \int_{\Omega} \nabla\varphi_k(x,y) \cdot \nabla\varphi_h(x,y)\, d\Omega \tag{1.15}$$

and

$$b_k = -\int_{\Omega} \nabla\mathscr{R}g \cdot \nabla\varphi_k(x,y)\, d\Omega \tag{1.16}$$

The solution of the linear system gives a unique approximation in V_h because the matrix $\mathbf{A}$ is non-singular (its entries are obtained as products of the elements of the basis). One can also notice that the matrix $\mathbf{A}$ will present many zero entries because of the compact support of the functions φ_k.

1.2.1 Example

As example, let us consider a simple domain $\Omega = [0,1] \times [0,1]$ with just one exit only in $\{1\} \times [1/3, 2/3]$ (Figure 1.1). For convenience, we suppose an uniform de-

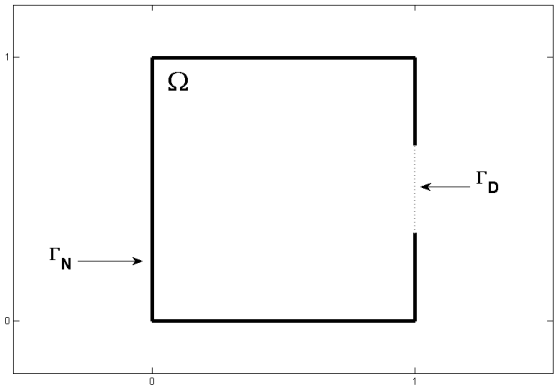

Figure 1.1: A square domain with a single exit.

composition of the domain with step h in both directions and we use the function $\mathscr{R}g = 2x^3 - 3x^2 + 2$ to take boundary data into account.
With reference to Fig. 1.2, an element of the basis can be written as

$$\varphi_k(x,y) = \varphi_{i_k}(x)\,\varphi_{j_k}(y) \tag{1.17}$$

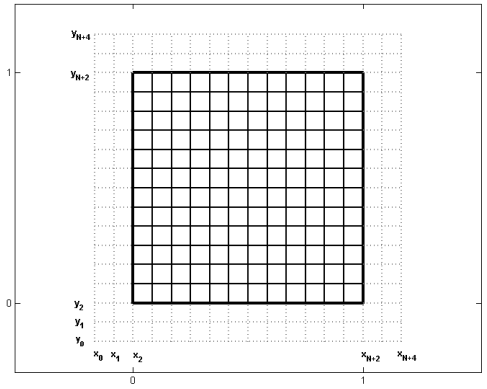

Figure 1.2: Uniform decomposition of the (extended) square domain; the generic element φ_k of the basis has support $[x_{i_k-1}, x_{i_k+2}] \times [y_{j_k-1}, y_{j_k+2}]$.

where $k = (i_k - 2)(N+2) + j_k$ and $1 \leq i_k, j_k \leq N+2$. The support of φ_{i_k} and φ_{j_k} are respectively the intervals $[x_{i_k-1}, x_{i_k+2}]$ and $[y_{j_k-1}, y_{j_k+2}]$; hence φ_k is non-zero in $(x_{i_k-1}, x_{i_k+2}) \times (y_{j_k-1}, y_{j_k+2})$ and entries $A_{k\ell}$ in the matrix $\mathbf{A}$ are non-zero if $|i_k - i_\ell| < 2$ or $|j_k - j_\ell| < 2$. For this reason, just few integrals have to be solved; more precisely one has to compute

$$\begin{aligned} \int_0^1 \varphi_i(x)\,dx &= \int_{x_{i-1}}^{x_i} \varphi_i(x)\,dx + \int_{x_i}^{x_{i+1}} \varphi_i(x)\,dx + \int_{x_{i+1}}^{x_{i+2}} \varphi_i(x)\,dx \\ &= \frac{h}{6} + \frac{2h}{3} + \frac{h}{6} = h \end{aligned} \tag{1.18}$$

and the products of element of the basis

$$\begin{aligned}\int_0^1 \varphi_i^2(x)\,dx &= \int_{x_{i-1}}^{x_i} \varphi_i^2(x)\,dx + \int_{x_i}^{x_{i+1}} \varphi_i^2(x)\,dx + \int_{x_{i+1}}^{x_{i+2}} \varphi_i^2(x)\,dx \\ &= \frac{h}{20} + \frac{9h}{20} + \frac{h}{20} = \frac{11h}{20}\end{aligned}$$

$$\begin{aligned}\int_0^1 \varphi_i(x)\,\varphi_{i+1}(x)\,dx &= \int_{x_i}^{x_{i+1}} \varphi_i(x)\,\varphi_{i+1}(x)\,dx + \int_{x_{i+1}}^{x_{i+2}} \varphi_i(x)\,\varphi_{i+1}(x)\,dx \\ &= \frac{13h}{120} + \frac{13h}{120} = \frac{13h}{60}\end{aligned} \tag{1.19}$$

$$\int_0^1 \varphi_i(x)\,\varphi_{i+2}(x)\,dx = \int_{x_{i+1}}^{x_{i+2}} \varphi_i(x)\,\varphi_{i+2}(x)\,dx = \frac{h}{120}$$

and of their derivatives

$$\begin{aligned}\int_0^1 \dot{\varphi}_i^2(x)\,dx &= \int_{x_{i-1}}^{x_i} \dot{\varphi}_i^2(x)\,dx + \int_{x_i}^{x_{i+1}} \dot{\varphi}_i^2(x)\,dx + \int_{x_{i+1}}^{x_{i+2}} \dot{\varphi}_i^2(x)\,dx \\ &= \frac{1}{3h} + \frac{1}{3h} + \frac{1}{3h} = \frac{1}{h}\end{aligned}$$

$$\begin{aligned}\int_0^1 \dot{\varphi}_i(x)\,\dot{\varphi}_{i+1}(x)\,dx &= \int_{x_i}^{x_{i+1}} \dot{\varphi}_i(x)\,\dot{\varphi}_{i+1}(x)\,dx + \int_{x_{i+1}}^{x_{i+2}} \dot{\varphi}_i(x)\,\dot{\varphi}_{i+1}(x)\,dx \\ &= -\frac{1}{6h} - \frac{1}{6h} = -\frac{1}{3h}\end{aligned} \tag{1.20}$$

$$\int_0^1 \dot{\varphi}_i(x)\,\dot{\varphi}_{i+2}(x)\,dx = \int_{x_{i+1}}^{x_{i+2}} \dot{\varphi}_i(x)\,\dot{\varphi}_{i+2}(x)\,dx = -\frac{1}{6h}$$

As concerns the term **b**, one has to evaluate

$$\begin{aligned}&\int_0^1 x(1-x)\,\dot{\varphi}_i(x)\,dx = \int_{x_{i-1}}^{x_i} x(1-x)\,\dot{\varphi}_i(x)\,dx + \int_{x_i}^{x_{i+1}} x(1-x)\,\dot{\varphi}_i(x)\,dx \\ &+ \int_{x_{i+1}}^{x_{i+2}} x(1-x)\,\dot{\varphi}_i(x)\,dx = \frac{1}{12}\left[-6x_i^2+6x_i+h(4x_i-2-h)\right] \\ &+ \frac{h}{6}(2x_{i+1}-1-h) + \frac{1}{12}\left[6x_{i+2}^2-6x_{i+2}-h(8x_{i+2}-4-3h)\right]\end{aligned} \tag{1.21}$$

The relevant discrete problem has a block band matrix

$$\mathbf{A} = \frac{1}{360}\begin{bmatrix} D_1 & E & F & 0 & 0 & 0 & \cdots & 0 & 0 & 0 & 0 & 0 & 0 \\ E & D_2 & 2E & F & 0 & 0 & \cdots & 0 & 0 & 0 & 0 & 0 & 0 \\ F & 2E & D_1+D_2 & 2E & F & 0 & \cdots & 0 & 0 & 0 & 0 & 0 & 0 \\ \vdots & \vdots & \vdots & \vdots & \vdots & \vdots & \ddots & \vdots & \vdots & \vdots & \vdots & \vdots & \vdots \\ 0 & 0 & 0 & 0 & 0 & 0 & \cdots & 0 & F & 2E & D_1+D_2 & 2\bar{E} & \bar{F} \\ 0 & 0 & 0 & 0 & 0 & 0 & \cdots & 0 & 0 & \bar{F} & 2\bar{E} & \bar{D}_2 & \bar{E} \\ 0 & 0 & 0 & 0 & 0 & 0 & \cdots & 0 & 0 & 0 & \bar{F} & \bar{E} & \bar{D}_1 \end{bmatrix} \tag{1.22}$$

whose blocks have the same band structure

$$
D_1 = \begin{bmatrix}
12 & 10 & -2 & 0 & 0 & 0 & \cdots & 0 & 0 & 0 & 0 & 0 & 0 \\
10 & 72 & 20 & -2 & 0 & 0 & \cdots & 0 & 0 & 0 & 0 & 0 & 0 \\
-2 & 20 & 84 & 20 & -2 & 0 & \cdots & 0 & 0 & 0 & 0 & 0 & 0 \\
\vdots & \vdots & \vdots & \vdots & \vdots & \vdots & \ddots & \vdots & \vdots & \vdots & \vdots & \vdots & \vdots \\
0 & 0 & 0 & 0 & 0 & 0 & \cdots & 0 & -2 & 20 & 84 & 20 & -2 \\
0 & 0 & 0 & 0 & 0 & 0 & \cdots & 0 & 0 & -2 & 20 & 72 & 10 \\
0 & 0 & 0 & 0 & 0 & 0 & \cdots & 0 & 0 & 0 & -2 & 10 & 12
\end{bmatrix}
$$

$$
D_2 = \begin{bmatrix}
72 & -4 & -28 & 0 & 0 & 0 & \cdots & 0 & 0 & 0 & 0 & 0 & 0 \\
-4 & 240 & -8 & -28 & 0 & 0 & \cdots & 0 & 0 & 0 & 0 & 0 & 0 \\
-28 & -8 & 312 & -8 & -28 & 0 & \cdots & 0 & 0 & 0 & 0 & 0 & 0 \\
\vdots & \vdots & \vdots & \vdots & \vdots & \vdots & \ddots & \vdots & \vdots & \vdots & \vdots & \vdots & \vdots \\
0 & 0 & 0 & 0 & 0 & 0 & \cdots & 0 & -28 & -8 & 312 & -8 & -28 \\
0 & 0 & 0 & 0 & 0 & 0 & \cdots & 0 & 0 & -28 & -8 & 240 & -4 \\
0 & 0 & 0 & 0 & 0 & 0 & \cdots & 0 & 0 & 0 & -28 & -4 & 72
\end{bmatrix}
$$

(1.23)

$$
E = \begin{bmatrix}
10 & -13 & -7 & 0 & 0 & 0 & \cdots & 0 & 0 & 0 & 0 & 0 & 0 \\
-13 & -4 & -26 & -7 & 0 & 0 & \cdots & 0 & 0 & 0 & 0 & 0 & 0 \\
-7 & -26 & 6 & -26 & -7 & 0 & \cdots & 0 & 0 & 0 & 0 & 0 & 0 \\
\vdots & \vdots & \vdots & \vdots & \vdots & \vdots & \ddots & \vdots & \vdots & \vdots & \vdots & \vdots & \vdots \\
0 & 0 & 0 & 0 & 0 & 0 & \cdots & 0 & -7 & -26 & 6 & -26 & -7 \\
0 & 0 & 0 & 0 & 0 & 0 & \cdots & 0 & 0 & -7 & -26 & -4 & -13 \\
0 & 0 & 0 & 0 & 0 & 0 & \cdots & 0 & 0 & 0 & -7 & -13 & 10
\end{bmatrix}
$$

$$
F = \begin{bmatrix}
-2 & -7 & -1 & 0 & 0 & 0 & \cdots & 0 & 0 & 0 & 0 & 0 & 0 \\
-7 & -28 & -14 & -1 & 0 & 0 & \cdots & 0 & 0 & 0 & 0 & 0 & 0 \\
-1 & -14 & -30 & -14 & -1 & 0 & \cdots & 0 & 0 & 0 & 0 & 0 & 0 \\
\vdots & \vdots & \vdots & \vdots & \vdots & \vdots & \ddots & \vdots & \vdots & \vdots & \vdots & \vdots & \vdots \\
0 & 0 & 0 & 0 & 0 & 0 & \cdots & 0 & -1 & -14 & -30 & -14 & -1 \\
0 & 0 & 0 & 0 & 0 & 0 & \cdots & 0 & 0 & -1 & -14 & -28 & -7 \\
0 & 0 & 0 & 0 & 0 & 0 & \cdots & 0 & 0 & 0 & -1 & -7 & -2
\end{bmatrix}
$$

Blocks $\bar{D}_1$, $\bar{D}_2$, $\bar{E}$ and $\bar{F}$ are extracted by the corresponding blocks D_1, D_2, E and F removing some rows and columns because of the presence of a Dirichlet condition on Γ_D.
As concerns term **b**, it takes the form

$$\mathbf{b} = \begin{bmatrix} b_1\xi \\ b_2\xi \\ \vdots \\ b_N\xi \end{bmatrix} \qquad \text{where} \qquad \xi = \begin{bmatrix} 1 \\ 5 \\ 6 \\ \vdots \\ 6 \\ 5 \\ 1 \end{bmatrix} \tag{1.24}$$

and

$$\begin{aligned} b_1 &= \frac{h^2(h-2)}{12} = -b_N \quad , \quad b_2 = \frac{h^2(13h-10)}{12} = -b_{N-1} \\ b_i &= h^2[(2i-3)h-1] \qquad \text{for } i = 3,4,\ldots,N-2. \end{aligned} \tag{1.25}$$

In figure 1.3 the approximate solution and the related desired velocity field show that the exit is an attractive zone and agents can't go through the walls.

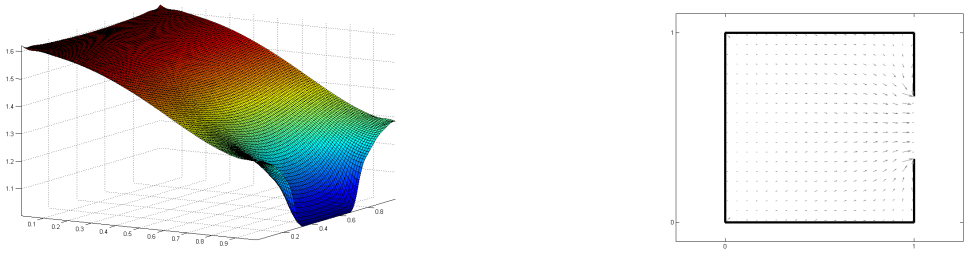

(a) Potential (b) Velocity field

Figure 1.3: Potential and velocity field related to a square domain with a single exit. A potential well in correspondence of the exit reproduces the desired attractive effect.

The same technique can be used for different configurations. In figure 1.4 a square

domain with two symmetric exits and the related potential are plotted. Also in this case, the technique catches correctly the presence of attractive and repulsive zones.

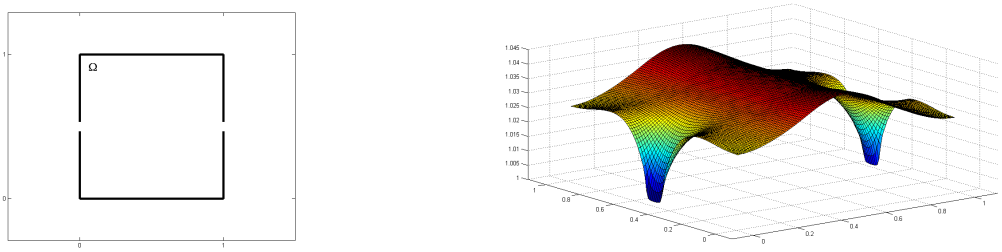

(a) Domain (b) Potential

Figure 1.4: Potential and velocity field related to a square domain with two symmetric exits. Also in this case the attractive zones present a potential well.

To confirm that this procedure is a good way to treat geometric restrictions, one can solve a simple model in which the interactions are neglected. The system of ordinary differential equations seen before reduces to

$$\begin{cases} \dot{\mathbf{x}}_i = \mathbf{v}_i \\ \dot{\mathbf{v}}_i = \dfrac{v_i^0 \mathbf{e}_i^0 - \mathbf{v}_i}{\tau_i} \end{cases} \tag{1.26}$$

We consider the first geometric domain and, for convenience, we suppose that all particles share the same value of the desired velocity magnitude and the same relaxation parameter: $v_i^0 = v^0 =$ constant and $\tau_i = \tau =$ constant for all $i = 1, \ldots, N$. From now on, out of the domain, the desired velocity for each agent is the actual velocity and hence the self-propelling term vanishes. We fix $N = 40$ and we simulate two different situations corresponding to different relaxation times. We solve numerically by using a classical explicit Runge-Kutta method of order 4 [30]: the approximate solution of

$$\dot{y} = f(t, y) \tag{1.27}$$

at time step $k+1$ can be deduced as follows

$$y^{k+1} = y^k + \frac{1}{6}(k_1 + 2k_2 + 2k_3 + k_4) \qquad k = 0, 1, \ldots, n-1 \tag{1.28}$$

where

$$\begin{aligned} k_1 &= hf\left(t_k, y^k\right),\ k_2 = hf\left(t_k + \frac{h}{2}, y^k + \frac{k_1}{2}\right) \\ k_3 &= hf\left(t_k + \frac{h}{2}, y^k + \frac{k_2}{2}\right),\ k_4 = hf\left(t_k + h, y^k + k_3\right) \end{aligned} \tag{1.29}$$

Figures 1.5 and 1.6 show that this approach is efficient provided that a small parame-

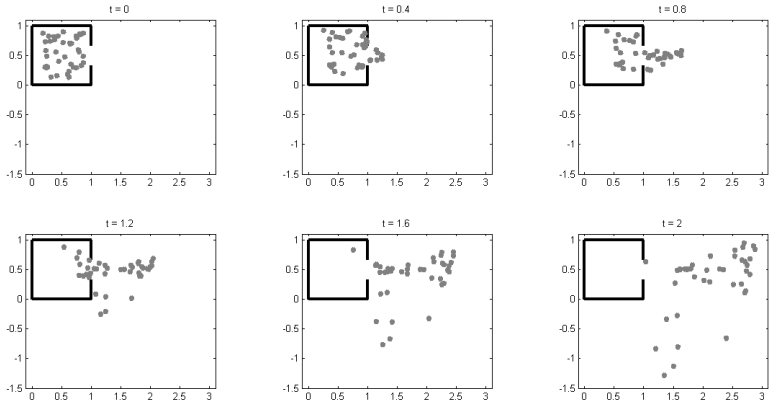

Figure 1.5: Agents dynamics without interactions: case $\tau = 0.1$. A small value of τ guarantees that agents do not cross the walls reproducing correctly the evacuation dynamics.

ter τ has been chosen. This means that each agent has to adapt its own velocity to the desired one as fast as possible and this was predictable if one would consider an initial configuration in which some agents are near the walls. In fact, in these situations an agent who moves towards the walls can cross the walls if he does not adapt his own velocity as fast as possible to desired one which is tangential to the boundary.

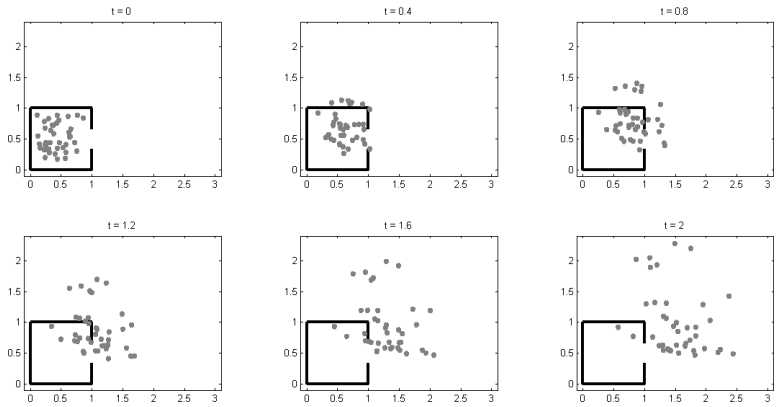

Figure 1.6: Agents dynamics without interactions: case $\tau = 1$. In presence of a larger value of τ agents can not adapt quickly their own velocities to desired ones and some of them can cross the walls.

1.3 Basic microscopic model

From now on let us consider the complete dynamics in which all phenomena are taken into account.

The first step is to determine a good choice of parameters in Morse potential. We confine ourselves to the case $C_a = 1$ and $C_r = 2$ (and hence $C = 2$ in (1.3)) and we vary parameters ℓ_a and ℓ_r for different fixed values of ℓ.

The interactions forces act along the direction connecting the two involved agents. As concerns the strength of these forces, some trends of the strength versus distance are shown in figure 1.7 where positive values correspond to repulsion while the negative ones are related to attractive effects .

In both cases we can notice that, for a fixed ℓ, the range in which distance admits positive values is wider as the parameters ℓ_a and ℓ_r increase; at the same time, the maximum attraction strength decreases. The optimal value for the threshold which separates repulsive and attractive effects has to be determined in each single case

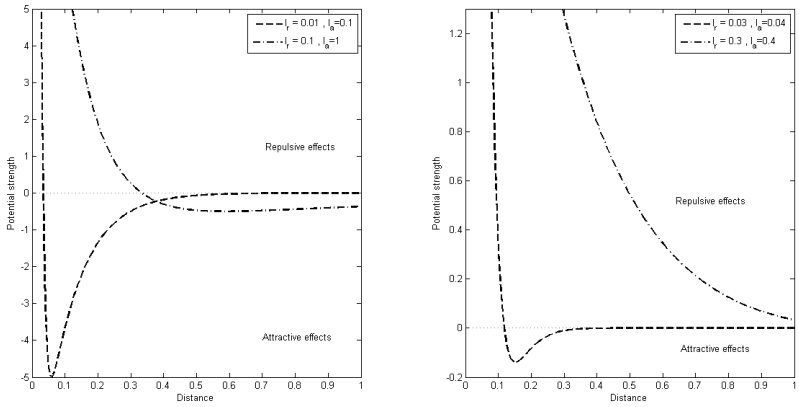

Figure 1.7: Potential strength for different values of the parameters: $\ell = 1/10$ on the left, $\ell = 3/4$ on the right. Trends show that parameters can not be chosen a priori and the choice depends on the features of each domain.

because of the different geometric characteristics of the domain. For example in the previous square domains with unit side the choice $\ell_r = 0.3$ and $\ell_a = 0.4$ seems unsuitable; in fact attractive effects come into play just for distance values greater than 1 and just repulsion has a significant role in the dynamics within the domain.
As concerns the mentioned domain with a single exit, we fix $\ell_r = 0.01$ and $\ell_a = 0.02$ (and hence $\ell = 0.5$).

As shown in Fig.1.8, crowd evacuation is described correctly and, in spite of strong repulsive effects, (almost) no agents cross the walls and sliding effects along the boundary are reproduced. Moreover, at the exit agents move together and cluster avoiding in this way an immediate dispersion outside the domain. One can notice that cluster effects were predictable; in fact, dynamics out of the domain is governed only by the Morse potential and hence, as noticed in [9], the choice of parameters (C, ℓ) implies cluster formation.
In this case we have assumed that each agent interacts with every single component of the crowd but this choice seems to be unrealistic. For this reason it is suitable to

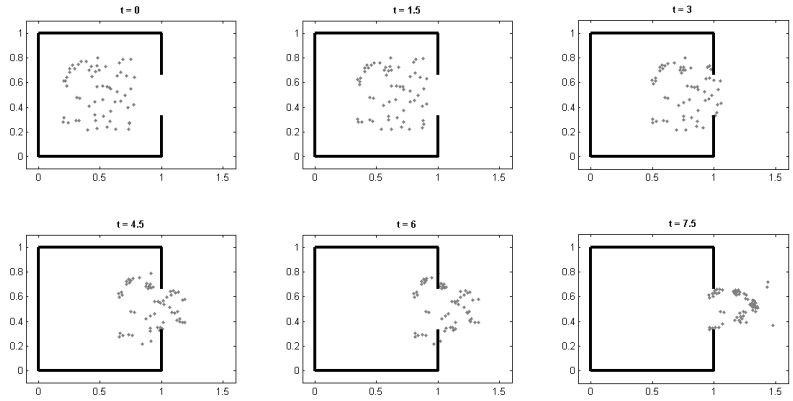

Figure 1.8: Dynamics of a crowd of 60 agents. Evacuation is correctly reproduced and no agent moves across the walls.

introduce a restriction on the number of interactions. It is reasonable to suppose that an agent interacts with the ones that it can see.

For this purpose, we introduce the concept of perception cone as illustrated in Fig.1.9. For the i-th agent, its position determines the cone vertex while its velocity vector individuates the limiting directions by rotations of angle $-\theta/2$ and $\theta/2$. Formally, the $i-$th agent will interact only with agents in

$$\mathscr{C}_i = \left\{ \mathbf{y} \in \mathbb{R}^2 \ : \ \frac{(\mathbf{x}_i - \mathbf{y}) \cdot \mathbf{v}_i}{|(\mathbf{x}_i - \mathbf{y})|\,|\mathbf{v}_i|} > \cos(\theta/2) \right\} \tag{1.30}$$

As clearly shown in Fig.1.9, by using this approach, interactions are not symmetric; in fact it may happen that $\mathbf{x}_B \in \mathscr{C}_A$ but $\mathbf{x}_A \notin \mathscr{C}_B$ or vice versa. The dynamics in presence of a perception angle $\theta = \pi/6$ is proposed in Fig.1.10 and, unlike the previous case, the same initial configuration does not lead to cluster phenomena at the exit because a lower number of interactions is admitted. Moreover, the presence of a perception region introduces a delay in evacuation dynamics (about 3.25%); probably, a smaller perturbation to the tendency to adapt velocity to the preferential one implies that agents look soon for the exit and hence an obstruction occurs close to the exit causing

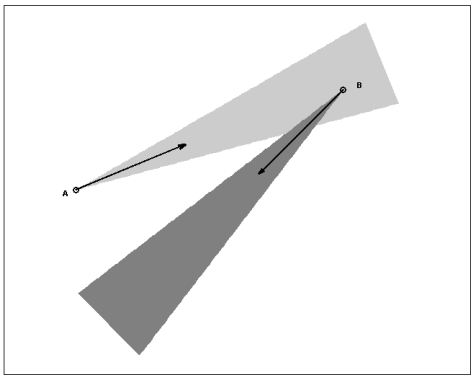

Figure 1.9: Perception region as infinite cone of angle θ and vertex individuated by the agent position.

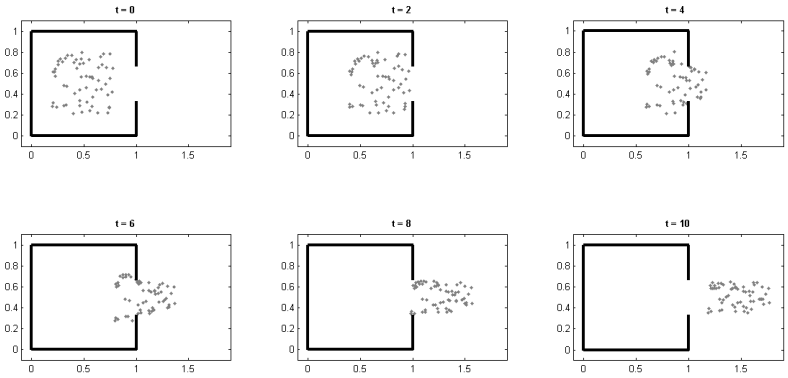

Figure 1.10: Crowd dynamics in presence of a perception angle ($\theta = \pi/6$). A lower number of interactions is admitted and evacuation dynamics is slower than the basic case.

a delay in the evacuation.
Obviously, the perception region can be described in other ways; in the next section we shall use also an easier form in which the perception zone is just a disk whose center is determined by the agent position and radius is fixed.

1.4 Panic in evacuation situations

As mentioned above, one of the most interesting aspects in the simulation of collective dynamics is the prevention of disastrous phenomena induced by panic and, therefore, it is important to mathematically reproduce this aspect.
For this purpose, we consider the approach proposed in [10] in which the panic implies a perturbation of the desired velocity by means of the average direction of agents in a neighborhood. To justify this assumption, one has to consider a situation in which pedestrians have to leave a smoke-filled room. In this case walls and exits are not visible at long range and hence they lose their utility as reference point. Therefore each agent tends to put his trust in people around him. For this reason every pedestrian moves along the following direction

$$\text{Norm}\left[(1-p_i)\,\mathbf{e}_i^0 + p_i < \mathbf{e}_j >_i\right] \tag{1.31}$$

which is a linear combination of the desired velocity $\mathbf{e}_i^0$ and of the average direction $< \mathbf{e}_j >_i$ of the neighbors in his perception region. The weight p_i is the panic parameter and it expresses the level of confidence in people around. Small values of p_i correspond to individualistic behavior: one tries to maintain his preferential direction but modifies slightly his velocity just to avoid crowding; greater values privilege collective motion neglecting the natural tendency to move towards the targets that one wants to reach.
In our simulations agents share the same constant panic value, $p_i = p = \text{constant}$.
Figure 1.11 still shows that evacuation is possible but panic introduces a delay (about 3.79% with respect to the case in absence of perception region and panic).
The presence of panic is strictly related also to other phenomena like symmetry breaking.

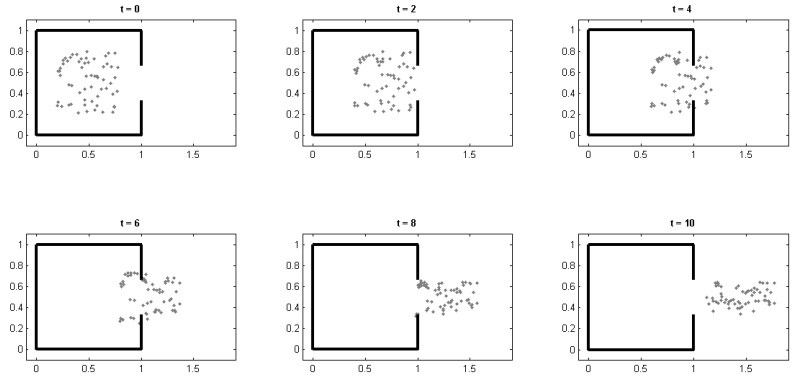

Figure 1.11: Crowd dynamics in presence of a perception angle and panic ($\theta = \pi/6$ and $p = 0.8$). In presence of panic a delay arises in a natural way in the evacuation dynamics.

Let us consider a room with two symmetric identical doors and usually, in normal conditions, one can notice that people use them in the same way. Some empirical observations show that the presence of panic induces agents to move together towards one of the two exits neglecting the other one. As before, the dominance of collective motion with respect to the individualism introduces a delay due to the obstruction of the selected door.
The same behavior has been observed also in different frameworks like biology.
As shown in [2], a collection of ants in a circular cell with two symmetric exits abandon using both exits in approximately equal proportions; if one introduces a repellent fluid, panic is created and one of the two exits is more used than the other one in the escape dynamics.
We test our approach on this particular biological problem; in this case we use a circular perception region instead of the previous infinite cone and, for convenience, we consider a square domain.
Figure 1.12 shows that, for small values of the panic parameter p, individualistic be-

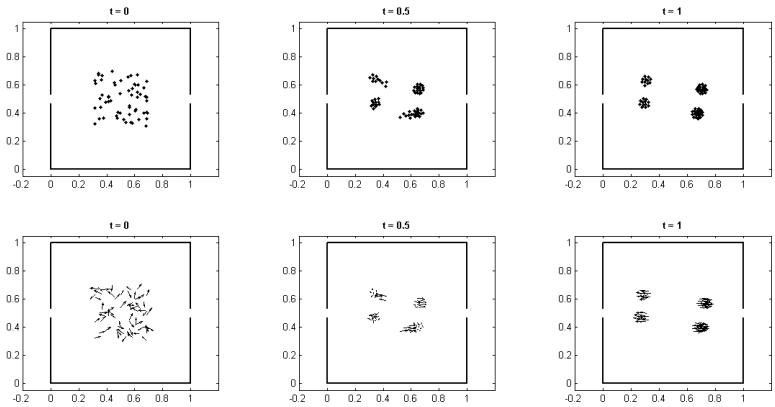

Figure 1.12: Positions and velocities for escaping ants in presence of panic : $p = 0.25$. Dynamics is very similar to the basic case in absence of panic.

havior is dominant; the introduced perturbation does not have a significant role in the evolution and agents tend to move as in absence of panic. Possible clustering effects are due to the interaction Morse potential.

In figures 1.13, 1.14 increasing values of p implies that dynamics is characterized essentially by the collective motion and agents tend to share a common value of velocity neglecting the main objective, i.e. evacuation, introducing in this way a delay. Moreover for greater values of p the symmetry breaking is correctly reproduced and just one exit is used during the escape.

1.5 Domains with obstacles

One of the most interesting and practical aspects in modeling crowd dynamics is how to describe mathematically the presence of obstacles in the domain and the way the agents interact with them.

In fact experimental data show that each obstacle can have different characterizations; it can play a ‘negative’ role, in the sense that it can be obstructive and it can delay the

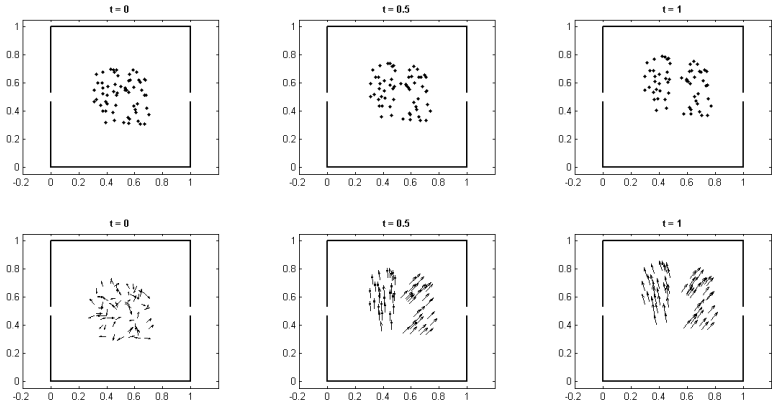

Figure 1.13: Positions and velocities for escaping ants in presence of panic : $p = 0.7$. Agents still separates in two similar groups but it is interesting to notice that, in each group, agents tend to share a common value of velocity.

escape, or, sometimes, it can be seen as a 'positive' obstacle, causing an unexpected faster evacuation of the crowd.

In this respect one can recall a classical example of positive role; in panic situations, splitting an exit in two parts by means of an obstacle can induce a spontaneous self-organization in the crowd and hence the evacuation occurs in a faster and more organized way.

The most natural way to deal with obstacles is to interpret them as holes in the domain and hence their edges constitute part of the boundary. This 'inner' boundary can be treated in the same way of the 'outer' one considering suitable Dirichlet or Neumann conditions.

The main problem of the approach we have seen before is to find a suitable extension $\mathscr{R}g$ whose restriction is equal to the boundary datum g and it results very complicated in the case of a inner-outer boundary. Moreover, once an appropriate extension can be found, then this function could present some oscillations hardly manageable from a numerical point of view.

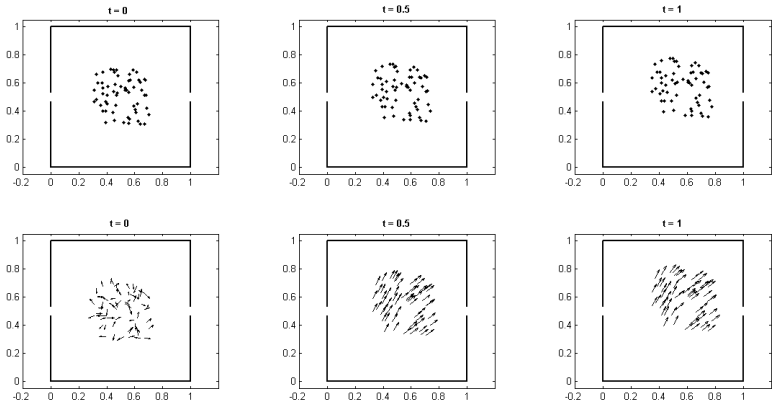

Figure 1.14: Positions and velocities for escaping ants in presence of panic : $p = 0.8$. Dynamics is dominated by the collective motion; agents move together towards one exit only sharing a common value of velocity.

For these reasons we try to bypass the problem as follows.
The main feature we want to reproduce is the impossibility for the agents to get through the obstacles and to do that it is sufficient to have some peaks for the potential function in correspondence to them. In fact, the corresponding gradient will push away agents towards lower potential zones.
A very simple way to realize that is to find an extension just related to outer boundary (this results easier because few conditions have to be satisfied) and to modify it adding some simpler functions which simulate the potential peaks. Therefore, starting from the Poisson problem in absence of obstacles

$$\Delta u = -\Delta \mathscr{R} g \tag{1.32}$$

one can obtain a similar problem in presence of them

$$\Delta u = -\Delta \left(\mathscr{R} g + \sum_i \psi_i \right) \tag{1.33}$$

where $\{\psi_i\}$ characterize the presence of obstacles. We choose to model peaks by using B-spline functions whose supports are located around the positions of the obstacles and this modification corresponds to impose a (not-well specified) Dirichlet condition on the inner boundary.

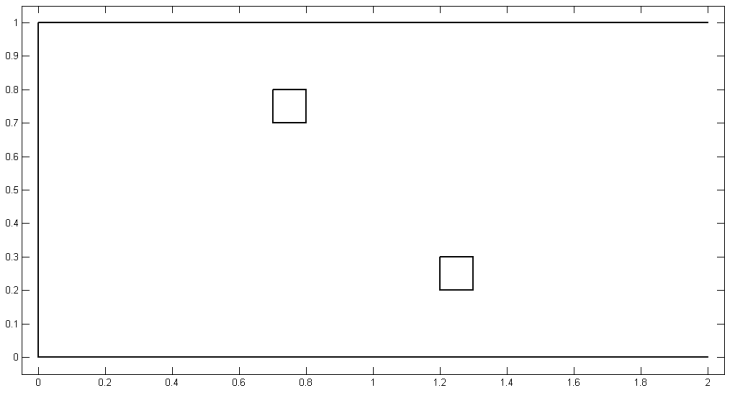

Figure 1.15: A corridor with two obstacles.

We test our approach in the case of a corridor with two obstacles inside (Figure 1.15). Simulations in figure 1.16 show that the repulsive effects are correctly reproduced, no agent gets through the obstacles and slide along the walls can be noticed. One can observe also that the presence of an obstacle has some effects only when an agent is very close to it; to have a longer range effect it is sufficient to consider a B-spline function around the obstacle whose support is wider than it. Finally, one can notice that the crowd does not gather once it overtakes the obstacles and, maybe this is related to a too wide exit. Numerical simulations in presence of smaller exits are in progress.

Managing obstacles and walls by means of a potential function can seem complicated and easier ways to proceed are desirable. For this reason, our first idea was to simulate interactions with the domain by means of a suitable Morse potential in which repulsive effects were reproduced by choosing $C_a = 0$ while the attractive ones by posing

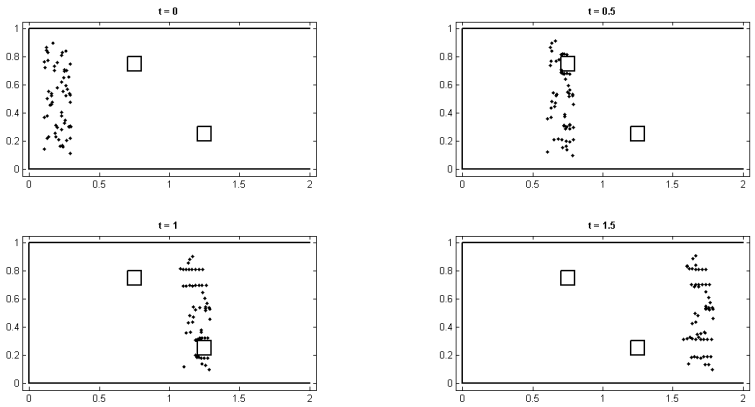

Figure 1.16: Dynamics of a crowd in a corridor in presence of obstacles. No agent moves across the obstacles and sliding effect are correctly reproduced.

$C_r = 0$. Unfortunately this approach can't reproduce the desired sliding effects.

Chapter 2

Mesoscopic and macroscopic models for crowd dynamics

2.1 Kinetic description

In the previous chapter we have proposed a simple model for collective motion and we have discussed some features like the geometric restrictions and the presence of panic in evacuation phenomena. This approach seems the most natural way to treat the dynamics when the crowd is composed by a small number of agents and it gives a more realistic representation of pedestrian movement.
As this number increases (for example in a collection of fishes or bacteria) continuum models are necessary, both from a theoretical and a computational point of view; in fact simulations for a large population is really difficult and it requires many computational resources because of the increasing number of differential equations. For this reason different approaches are required and they are based on the analysis of the evolution of other quantities: distribution functions at kinetic level and density and mean velocity at macroscopic one.
The first step is to propose a mesoscopic description of the problem by considering a distribution function for agents in the phase space: $f = f(\mathbf{x}, \mathbf{v}, t)$ where $\mathbf{x}, \mathbf{v} \in \mathbb{R}^d$ denote respectively position and microscopic velocity. Its evolution is governed by

a Boltzmann-type equation which will be deduced by means of standard tools of kinetic theory (grazing collision limit or mean field limit). Later, we shall propose a macroscopic model obtained by the previous kinetic one by using hydrodynamic limit procedure and suitable closure assumptions.
Before presenting the kinetic and macroscopic model, let us remind the microscopic description from which we shall deduce the other ones. We consider a set of N agents who move according to the following system of ordinary differential equations

$$\begin{cases} \dot{\mathbf{x}}_i = \mathbf{v}_i \\ \\ \dot{\mathbf{v}}_i = \mathscr{S}(\mathbf{v}_i) - \sum_{j \neq i} \nabla U\left(\left\|\mathbf{x}_i - \mathbf{x}_j\right\|\right) \end{cases} \tag{2.1}$$

The quantities

$$\mathscr{S}(\mathbf{v}_i) = \frac{v_i^0 \mathbf{e}_i^0 - \mathbf{v}_i}{\tau} \tag{2.2}$$

and

$$U\left(\left\|\mathbf{x}_i - \mathbf{x}_j\right\|\right) = C_r \exp\left(-\frac{\left\|\mathbf{x}_i - \mathbf{x}_j\right\|}{\ell_r}\right) - C_a \exp\left(-\frac{\left\|\mathbf{x}_i - \mathbf{x}_j\right\|}{\ell_a}\right) \tag{2.3}$$

denote respectively the self-propelling term and the Morse repulsion/attraction potential and describe respectively the tendency of agents to move along preferential directions and the interactions between agents.

2.1.1 Derivation of Boltzmann-like equations

The key point to deduce kinetic models from the corresponding discrete ones is the description of the binary collisions involving two generic agents.
In our problem, let assume that two agents in position, respectively, $\mathbf{x}$ and $\mathbf{y}$ who move with velocity $\mathbf{v}$ and $\mathbf{w}$ modify their own velocities according to the interaction rule

$$\mathbf{v}^* = \mathscr{C}(\mathbf{x}, \mathbf{v}; \mathbf{y}, \mathbf{w}) \qquad \text{and} \qquad \mathbf{w}^* = \mathscr{C}(\mathbf{y}, \mathbf{w}; \mathbf{x}, \mathbf{v}) \tag{2.4}$$

where $\mathbf{v}^*$ and $\mathbf{w}^*$ denote post-interaction velocities and

$$\mathscr{C}(\mathbf{x}, \mathbf{v}; \mathbf{y}, \mathbf{w}) = \mathbf{v} + \eta\left[\mathscr{S}(\mathbf{v}) - \nabla U(\|\mathbf{x} - \mathbf{y}\|)\right] \tag{2.5}$$

is obtained by approximating derivative by its different quotient and η indicate the strength of the interaction.
The evolution is described by a Boltzmann-like equation

$$\left[\frac{\partial f}{\partial t} + \mathbf{v}\cdot\nabla_{\mathbf{x}} f\right](\mathbf{x},\mathbf{v},t) = Q(f,f)(\mathbf{x},\mathbf{v},t) \tag{2.6}$$

whose collision operator Q takes the interactions into account and it has the following form

$$\begin{aligned} Q(f,f) = \frac{1}{\varepsilon}\int_{\mathbb{R}^d}\int_{\mathbb{R}^d}\Bigg[&\frac{1}{J(\mathbf{x},\mathbf{v};\mathbf{y},\mathbf{w})} f(\mathbf{x},\mathbf{v}_*,t) f(\mathbf{y},\mathbf{w}_*,t) \\ &- f(\mathbf{x},\mathbf{v},t) f(\mathbf{y},\mathbf{w},t)\Bigg] d\mathbf{w} d\mathbf{y} \end{aligned} \tag{2.7}$$

where $\mathbf{v}_*$ and $\mathbf{w}_*$ are the pre-interaction velocities which generate $\mathbf{v}$ and $\mathbf{w}$ as post-interaction ones and ε is a small parameter (typically a Knudsen number); moreover J is the jacobian matrix of the transformation which links pre- and post-interaction quantities. The factor $1/\varepsilon$ implies that motion is strongly influenced by interactions between agents.
The presence of the jacobian matrix can be avoided by using the weak formulation; this means that a distribution function f is a weak solution of the problem with initial datum f_0 if it satisfies

$$\begin{aligned} &\frac{\partial}{\partial t}\int_{\mathbb{R}^{2d}} \varphi(\mathbf{x},\mathbf{v}) f(\mathbf{x},\mathbf{v},t)\, d\mathbf{x} d\mathbf{v} + \int_{\mathbb{R}^{2d}} [\mathbf{v}\cdot\nabla_{\mathbf{x}}\varphi(\mathbf{x},\mathbf{v})] f(\mathbf{x},\mathbf{v},t)\, d\mathbf{x} d\mathbf{v} = \\ &\qquad = \frac{1}{\varepsilon}\int_{\mathbb{R}^{4d}} [\varphi(\mathbf{x},\mathbf{v}^*) - \varphi(\mathbf{x},\mathbf{v})] f(\mathbf{x},\mathbf{v},t) f(\mathbf{y},\mathbf{w},t)\, d\mathbf{x} d\mathbf{v} d\mathbf{y} d\mathbf{w} \end{aligned} \tag{2.8}$$

for every $t > 0$ and for every smooth function φ with compact support, and such that

$$\lim_{t\to 0^+}\int_{\mathbb{R}^{2d}} \varphi(\mathbf{x},\mathbf{v}) f(\mathbf{x},\mathbf{v},t)\, d\mathbf{x} d\mathbf{v} = \int_{\mathbb{R}^{2d}} \varphi(\mathbf{x},\mathbf{v}) f_0(\mathbf{x},\mathbf{v})\, d\mathbf{x} d\mathbf{v} \tag{2.9}$$

Now, let us consider the Taylor expansion of $\varphi(\mathbf{x},\mathbf{v}^*)-\varphi(\mathbf{x},\mathbf{v})$ at the right-hand side of (2.8); stopping at the second order one has

$$\begin{aligned}
&\int_{\mathbb{R}^{4d}}[\varphi(\mathbf{x},\mathbf{v}^*)-\varphi(\mathbf{x},\mathbf{v})]f(\mathbf{x},\mathbf{v},t)f(\mathbf{y},\mathbf{w},t)\,d\mathbf{x}d\mathbf{v}d\mathbf{y}d\mathbf{w}=\\
&\quad=\int_{\mathbb{R}^{4d}}[\nabla_{\mathbf{v}}\varphi(\mathbf{x},\mathbf{v})\cdot(\mathbf{v}^*-\mathbf{v})]f(\mathbf{x},\mathbf{v},t)f(\mathbf{y},\mathbf{w},t)\,d\mathbf{x}d\mathbf{v}d\mathbf{y}d\mathbf{w}+\\
&\quad+\frac{1}{2}\int_{\mathbb{R}^{4d}}\left[\sum_{\substack{h_1,\dots,h_d=0\\ h_1+\dots+h_d=2}}^{2}\frac{\partial^2\varphi(\mathbf{x},\tilde{\mathbf{v}})}{\partial v_1^{h_1}\dots\partial v_d^{h_d}}(v_1^*-v_1)^{h_1}\dots(v_d^*-v_d)^{h_d}\right]\times\\
&\qquad\qquad\times f(\mathbf{x},\mathbf{v},t)f(\mathbf{y},\mathbf{w},t)\,d\mathbf{x}d\mathbf{v}d\mathbf{y}d\mathbf{w}
\end{aligned}\tag{2.10}$$

where $\tilde{\mathbf{v}}=\theta\mathbf{v}+(1-\theta)\mathbf{v}^*$, $0\le\theta\le 1$ and the sum denotes all possible choices of exponents h_i such that $0\le h_i\le 2\ \forall i$ and $h_1+\dots+h_d=2$. After noticing that

$$\mathbf{v}^*-\mathbf{v}=\eta\left[\mathscr{S}(\mathbf{v})-\nabla U(\|\mathbf{x}-\mathbf{y}\|)\right]=:\eta\mathscr{F}^1 \tag{2.11}$$

one can rewrite the interaction term as follows

$$\begin{aligned}
&\frac{1}{\varepsilon}\int_{\mathbb{R}^{4d}}[\varphi(\mathbf{x},\mathbf{v}^*)-\varphi(\mathbf{x},\mathbf{v})]f(\mathbf{x},\mathbf{v},t)f(\mathbf{y},\mathbf{w},t)\,d\mathbf{x}d\mathbf{v}d\mathbf{y}d\mathbf{w}=\\
&\quad=\frac{\eta}{\varepsilon}\int_{\mathbb{R}^{4d}}\left[\nabla_{\mathbf{v}}\varphi(\mathbf{x},\mathbf{v})\cdot\mathscr{F}^1\right]f(\mathbf{x},\mathbf{v},t)f(\mathbf{y},\mathbf{w},t)\,d\mathbf{x}d\mathbf{v}d\mathbf{y}d\mathbf{w}+\\
&\quad+\frac{\eta^2}{2\varepsilon}\int_{\mathbb{R}^{4d}}\left[\sum_{\substack{h_1,\dots,h_d=0\\ h_1+\dots+h_d=2}}^{2}\frac{\partial^2\varphi(\mathbf{x},\tilde{\mathbf{v}})}{\partial v_1^{h_1}\dots\partial v_d^{h_d}}\left(\mathscr{F}_1^1\right)^{h_1}\dots\left(\mathscr{F}_d^1\right)^{h_d}\right]\times\\
&\qquad\qquad\times f(\mathbf{x},\mathbf{v},t)f(\mathbf{y},\mathbf{w},t)\,d\mathbf{x}d\mathbf{v}d\mathbf{y}d\mathbf{w}
\end{aligned}\tag{2.12}$$

Let us consider a small interaction strength

$$\eta\ll 1\quad\text{ such that }\quad\frac{\eta}{\varepsilon}=\lambda\quad\text{ and }\quad\frac{\eta^2}{\varepsilon}\ll 1 \tag{2.13}$$

and, hence, the interaction operator can be approximated only by the first order term. The resulting equation is associated to the strong form one

$$\frac{\partial f}{\partial t}+\mathbf{v}\cdot\nabla_{\mathbf{x}}f=\lambda\left\{(\nabla_{\mathbf{x}}U*\rho)\cdot\nabla_{\mathbf{v}}f-\nabla_{\mathbf{v}}\cdot[\mathscr{S}(\mathbf{v})f]\right\} \tag{2.14}$$

where $*$ denotes the $\mathbf{x}-$convolution and

$$\rho(\mathbf{x},t) = \int_{\mathbb{R}^d} f(\mathbf{x},\mathbf{v},t)\, d\mathbf{v} \tag{2.15}$$

is the density function in the configuration space.
The same equation can be deduced in a different way by using the mean field limit technique.
Let us introduce the atomic distribution function given by

$$f^N(\mathbf{x},\mathbf{v},t) = \frac{1}{N}\sum_{i=1}^{N} \delta(\mathbf{x}-\mathbf{x}_i(t))\,\delta(\mathbf{v}-\mathbf{v}_i(t)) \tag{2.16}$$

where δ denotes the Dirac delta distribution. Now, let us consider a test function $\varphi \in \mathscr{C}_0^1\left(\mathbb{R}^{2d}\right)$ and we compute the derivative of the $L^2\left(\mathbb{R}^{2d}\right)-$product

$$\begin{aligned}
\frac{d}{dt}\left\langle f^N(t),\varphi\right\rangle &= \frac{1}{N}\sum_{i=1}^{N}\frac{d}{dt}\varphi(\mathbf{x}_i(t),\mathbf{v}_i(t)) \\
&= \frac{1}{N}\sum_{i=1}^{N}\nabla_{\mathbf{x}}\varphi(\mathbf{x}_i(t),\mathbf{v}_i(t))\cdot\mathbf{v}_i(t) + \frac{1}{N}\sum_{i=1}^{N}\nabla_{\mathbf{v}}\varphi(\mathbf{x}_i(t),\mathbf{v}_i(t))\cdot\dot{\mathbf{v}}_i(t) \\
&= \frac{1}{N}\sum_{i=1}^{N}\nabla_{\mathbf{x}}\varphi(\mathbf{x}_i(t),\mathbf{v}_i(t))\cdot\mathbf{v}_i(t) + \frac{1}{N}\sum_{i=1}^{N}\nabla_{\mathbf{v}}\varphi(\mathbf{x}_i(t),\mathbf{v}_i(t))\cdot\mathscr{S}(\mathbf{v}_i) \\
&\qquad - \frac{1}{N^2}\sum_{i=1}^{N}\sum_{\substack{j=1\\ j\neq i}}^{N}\nabla_{\mathbf{v}}\varphi(\mathbf{x}_i(t),\mathbf{v}_i(t))\cdot\nabla U\left(\left\|\mathbf{x}_i-\mathbf{x}_j\right\|\right) \\
&= \left\langle f^N(t),\nabla_{\mathbf{x}}\varphi(\mathbf{x},\mathbf{v})\cdot\mathbf{v}\right\rangle + \left\langle f^N(t),\nabla_{\mathbf{v}}\varphi(\mathbf{x},\mathbf{v})\cdot\mathscr{S}(\mathbf{v})\right\rangle \\
&\qquad - \left[\frac{1}{N}\sum_{i=1}^{N}\left(\frac{1}{N}\sum_{\substack{j=1\\ j\neq i}}^{N}\nabla U\left(\left\|\mathbf{x}_i-\mathbf{x}_j\right\|\right)\right)\nabla_{\mathbf{v}}\varphi(\mathbf{x}_i(t),\mathbf{v}_i(t))\right] \\
&= \left\langle f^N(t),\nabla_{\mathbf{x}}\varphi(\mathbf{x},\mathbf{v})\cdot\mathbf{v}\right\rangle + \left\langle f^N(t),\nabla_{\mathbf{v}}\varphi(\mathbf{x},\mathbf{v})\cdot\mathscr{S}(\mathbf{v})\right\rangle \\
&\qquad - \left\langle f^N(t),\left(\frac{1}{N}\sum_{\substack{j=1\\ \mathbf{x}_j\neq\mathbf{x}}}^{N}\nabla U\left(\left\|\mathbf{x}-\mathbf{x}_j\right\|\right)\right)\cdot\nabla_{\mathbf{v}}\varphi(\mathbf{x},\mathbf{v})\right\rangle
\end{aligned} \tag{2.17}$$

Noticing that

$$\frac{1}{N}\sum_{\substack{j=1\\ \mathbf{x}_j\neq\mathbf{x}}}^{N}\nabla U\left(\left\|\mathbf{x}-\mathbf{x}_j\right\|\right)=\frac{1}{N}\sum_{\substack{j=1\\ \mathbf{x}_j\neq\mathbf{x}}}^{N}\left\langle\nabla U\left(\|\mathbf{x}-\mathbf{y}\|\right)\delta\left(\mathbf{y}-\mathbf{x}_j\right)\right\rangle_{\mathbf{x}}=\nabla U*\rho^N\left(\mathbf{x},t\right) \quad (2.18)$$

one can conclude that the atomic distribution function satisfies

$$\frac{d}{dt}\left\langle f^N\left(t\right),\varphi\right\rangle=\left\langle f^N\left(t\right),\nabla_{\mathbf{x}}\varphi\cdot\mathbf{v}+\nabla_{\mathbf{v}}\varphi\cdot\mathscr{S}\left(\mathbf{v}\right)-\nabla U*\rho^N\cdot\nabla_{\mathbf{v}}\varphi\right\rangle \quad (2.19)$$

which, in strong form, can be read as

$$\frac{\partial f^N}{\partial t}+\mathbf{v}\cdot\nabla_{\mathbf{x}}f^N=\left\{\left(\nabla_{\mathbf{x}}U*\rho\right)\cdot\nabla_{\mathbf{v}}f^N-\nabla_{\mathbf{v}}\cdot\left[\mathscr{S}\left(\mathbf{v}\right)f^N\right]\right\} \quad (2.20)$$

Passing to the limit, under suitable hypothesis of convergence, one can obtain again equation (2.14).

2.1.2 Numerical methods

Computing numerical solutions of Boltzmann-like equations has a very expensive cost because of the large number of variables and of the presence of a nonlinear multidimensional collision integral. Therefore, a numerical scheme in which a suitable decomposition of the multidimensional domain is required, seems impracticable.
For this reason, since 1970's [31, 32], the main approaches to solve numerically gas dynamics equations are based on probabilistic Monte Carlo methods. This kind of approaches presents many advantages: first the computational cost is strongly reduced with respect to the order of number of involved agents; second these methods do not require artificial boundary conditions (in principle every position and velocity are admissible).
In presence of bounded domains one has to impose suitable boundary conditions and the most natural choice is a sort of impermeability condition which prevents the mass flux through the walls. In our numerical simulations, under suitable choices of the initial configuration, this condition is guaranteed by the self-propelling term which takes account of the geometrical restrictions of the domain.
We refer to [12] for an overview of direct simulation and time relaxed Monte Carlo

techniques.
As in many of these methods, the starting point of our procedure is a splitting of the problem in two different steps

- transport part
$$\frac{\partial f}{\partial t} + \mathbf{v} \cdot \nabla_{\mathbf{x}} f = 0 \tag{2.21}$$
which will be solved by the exact free flow of the sample particles $\mathbf{x}_i(t+\Delta t) = \mathbf{x}_i(t) + \mathbf{v}_i(t)\Delta t$

- collision part
$$\frac{\partial f}{\partial t} = Q(f,f) \tag{2.22}$$
for which we use a Monte Carlo scheme.

The first step in Monte Carlo methods for kinetic equations is to select some values of the variables which are compatible with the initial datum. For this reason, before discussing the chosen algorithm, let us present the acceptance-rejection method which will be useful later to sample. The idea is really simple and we present that in 1-D case.
Let f be defined in (a,b) and let $f_{\max}$ be a constant such that $f_{\max} > f(x)$ for every $x \in (a,b)$. Let us consider two sequences of random numbers $\{\eta_i\}$ and $\{\bar{\eta}_i\}$, uniformly distributed in $(0,1)$, and let us proceed as follows

- from $\{\eta_i\}$ we generate the sequence $\{x_i\}$ in (a,b) by using
$$x_i = (b-a)\eta_i + a \tag{2.23}$$

- from $\{\bar{\eta}_i\}$ we generate the sequence $\{y_i\}$ in $(0, f_{\max})$ by using
$$y_i = f_{\max}\bar{\eta}_i \tag{2.24}$$

- if $y_i < f(x_i)$ then x_i is accepted; otherwise it is rejected.

The sequence of the accepted x_i is a sample compatible with the initial datum.
Now, we are ready to discuss the Monte Carlo algorithm. We consider a Nanbu-like asymptotic method in a symmetric version as proposed in [33] whose main utility is the low computational cost, reducing complexity from $O\left(N^2\right)$ (expected cost for a system of N interacting particles) to $O(N)$.
In order to justify the algorithm that we shall present in the sequel, one can notice that, splitting the collision operator in gain and loss term, the collision step can be rewritten as follows

$$\frac{\partial f}{\partial t} = \frac{1}{\varepsilon}\left[Q^+(f,f) - \mu f\right] \tag{2.25}$$

where Q^+ denotes the gain part and

$$\mu = \int_{\mathbb{R}^{2d}} f(\mathbf{x},\mathbf{v},t)\, d\mathbf{x}d\mathbf{v} \tag{2.26}$$

is assumed constant without loss of generality ($\mu = 1$).
At this point, if one consider a forward Euler scheme, the discrete equation reads as

$$f^{n+1} = \left(1 - \frac{\Delta t}{\varepsilon}\right) f^n + \frac{\Delta t}{\varepsilon} Q^+(f^n, f^n) \tag{2.27}$$

This means that an agent does not interact with the other ones with probability $1 - \Delta t/\varepsilon$ while interactions occur with probability $\Delta t/\varepsilon$.
We are interested in small values of ε and hence a natural choice is $\Delta t = \varepsilon$. A solution of (2.27) in $[0,T]$, $n_{\text{tot}} = T/\Delta t$ and $\Delta t = \varepsilon$, is given by

- sampling from the initial distribution f_0: $\left(\mathbf{x}_k^0, \mathbf{v}_k^0\right)$ with $k = 1, \ldots, N$
- for $n = 0$ to $n_{\text{tot}} - 1$
  - set $N_c = \text{Iround}\,(N/2)$
  - select N_c random pairs (i,j) of agents uniformly without repetition at time level n
  - compute the post-interaction velocities $\mathbf{v}_i^*$ and $\mathbf{v}_j^*$ for each pair (i,j) with strength $\eta = \varepsilon$ by using the interaction rules

– set $\left(\mathbf{x}_i^{n+1}, \mathbf{v}_i^{n+1}\right) = \left(\mathbf{x}_i^n, \mathbf{v}_i^*\right)$ and $\left(\mathbf{x}_j^{n+1}, \mathbf{v}_j^{n+1}\right) = \left(\mathbf{x}_j^n, \mathbf{v}_j^*\right)$ for all agents who changed their velocities; otherwise $\left(\mathbf{x}_h^{n+1}, \mathbf{v}_h^{n+1}\right) = \left(\mathbf{x}_h^n, \mathbf{v}_h^n\right)$

- end of cycle

where Iround denotes the integer stochastic rounding.

2.1.3 Numerical simulation

We consider now a mesoscopic model for two different situations presented in the previous chapter.
In the Monte Carlo method described above we sample $N = 5000$ agents and we choose a time step $\Delta t = 0.001$.
Figure 2.1 shows that evacuation is correctly reproduced. In fact, starting from an

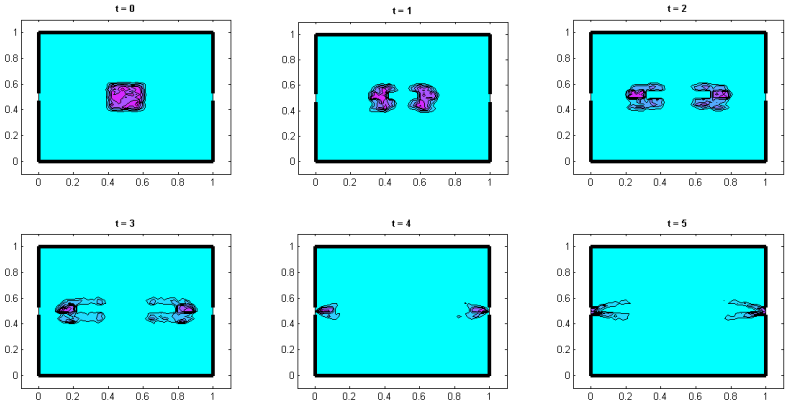

Figure 2.1: Mesoscopic description of the evacuation of a crowd in a domain with two exits. As in the microscopic case, the crowd separates in two different comparable groups and exits are used approximately in the same way.

initial configuration in which the population is concentrated in the middle of the walking area, dynamics divides agents in two different groups moving in opposite

directions. No panic phenomena have been introduced and hence the two identical exits are used in the same way and groups are comparable.

Also in figure 2.2 evacuation dynamics is correctly reproduced as expected. Unlike

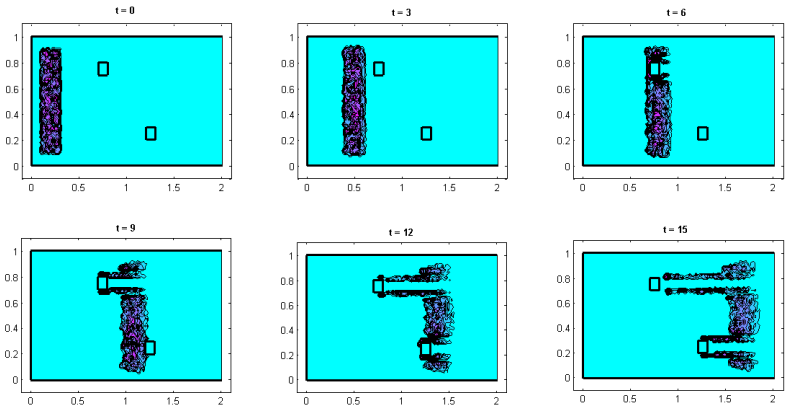

Figure 2.2: Mesoscopic description of the evacuation of a crowd in a domain in presence of obstacles. Obstacles are avoided by the entire crowd and sliding effects are correctly reproduced.

the previous case, now the walking area presents some obstacles in the middle which are avoided by the entire population moving towards the exit. Sliding effects occur also at mesoscopic level.

2.2 Macroscopic description

2.2.1 Derivation of the model

Now we are interested to deduce a set of partial differential equations to describe the crowd dynamics at the macroscopic level. The starting point is the previous kinetic model

$$\frac{\partial f}{\partial t} + \mathbf{v} \cdot \nabla_{\mathbf{x}} f = \lambda \left\{ (\nabla_{\mathbf{x}} U * \rho) \cdot \nabla_{\mathbf{v}} f - \nabla_{\mathbf{v}} \cdot [\mathscr{S}(\mathbf{v}) f] \right\} \tag{2.28}$$

It is well-known that kinetic descriptions are very expensive from a computational point of view when the distribution functions are defined in "high" dimension spaces as seen in the previous applications where positions and velocities are vectors in $\mathbb{R}^2$. In this regard, by taking the hydrodynamic limit, one can reduce the complexity of the problem by reducing its dimensionality.

As usually done in kinetic theory, we are interested in the evolution of the macroscopic quantities defined as moments of the distribution function f

$$\rho\mathbf{u} = \int_{\mathbb{R}^d} \mathbf{v} f(\mathbf{x},\mathbf{v},t)\, d\mathbf{v} \qquad \text{and} \qquad d\rho T = \int_{\mathbb{R}^d} (\mathbf{v}-\mathbf{u})^2 f(\mathbf{x},\mathbf{v},t)\, d\mathbf{v} \tag{2.29}$$

where ρ, $\mathbf{u}$ and T indicate, respectively, density, mean velocity of the crowd and T gives a measure of the deviation of $\mathbf{v}$ with respect to $\mathbf{u}$.

In order to obtain macroscopic equations, we have to consider the weak formulation of the Boltzmann-like one (2.28).

By using the unit constant as test function in the weak form, one can notice that the right-hand side in (2.28) vanishes. As regards the left-hand side, one can observe that

$$\begin{aligned} &\int \frac{\partial f}{\partial t}(\mathbf{x},\mathbf{v},t)\, d\mathbf{v} + \int \mathbf{v}\cdot\nabla_{\mathbf{x}} f(\mathbf{x},\mathbf{v},t)\, d\mathbf{v} \\ &\quad = \frac{\partial}{\partial t}\int f(\mathbf{x},\mathbf{v},t)\, d\mathbf{v} + \nabla_{\mathbf{x}}\cdot\int \mathbf{v} f(\mathbf{x},\mathbf{v},t)\, d\mathbf{v} = \frac{\partial\rho}{\partial t} + \nabla_{\mathbf{x}}\cdot(\rho\mathbf{u}) \end{aligned} \tag{2.30}$$

under suitable assumptions. Therefore, density satisfies the usual continuity equation

$$\frac{\partial\rho}{\partial t} + \nabla_{\mathbf{x}}\cdot(\rho\mathbf{u}) = 0 \tag{2.31}$$

Now we use the identity $\varphi(\mathbf{v}) = \mathbf{v}$ as test function to deduce a macroscopic momentum equation; at the left-hand side, we obtain

$$\frac{\partial}{\partial t}(\rho\mathbf{u}) + \nabla_{\mathbf{x}}\cdot(\rho\mathbf{u}\otimes\mathbf{u} + \mathbf{P}) \tag{2.32}$$

where $\otimes$ denotes the tensor product and $\mathbf{P}$ is a tensor which takes account of the moments of order 2.

In order to have a closed set of partial differential equations, we assume that

- fluctuations are negligible i.e. $T(\mathbf{x},t)=0$
  $\Rightarrow$ diagonal part of $\mathbf{P}$ vanishes
- the velocity distribution is monokinetic i.e. $f(\mathbf{x},\mathbf{v},t)=\rho(\mathbf{x},t)\,\delta(\mathbf{v}-\mathbf{u}(\mathbf{x},t))$
  $\Rightarrow$ non-diagonal part of $\mathbf{P}$ vanishes

As concerns the right-hand side, by using integration by parts, one has

$$\begin{aligned}\int (\nabla_{\mathbf{x}} U * \rho)\cdot\nabla_{\mathbf{v}} f v_i d\mathbf{v} = \\ = \sum_j \int \left(\frac{\partial U}{\partial x_j} * \rho\right)\frac{\partial f}{\partial v_j} v_i d\mathbf{v} = \sum_j \int \frac{\partial}{\partial v_j}\left(\frac{\partial U}{\partial x_j} * \rho f\right) v_i d\mathbf{v} \\ = -\sum_j \left(\frac{\partial U}{\partial x_j} * \rho\right)\int f\delta_{ij} d\mathbf{v} = -\rho\left(\frac{\partial U}{\partial x_i} * \rho\right)\end{aligned} \tag{2.33}$$

and analogously

$$-\int \nabla_{\mathbf{v}}\cdot[\mathscr{S}(\mathbf{v})f(\mathbf{v})]\,v_i d\mathbf{v} = \rho\mathscr{S}_i(\mathbf{u}) \tag{2.34}$$

where

$$\mathscr{S}(\mathbf{u}) = \frac{v^0\mathbf{e}^0(\mathbf{x})-\mathbf{u}}{\tau} \tag{2.35}$$

and $\mathbf{e}^0(\mathbf{x})$ is the field of the desired directions.
Summing up, mass and momentum equations fulfill

$$\begin{cases}\dfrac{\partial\rho}{\partial t}+\nabla_{\mathbf{x}}\cdot(\rho\mathbf{u}) = 0 \\ \\ \dfrac{\partial}{\partial t}(\rho\mathbf{u})+\nabla_{\mathbf{x}}\cdot(\rho\mathbf{u}\otimes\mathbf{u}) = \rho\mathscr{S}(\mathbf{u})-\rho(\nabla_{\mathbf{x}}U*\rho)\end{cases} \tag{2.36}$$

2.2.2 Numerical methods

For sake of simplicity, from now on, let us consider the 1-D formulation of the previous macroscopic model

$$\begin{cases}\dfrac{\partial\rho}{\partial t}+\dfrac{\partial}{\partial x}(\rho u) = 0 \\ \\ \dfrac{\partial}{\partial t}(\rho u)+\dfrac{\partial}{\partial x}(\rho u^2) = \rho\mathscr{S}(u)-\rho\left(\dfrac{\partial}{\partial x}U*\rho\right)\end{cases} \tag{2.37}$$

or, equivalently,

$$\begin{cases} \dfrac{\partial \rho}{\partial t} + \dfrac{\partial}{\partial x}(\rho u) = 0 \\ \\ \dfrac{\partial u}{\partial t} + u\dfrac{\partial u}{\partial x} = \mathscr{S}(u) - \left(\dfrac{\partial}{\partial x} U * \rho\right) \end{cases} \tag{2.38}$$

It is easy to prove that this set of partial differential equations constitutes a hyperbolic system and it is well-known that finding analytical and numerical solutions is really hard, especially when some discontinuities appear.

Before presenting the numerical technique we will use in the sequel, the first step is to consider a suitable splitting of the problem.

From the previous system we deduce two different sub-problems

$$A: \begin{cases} \dfrac{\partial \rho}{\partial t} + \dfrac{\partial}{\partial x}(\rho u) = 0 \\ \\ \dfrac{\partial u}{\partial t} + u\dfrac{\partial u}{\partial x} = 0 \end{cases} \qquad B: \begin{cases} \dfrac{\partial \rho}{\partial t} = 0 \\ \\ \dfrac{\partial u}{\partial t} = \mathscr{S}(u) - \left(\dfrac{\partial}{\partial x} U * \rho\right) \end{cases} \tag{2.39}$$

Step A (transport step) takes the hyperbolic structure into account but it neglects source terms. The system of balance equations reduces to a system of conservation laws. On the other side, step B (collision step) includes interactions between different agents or between agents and domain but it just takes account of time-dependence. In this case partial differential equations become ordinary differential equations.

As concerns step B, a simple forward Euler scheme has been implemented.

As regards the hyperbolic system A, besides difficulties due to non-linearity, the main purpose is a good treatment of possible discontinuous solutions. For these reasons we choose to work with Lax-Friedrichs method [34]. Let us introduce it in a generic case. Let us suppose we want to solve the non-linear problem

$$\frac{\partial u}{\partial t} + \frac{\partial}{\partial x} f(u) = 0 \tag{2.40}$$

where $u = u(x,t)$ is the unknown field. Let us indicate by U an approximation of the exact solution u: one has $U_j^n = u(x_j, t^n)$ where $\{x_j\}_j$ and $\{t^n\}_n$ denote, respectively,

suitable decompositions in space and time. The discrete solution at time step $n+1$ can be computed as follows

$$U_j^{n+1} = \frac{1}{2}\left(U_{j-1}^n + U_{j+1}^n\right) - \frac{k}{2h}\left[f\left(U_{j+1}^n\right) - f\left(U_{j-1}^n\right)\right] \tag{2.41}$$

where k and h are time and space discretization steps.
It is easy to notice that computations in the first and last knots require to assume some boundary conditions; for this reason we shall extend the solution in a constant way by taking the values in boundary knots.
Let us show now the reason for which Lax-Friedrichs scheme seems a good choice. We shall say that a method is in conservation form if it can be written in the form

$$U_j^{n+1} = U_j^n - \frac{k}{h}\left[F\left(U_{j-p}^n, U_{j-p+1}^n, \ldots, U_{j+q}^n\right) - F\left(U_{j-p-1}^n, U_{j-p}^n, \ldots, U_{j+q-1}^n\right)\right] \tag{2.42}$$

where F is a function of $p+q+1$ arguments and it is called numerical flux function. This requirement guarantees that the algorithm does not converge to non-solutions. Noting that Lax-Friedrichs can be rewritten by using the following numerical flux

$$F\left(U_j, U_{j+1}\right) = \frac{h}{2k}\left(U_j - U_{j+1}\right) + \frac{1}{2}\left[f\left(U_j\right) + f\left(U_{j+1}\right)\right] \tag{2.43}$$

one can conclude that it will build up a physical solution.

2.2.3 Numerical simulations

In this section we analyze the evolution of the problem (2.37) for different initial configurations in 1-D space.
As concerns the initial velocity let us fix the same datum in every situation and we consider the constant function $u_0(x) = -1 \ \forall x$. This means that agents move in the opposite direction with respect to the positive desired one $v^0 = 1$.
As regards density datum we consider some functions ρ_0 with unit total density (the

integral of ρ_0 over the domain is equal to 1)

$$(\mathbf{A}) \quad \rho_0(x) = \begin{cases} 1 \text{ if } -1/2 < x < 1/2 \\ 0 \text{ otherwise} \end{cases}$$

$$(\mathbf{B}) \quad \rho_0(x) = \begin{cases} 1 \text{ if } -3/4 < x < -1/4 \text{ and } 1/4 < x < 3/4 \\ 0 \text{ otherwise} \end{cases} \tag{2.44}$$

$$(\mathbf{C}) \quad \rho_0(x) = \begin{cases} 2 \text{ if } 1/4 < x < 3/4 \\ 0 \text{ otherwise} \end{cases}$$

All the simulations show that a sufficiently small spatial step is required; in fact,

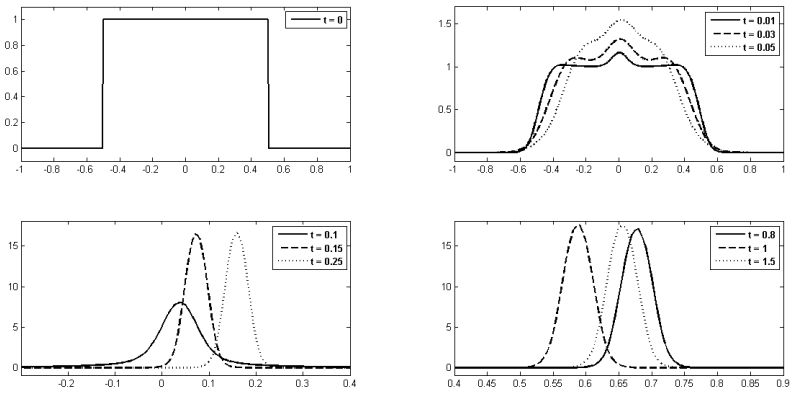

Figure 2.3: Evolution of a crowd with initial configuration **A**.

a small number of points in the space discretization introduces oscillations in correspondence of discontinuities. Moreover a suitable small time step has to be coupled. In each figure one can notice that, at the beginning, dynamics tend to regularize the initial piecewise constant data until they assume a Gaussian-like profile or, in other

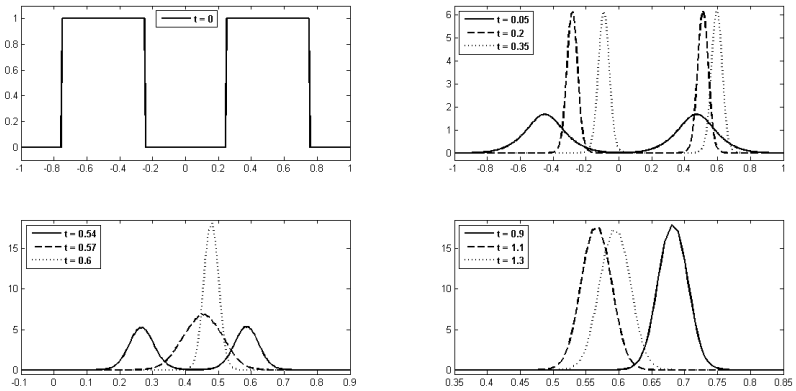

Figure 2.4: Evolution of a crowd with initial configuration **B**.

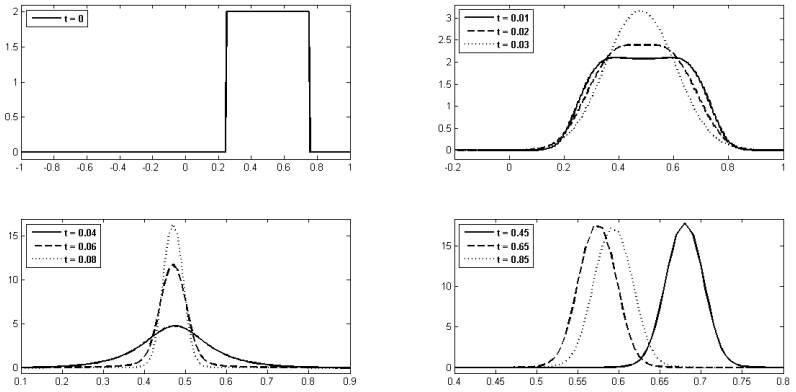

Figure 2.5: Evolution of a crowd with initial configuration **C**.

words, agents tend to concentrate in a small neighborhood around a position.
Then this profile moves as a wave adapting its direction to desired one and, in this way, the initial tendency to move in the opposite direction is totally absorbed by the

self-propelling term.
At last, one can notice some oscillations around a position which gets us supposing the existence of an equilibrium configuration of Gaussian type. Hence, in other words, the tendency of agents to adapt its own velocity to the desired one is balanced by the particle interactions.

Chapter 3

Multi-temperature models for inert and reactive gas mixtures

3.1 Introduction

It is well known that in thermally non-equilibrium conditions a single temperature model for a gas mixture is not valid and more accurate models of kinetics, gas dynamics and transport properties are required [35]. For example, a multi-temperature description arises spontaneously when atomic masses of components are disparate, in physics of plasmas at high temperature as well as in several problems of aerothermodynamics [7, 8]. Clearly a multi-temperature approach presents many practical difficulties such as measuring the temperature of each component or handling a larger number of variables; nevertheless a macroscopic theory of homogenous mixtures is developed in the framework of rational thermodynamics [36] and it is based on the assumption that each constituent obeys the same balance laws as a single fluid [13, 14]. At this point a consistent formal derivation of multi-temperature fluid-dynamics is desirable and it can be obtained as an asymptotic limit starting from suitable kinetic descriptions [4, 37]. In this regard, some hydrodynamic models, even for reactive gases, were already considered [38] but they were all leading to some single-temperature descriptions. In order to avoid this restriction, it is clear that one should deal with a gas

in which equilibration within each species is faster than equalization of species parameters in the gas as a whole. Of course, the task becomes quite heavy if one wants to include also other processes like the occurrence of chemical reactions or take account of the internal molecular structure [39, 40].
In this chapter, first we recall a very simple model for a mixture of monoatomic gases which takes into account just elastic mechanical interactions. We consider a two-scale process where the fast dominant phenomenon is constituted by resonant collisions between particles of the same species; interactions involving different components belong to the slow process [15]. At the kinetic level, rescaled equations for a mixture of Q components read as

$$\frac{\partial f_i}{\partial t} + \mathbf{v} \cdot \nabla_{\mathbf{x}} f_i = \frac{1}{\varepsilon} I_{ii}[f_i, f_i] + \sum_{j \neq i} I_{ij}[f_i, f_j] \qquad \text{for } i = 1, \ldots, Q \tag{3.1}$$

where f_i denotes the distribution function of the $i-$th species and I_{ij} is the collision operator related to interactions between species i and j. It takes the form

$$I_{ij}[f_i, f_j] = \iint B_{ij}\left(g, \hat{n} \cdot \hat{n}'\right)\left[f_i(\mathbf{v}^*) f_j(\mathbf{w}^*) - f_i(\mathbf{v}) f_j(\mathbf{w})\right] d\mathbf{w} d\hat{n}' \tag{3.2}$$

and it involves the collision kernel B_{ij} depending on the relative speed $g = |\mathbf{v} - \mathbf{w}|$ and on the deflection angle $\hat{n} \cdot \hat{n}'$. Finally, Knudsen number ε is a small parameter and its role is to amplify the effect of resonant collisions.
Starting from the previous set of integro-differential Boltzmann-like equations we deduce a macroscopic description by a hydrodynamic limit ($\varepsilon \to 0$) and by a suitable closure at Euler level. The evolution of the macroscopic quantities turns out to be governed by a multi-velocity and multi-temperature set of partial differential equations and one has to handle Q mass densities, velocities and temperatures.
Later we shall extend the model to the reactive case when components undergo the following bimolecular reversible chemical reaction

$$(1,2) \rightleftharpoons (3,4) \tag{3.3}$$

which involves four different species ($Q \geq 4$). We suppose that each component is endowed with an internal energy due to the chemical links E_i; the quantity $\Delta E =$

$E_3 + E_4 - E_1 - E_2$ is fixed positive and it represents the activation energy of the endothermic reaction. Under the assumption $\Delta E = 0$, some interesting results, like hydrodynamic equations at Euler level and existence, uniqueness and stability of equilibria, have been deduced [15]. Also a single-velocity and multi-temperature model can be obtained by the previous general one assuming the equalization of species velocities and it can be tested on classical problems, like the steady shock waves problem [17].
At the end we shall propose a possible extension to polyatomic gases [16] by considering a discrete set of energy levels to mimic the internal structure. The finite spectrum can be replaced by a continuous one and some results, like the determination and analysis of production terms, have been presented recently [41].

3.2 Monoatomic inert gases

In this section we recall the main features of a multi-temperature description for a non-reactive mixture of monoatomics gases and we refer to [15] for more details.
The starting point is the set of Boltzmann-type equations governing the distribution functions of the involved species

$$\frac{\partial f_i}{\partial t} + \mathbf{v} \cdot \nabla_{\mathbf{x}} f_i = \frac{1}{\varepsilon} I_{ii}[f_i, f_i] + \sum_{j \neq i} I_{ij}[f_i, f_j] \qquad \text{for } i = 1, \ldots, Q \tag{3.4}$$

where I_{ij} is the elastic scattering operator for (i, j) encounters. The quantity ε is a small parameter and it represents the ratio of the mean free path of the collisions within each single species to any of the other characteristic lengths which are supposed to be longer than the previous one.
One can prove [4] that collision equilibria for the whole equations (3.4) are provided by the seven parameter family of Maxwellians

$$f_i^M(\mathbf{v}) = n_i \left(\frac{m_i}{2\pi T}\right)^{3/2} \exp\left[-\frac{m_i}{2T}(\mathbf{v} - \mathbf{u})^2\right] \tag{3.5}$$

sharing common values $\mathbf{u}$ and T, respectively, for mass velocity and temperature.
Moreover, entropy dissipation and stability of equilibria are given by the Lyapunov

function for mixtures

$$H[\mathbf{f}] = \sum_{i=1}^{Q} \int f_i \log f_i d\mathbf{v} \tag{3.6}$$

As usual, macroscopic fields for each species are defined as moments of the relevant distribution function and we want to propose a description of their evolution.
We are interested in the hydrodynamic closure in the asymptotic limit $\varepsilon \to 0$ of (3.4) and in particular we concentrate on the zero-th order approximation (at Euler level). The first step in this regard is determining the collision invariants and equilibria for the dominant part of the collision operator. It is not difficult to prove that the local equilibria solving $I_{ii} = 0 \ \forall i$ constitute a $5Q-$parameter family of local Maxwellians

$$M_i(\mathbf{v}) = n_i \left(\frac{m_i}{2\pi T_i}\right)^{3/2} \exp\left[-\frac{m_i}{2T_i}(\mathbf{v}-\mathbf{u}_i)^2\right] \tag{3.7}$$

with free parameters n_i, $\mathbf{u}_i$ and T_i and that such dominant operators admit $5Q$ independent collision invariants corresponding to preservation of number density, momentum and kinetic energy within each single species.
In order to obtain a macroscopic description for the mixture, one can use collision invariants as test functions in the weak form of (3.4) whose production term at the right-hand side becomes

$$\int \varphi_i(\mathbf{v}) I_{ij}[f_i, f_j](\mathbf{v}) d\mathbf{v} = \iiint B_{ij}\left(g, \hat{n}\cdot\hat{n}'\right)\left[\varphi_i(\mathbf{v}_{ij}) - \varphi_i(\mathbf{v})\right] f_i(\mathbf{v}) f_j(\mathbf{w}) d\mathbf{v} d\mathbf{w} d\hat{n}' \tag{3.8}$$

where φ_i indicates the generic collision invariant and $\mathbf{v}$, $\mathbf{v}_{ij}$ are, respectively, pre- and post-collision velocities.
The set of partial differential equations for densities n_i, mass velocities $\mathbf{u}_i$ and tem-

peratures T_i results

$$\begin{cases} \dfrac{\partial n_i}{\partial t} + \nabla_{\mathbf{x}} \cdot (n_i \mathbf{u_i}) = 0 \\ \\ \dfrac{\partial}{\partial t}(\rho_i \mathbf{u}_i) + \nabla_{\mathbf{x}} \cdot (\rho_i \mathbf{u}_i \otimes \mathbf{u}_i) + \nabla_{\mathbf{x}} \cdot \mathbf{P}_i = \displaystyle\sum_{j \neq i} \mathbf{R}_{ij} \\ \\ \dfrac{\partial}{\partial t}\left(\dfrac{1}{2}\rho_i u_i^2 + \dfrac{3}{2} n_i T_i\right) + \nabla_{\mathbf{x}} \cdot \left[\left(\dfrac{1}{2}\rho_i u_i^2 + \dfrac{3}{2} n_i T_i\right)\mathbf{u}_i + \mathbf{P}_i \cdot \mathbf{u}_i + \mathbf{q}_i\right] = \displaystyle\sum_{j \neq i} S_{ij} \end{cases} \tag{3.9}$$

where $\mathbf{P}_i$ and $\mathbf{q}_i$ denote respectively pressure tensor and heat flux for the $i-$th component; $\mathbf{R}_{ij}$ and S_{ij} are integrals of the collision kernels B_{ij} $(i \neq j)$ representing momentum and energy exchanges between particles of different species.

The previous system is not a closed set of equations and a closure is required. It can be done in a natural way at different levels of accuracy by a suitable expansion of the distribution function f_i around the corresponding local equilibrium M_i. The easiest approximation is the zero-th order one, obtained just by replacing f_i by M_i in the non-hydrodynamic fields $\mathbf{P}_i$ and $\mathbf{q}_i$ and in the collision contributions. This implies that the stress tensors get a diagonal form, $\mathbf{P}_i = n_i T_i \mathbf{I}$, and the heat fluxes $\mathbf{q}_i$ vanish. Hence this lead us to the following system of Euler-type equations

$$\begin{cases} \dfrac{\partial n_i}{\partial t} + \nabla_{\mathbf{x}} \cdot (n_i \mathbf{u_i}) = 0 \\ \\ \dfrac{\partial}{\partial t}(\rho_i \mathbf{u}_i) + \nabla_{\mathbf{x}} \cdot (\rho_i \mathbf{u}_i \otimes \mathbf{u}_i) + \nabla_{\mathbf{x}} (n_i T_i) = \displaystyle\sum_{j \neq i} \mathbf{R}_{ij} \\ \\ \dfrac{\partial}{\partial t}\left(\dfrac{1}{2}\rho_i u_i^2 + \dfrac{3}{2} n_i T_i\right) + \nabla_{\mathbf{x}} \cdot \left[\left(\dfrac{1}{2}\rho_i u_i^2 + \dfrac{5}{2} n_i T_i\right)\mathbf{u}_i\right] = \displaystyle\sum_{j \neq i} S_{ij} \end{cases} \tag{3.10}$$

where now $\mathbf{R}_{ij}$ and S_{ij} are suitable integrals of the collision operators I_{ij} with Gaussian M_i, M_j in place of actual distributions f_i, f_j. Source terms at the right-hand side depend on the collision kernel or, in other words, on the way we describe the interactions between particles. From now on we suppose to model particles as Maxwell

molecules for which moments of the collision kernels become constant.
In order to compute integrals at the right hand side one can notice that the product of Maxwellians can be cast as

$$\begin{aligned} M_i(\mathbf{v})M_j(\mathbf{w}) = n_i n_j \left(\frac{m_i}{2\pi T_i}\right)^{\frac{3}{2}} \left(\frac{m_j}{2\pi T_j}\right)^{\frac{3}{2}} \times \\ \times \exp\left[-\eta_{ij}\left(\mathbf{G}_{ij}+\gamma_{ij}\mathbf{g}-\delta_{ij}\right)^2\right] \exp\left\{-\beta_{ij}\left[\mathbf{g}-(\mathbf{u}_i-\mathbf{u}_j)\right]^2\right\} \end{aligned} \tag{3.11}$$

where

$$\begin{aligned} \eta_{ij} = \frac{m_i}{2T_i}+\frac{m_j}{2T_j}, \beta_{ij} = \left(\frac{2T_i}{m_i}+\frac{2T_j}{m_j}\right)^{-1} \\ \gamma_{ij} = \frac{\mu_{ij}}{\eta_{ij}}\left(\frac{1}{2T_i}-\frac{1}{2T_j}\right), \delta_{ij} = \frac{1}{\eta_{ij}}\left(\frac{m_i}{2T_i}\mathbf{u}_i+\frac{m_j}{2T_j}\mathbf{u}_j\right) \end{aligned} \tag{3.12}$$

and $\mathbf{G}_{ij}$ is the center of mass velocity $\alpha_{ij}\mathbf{v}+\alpha_{ji}\mathbf{w}$, $\mu_{ij} = m_i m_j/(m_i+m_j)$ is the reduced mass and $\alpha_{ij} = m_i/(m_i+m_j)$ is the mass ratio. Since $d\mathbf{v}d\mathbf{w} = d\mathbf{G}_{ij}d\mathbf{g}$, the integration over $\mathbf{G}_{ij} \in \mathbb{R}^3$ may be performed explicitly and, under the assumption of Maxwell molecules, also integrations over $\mathbf{g}$ can be computed and hence slow collision terms read as

$$\mathbf{R}_{ij} = -\mu_{ij} n_i n_j \bar{B}_{ij}(\mathbf{u}_i-\mathbf{u}_j) \tag{3.13}$$

and

$$\mathbf{S}_{ij} = -\mu_{ij} n_i n_j \bar{B}_{ij}\left[(\alpha_{ij}\mathbf{u}_i+\alpha_{ji}\mathbf{u}_j)\cdot(\mathbf{u}_i-\mathbf{u}_j)+3\frac{T_i-T_j}{m_i+m_j}\right] \tag{3.14}$$

where $\bar{B}_{ij}$ is the constant collision frequency for (i,j) interactions

$$\bar{B}_{ij} = B^0_{ij}-B^1_{ij} \qquad B^\ell_{ij} = \int \left(\hat{n}\cdot\hat{n}'\right)^\ell B_{ij}\left(g,\hat{n}\cdot\hat{n}'\right) d\hat{n}' \tag{3.15}$$

An important robustness test concerns the study of equilibria and their stability. It may be easily proved that equilibria are characterized by

- equalization of species velocities $\mathbf{u}_1 = \mathbf{u}_2 = \ldots = \mathbf{u}_N$
- equalization of species temperatures $T_1 = T_2 = \ldots = T_N$

Existence and uniqueness of the configuration of equilibrium are guaranteed once the initial configuration has been fixed. Moreover a Lyapunov function correctly reproduces entropy dissipation and relaxation to the equilibrium. This function is obtained by the restriction of the mixture Boltzmann H-functional to the subspace of the distribution functions defined by the local Maxwellians M_i and it reads as

$$H = \sum_i n_i \left[\log n_i + \frac{3}{2} \log \left(\frac{m_i}{2\pi T_i} \right) - \frac{3}{2} \right] \tag{3.16}$$

In order to show that H is a Lyapunov function for this problem, one has to prove that

$$\dot{H} \leq 0 \quad (\dot{H} = 0 \text{ if } H = H^{\text{eq}}) \qquad \text{and} \qquad H - H^{\text{eq}} > 0 \tag{3.17}$$

where H^{eq} is the value of the function H in the equilibrium state.
As concerns the first inequality one can notice that

$$\begin{aligned} \dot{H} = &- \sum_{i=1}^{Q} \frac{1}{T_i} \sum_{\substack{j=1 \\ j \neq i}}^{Q} (S_{ij} - \mathbf{R}_{ij} \cdot \mathbf{u}_i) = \sum_{i=1}^{Q} \sum_{\substack{j=1 \\ j \neq i}}^{Q} \frac{\mu_{ij} n_i n_j \nu_{ij}}{T_i} \times \\ &\times \left[(\mathbf{u}_i - \mathbf{u}_j) \cdot (\alpha_{ij} \mathbf{u}_i + \alpha_{ji} \mathbf{u}_j) + 3 \frac{T_i - T_j}{m_i + m_j} - \mathbf{u}_i \cdot (\mathbf{u}_i - \mathbf{u}_j) \right] =: \sum_{i=1}^{Q} \sum_{\substack{j=1 \\ j \neq i}}^{Q} \xi^{ij} \end{aligned} \tag{3.18}$$

and

$$\begin{aligned} \xi^{ij} + \xi^{ji} &= 3 \frac{\mu_{ij} n_i n_j \nu_{ij}}{m_i + m_j} \left[\frac{T_i - T_j}{T_i} + \frac{T_j - T_i}{T_j} \right] \\ &+ \frac{\mu_{ij} n_i n_j \nu_{ij}}{T_i} \left[(\mathbf{u}_i - \mathbf{u}_j) \cdot (\alpha_{ij} \mathbf{u}_i + \alpha_{ji} \mathbf{u}_j) - \mathbf{u}_i \cdot (\mathbf{u}_i - \mathbf{u}_j) \right] \\ &- \frac{\mu_{ij} n_i n_j \nu_{ij}}{T_j} \left[(\mathbf{u}_i - \mathbf{u}_j) \cdot (\alpha_{ij} \mathbf{u}_i + \alpha_{ji} \mathbf{u}_j) - \mathbf{u}_j \cdot (\mathbf{u}_i - \mathbf{u}_j) \right] \\ &= 3 \frac{\mu_{ij} n_i n_j \nu_{ij}}{(m_i + m_j) T_i T_j} \left[T_i T_j - T_j^2 + T_j T_i - T_i^2 \right] \\ &+ \mu_{ij} n_i n_j \nu_{ij} \left[- \frac{\alpha_{ji}}{T_i} (\mathbf{u}_i - \mathbf{u}_j)^2 - \frac{\alpha_{ij}}{T_j} (\mathbf{u}_i - \mathbf{u}_j)^2 \right] \\ &= -3 \frac{\mu_{ij} n_i n_j \nu_{ij}}{(m_i + m_j) T_i T_j} (T_i - T_j)^2 \\ &\quad - \frac{\mu_{ij} n_i n_j \nu_{ij}}{m_i + m_j} \left(\frac{m_j}{T_i} + \frac{m_i}{T_j} \right) (\mathbf{u}_i - \mathbf{u}_j)^2 \leq 0 \end{aligned} \tag{3.19}$$

As regards the second inequality, it is sufficient to recall that Boltzmann functional admits minimum when the distribution functions are Maxwellian-type functions sharing the same value for mass velocities and temperatures and to notice that the function H is nothing else but the Boltzmann functional restricted to a subspace in which the minimum is included.

3.3 Reactive case

An important extension of the previous model concerns the occurrence of chemical processes in the evolution of the mixture. For sake of simplicity, we introduce a single reversible bimolecular reaction

$$(1,2) \rightleftharpoons (3,4) \tag{3.20}$$

and only four participating species are considered. We suppose also that each component has an internal energy E_i due to the chemical links.
We follow the previous scheme to analyze this reactive case starting from the Boltzmann-type equations which are scaled as follows

$$\frac{\partial f_i}{\partial t} + \mathbf{v} \cdot \nabla_{\mathbf{x}} f_i = \frac{1}{\varepsilon} I_{ii}[f_i, f_i] + \sum_{j \neq i} I_{ij}[f_i, f_j] + J_i[\mathbf{f}] \qquad \text{for } i = 1, \ldots, 4 \tag{3.21}$$

The production term takes account of the chemical interactions and takes the form

$$\begin{aligned} J_i[\mathbf{f}] = \iint U\left(g^2 - \delta_{ij}^{hk}\right) g B_{ij}^{hk}\left(g, \hat{n} \cdot \hat{n}'\right) \times \\ \times \left[\left(\frac{\mu_{ij}}{\mu_{hk}} \right)^3 f_h\left(\mathbf{v}_{ij}^{hk}\right) f_k\left(\mathbf{w}_{ij}^{hk}\right) - f_i(\mathbf{v}) f_j(\mathbf{w}) \right] d\mathbf{v} d\hat{n}' \end{aligned} \tag{3.22}$$

where U is the unit step function, $\delta_{ij}^{hk} = 2\Delta E / \mu_{ij}$ and (i, j, h, k) is one of the following sequences

$$(1,2,3,4) \quad , \quad (2,1,4,3) \quad , \quad (3,4,1,2) \quad , \quad (4,3,2,1) \tag{3.23}$$

The occurrence of the endothermic reaction is strictly related to the internal energy. In fact, the quantity $\Delta E = E_3 + E_4 - E_1 - E_2$ represents an activation energy and it

introduces a threshold for the endothermic reaction: it may occur if the impinging kinetic energy overcomes a potential barrier proportional to ΔE.
As in the previous inert case, also for the reactive one it is possible determining equilibria

$$f_i^M(\mathbf{v}) = n_i \left(\frac{m_i}{2\pi T}\right)^{3/2} \exp\left[-\frac{m_i}{2T}(\mathbf{v}-\mathbf{u})^2\right] \tag{3.24}$$

where number densities are related by the classical Mass Action Law

$$\frac{n_1 n_2}{n_3 n_4} = \left(\frac{\mu_{12}}{\mu_{34}}\right)^{3/2} e^{\Delta E/T} \tag{3.25}$$

One can reproduce also the stability of equilibria and the entropy dissipation by a Boltzmann H-functional in chemical version

$$H[\mathbf{f}] = \sum_{i=1}^{4} \int f_i \log\left(\frac{f_i}{m_i^3}\right) d\mathbf{v} \tag{3.26}$$

We can pass to the hydrodynamic limit of (3.21) when $\varepsilon \to 0$; the evolution of the 20 macroscopic fields is governed by a set of partial differential differential equations

$$\begin{cases} \dfrac{\partial n_i}{\partial t} + \nabla_{\mathbf{x}} \cdot (n_i \mathbf{u_i}) = Q_i \\ \\ \dfrac{\partial}{\partial t}(\rho_i \mathbf{u}_i) + \nabla_{\mathbf{x}} \cdot (\rho_i \mathbf{u}_i \otimes \mathbf{u}_i) + \nabla_{\mathbf{x}} \cdot \mathbf{P}_i = \displaystyle\sum_{j \neq i} \mathbf{R}_{ij} + \mathbf{R}_i \\ \\ \dfrac{\partial}{\partial t}\left(\dfrac{1}{2}\rho_i u_i^2 + \dfrac{3}{2} n_i T_i\right) + \nabla_{\mathbf{x}} \cdot \left[\left(\dfrac{1}{2}\rho_i u_i^2 + \dfrac{3}{2} n_i T_i\right)\mathbf{u}_i + \mathbf{P}_i \cdot \mathbf{u}_i + \mathbf{q}_i\right] = \displaystyle\sum_{j \neq i} S_{ij} + S_i \end{cases} \tag{3.27}$$

where Q_i, $\mathbf{R}_i$ and S_i denote the exchange of mass, momentum and energy due to the chemical reaction. A first difference with respect to the inert case is that in the reactive frame number densities are not preserved across the reaction and a source term Q_i appears.
As in the previous section a closure procedure is required and at Euler level, under

the assumption of Maxwell molecules, the macroscopic equations become

$$\begin{cases} \dfrac{\partial n_i}{\partial t} + \nabla_{\mathbf{x}} \cdot (n_i \mathbf{u_i}) = Q_i \\ \\ \dfrac{\partial}{\partial t}(\rho_i \mathbf{u}_i) + \nabla_{\mathbf{x}} \cdot (\rho_i \mathbf{u}_i \otimes \mathbf{u}_i) + \nabla_{\mathbf{x}}(n_i T_i) = \displaystyle\sum_{j \neq i} \mathbf{R}_{ij} + \mathbf{R}_i \\ \\ \dfrac{\partial}{\partial t}\left(\dfrac{1}{2}\rho_i u_i^2 + \dfrac{3}{2} n_i T_i\right) + \nabla_{\mathbf{x}} \cdot \left[\left(\dfrac{1}{2}\rho_i u_i^2 + \dfrac{5}{2} n_i T_i\right)\mathbf{u}_i\right] = \displaystyle\sum_{j \neq i} S_{ij} + S_i \end{cases} \tag{3.28}$$

where the source terms are integrals of the Boltzmann (inert and reactive) operators with f_i replaced by M_i.

The integrations at the right-hand side are not possible in the most general case but for the density equations. It is easy to see that

$$Q_1 = Q_2 = -Q_3 = -Q_4 \tag{3.29}$$

and then conservation of pairs of densities (for instance $n_1 - n_2$, $n_1 + n_3$, $n_1 + n_4$) are reproduced as the conservation of total density.

A closed analytical form can be deduced only in some special cases discussed in the following subsections.

3.3.1 Vanishing activation energy

When the activation energy $\Delta E = 0$, one can compute explicitly all the source terms in Euler-type equations. More precisely, one has

$$Q_i = B_0 \left[\left(\frac{\mu_{12}}{\mu_{34}}\right)^{\frac{3}{4}(1+\lambda_i)} n_h n_k - \left(\frac{\mu_{12}}{\mu_{34}}\right)^{\frac{3}{4}(1-\lambda_i)} n_i n_j \right] \tag{3.30}$$

where B_0 is the moment of the reactive collision kernel of order 0 and $\lambda_1 = \lambda_2 = 1 = -\lambda_3 = -\lambda_4$ are the stoichiometric coefficients. Moreover

$$\begin{aligned} \mathbf{R}_i = {} & B_0 \left(\frac{\mu_{12}}{\mu_{34}}\right)^{\frac{3}{4}(1+\lambda_i)} n_h n_k \alpha_{ij} (m_h \mathbf{u}_h + m_k \mathbf{u}_k) \\ & - B_0 \left(\frac{\mu_{12}}{\mu_{34}}\right)^{\frac{3}{4}(1-\lambda_i)} n_i n_j m_i \mathbf{u}_i + B_1 \left(\frac{\mu_{12}}{\mu_{34}}\right)^{\frac{3+5\lambda_i}{4}} n_h n_k \mu_{hk} (\mathbf{u}_h - \mathbf{u}_k) \end{aligned} \tag{3.31}$$

and

$$\begin{aligned} S_i = {} & B_0 \left(\frac{\mu_{12}}{\mu_{34}}\right)^{\frac{3}{4}(1+\lambda_i)} n_h n_k \left[\frac{1}{2} m_i \left(\alpha_{hk}\mathbf{u}_h + \alpha_{kh}\mathbf{u}_k\right)^2 + \frac{1}{2}\alpha_{ji}\mu_{hk}\left(\mathbf{u}_h - \mathbf{u}_k\right)^2 \right. \\ & \left. + \frac{3}{2}\alpha_{ij}\left(\alpha_{hk}T_h + \alpha_{kh}T_k\right) + \frac{3}{2}\alpha_{ji}\left(\alpha_{kh}T_h + \alpha_{hk}T_k\right)\right] \\ & - B_0 \left(\frac{\mu_{12}}{\mu_{34}}\right)^{\frac{3}{4}(1-\lambda_i)} n_i n_j \left(\frac{1}{2} m_i u_i^2 + \frac{3}{2} T_i\right) + B_1 \left(\frac{\mu_{12}}{\mu_{34}}\right)^{\frac{3+5\lambda_i}{4}} n_h n_k \mu_{hk} \\ & \times \left[\left(\alpha_{hk}\mathbf{u}_h + \alpha_{kh}\mathbf{u}_k\right)\cdot\left(\mathbf{u}_h - \mathbf{u}_k\right) + \frac{3}{m_h + m_k}\left(T_h - T_k\right)\right] \end{aligned} \tag{3.32}$$

where $(i,j,h,k) \in \{(1,2,3,4),(2,1,4,3),(3,4,1,2),(4,3,2,1)\}$, $\lambda_1 = \lambda_2 = 1 = -\lambda_3 = -\lambda_4$ and B_1 is the moment of the reactive collision kernel of order 1

$$B_\ell = \int \left(\hat{n}\cdot\hat{n}'\right)^\ell B_{12}^{34}\left(g, \hat{n}\cdot\hat{n}'\right) d\hat{n}' \tag{3.33}$$

which is constant under the assumption of Maxwell molecule.
It is not difficult to prove that

$$\sum_i \mathbf{R}_i = \mathbf{0} \qquad \text{and} \qquad \sum_i S_i = -\Delta E Q_1 = 0 \tag{3.34}$$

and hence total momentum and total energy are preserved also in this reactive case.
Existence and uniqueness of the configuration of equilibrium is guaranteed once the initial configuration is fixed and it is characterized not only by the previous conditions of equalization of mass velocities and temperatures but also by the so-called Mass Action Law in a simpler form (corresponding to $\Delta E = 0$)

$$\frac{n_1 n_2}{n_3 n_4} = \left(\frac{\mu_{12}}{\mu_{34}}\right)^{3/2} \tag{3.35}$$

This equation is easily deduced by the continuity equations. The equalization of species velocities and temperature can be proved by rewriting conditions

$$\sum_{j\neq i} \mathbf{R}_{ij} + \mathbf{R}_i = \mathbf{0} \qquad \text{and} \qquad \sum_{j\neq i} S_{ij} + S_i = 0 \tag{3.36}$$

as suitable homogenous linear systems whose matrices are negative definite.
As in the previous section, one can reproduce entropy dissipation and relaxation to equilibrium by using the Lyapunov function

$$H = \sum_i n_i \left[\log\left(\frac{n_i}{m_i^3}\right) + \frac{3}{2}\log\left(\frac{m_i}{2\pi T_i}\right) - \frac{3}{2} \right] \tag{3.37}$$

obtained as the restriction of reactive Boltzmann H-functional to the subspace of local Maxwellians (the sketch of the proof is the same as that in the inert case).

3.3.2 Single-velocity and multi-temperature case

Some recent results in rational thermodynamics show that there are significant physical scenarios in which the mechanical relaxation time is shorter than the thermal one i.e. the equalization of species velocities is faster than the equalization of temperatures so that a single-velocity and multi-temperature Euler description is useful to describe the last stage of the evolution [42].
Under the assumption of equalization of mass velocities, one can rewrite the Euler system as follows

$$\begin{cases} \dfrac{\partial n_i}{\partial t} + \nabla_{\mathbf{x}} \cdot (n_i \mathbf{u}) = Q_i \\ \\ \dfrac{\partial}{\partial t}(\rho \mathbf{u}) + \nabla_{\mathbf{x}} \cdot (\rho \mathbf{u} \otimes \mathbf{u}) + \nabla_{\mathbf{x}}(nT) = 0 \\ \\ \dfrac{\partial}{\partial t}\left(\dfrac{1}{2}\rho_i u^2 + \dfrac{3}{2} n_i T_i\right) + \nabla_{\mathbf{x}} \cdot \left[\left(\dfrac{1}{2}\rho_i u^2 + \dfrac{5}{2} n_i T_i\right)\mathbf{u}\right] = \displaystyle\sum_{j \neq i} S_{ij} + S_i \end{cases} \tag{3.38}$$

where the balance equations for momenta are replaced by the conservation of global momentum and $n = \sum_i n_i$, $\rho = \sum_i m_i n_i$ and $nT = \sum_i n_i T_i$.
Also in this case, source terms have a closed form. In energy equations one has that mechanical terms reduce as follows

$$S_{ij} = -3\alpha_{ij}\alpha_{ji} n_i n_j \bar{B}_{ij} (T_i - T_j) \tag{3.39}$$

As concerns chemical source terms

$$
\begin{aligned}
Q_1 \;=\; & \frac{2}{\sqrt{\pi}} B_0 \left[n_3 n_4 \left(\frac{\mu_{12}}{\mu_{34}} \right)^{3/2} \exp\left(\frac{\Delta E}{\alpha_{43} T_3 + \alpha_{34} T_4} \right) \right. \\
& \left. \times \Gamma\left(\frac{3}{2}, \frac{\Delta E}{\alpha_{43} T_3 + \alpha_{34} T_4} \right) - n_1 n_2 \Gamma\left(\frac{3}{2}, \frac{\Delta E}{\alpha_{21} T_1 + \alpha_{12} T_2} \right) \right]
\end{aligned}
\tag{3.40}
$$

and

$$
Q_1 \;=\; Q_2 \;=\; -Q_3 \;=\; -Q_4 \tag{3.41}
$$

For $i = 1$ (and similarly for $i = 2$) the reactive energy exchange rate becomes

$$
\begin{aligned}
S_1 = & \left(\frac{\mu_{12}}{\mu_{34}} \right)^{3/2} n_3 n_4 \left(\frac{m_3}{2\pi T_3} \right)^{3/2} \left(\frac{m_4}{2\pi T_4} \right)^{3/2} \frac{1}{2} m_1 \times \\
& \times \iint \left\{ B_0 \left[G_{34}^2 + \alpha_{21}^2 \frac{\mu_{34}}{\mu_{12}} \left(g^2 + \frac{2\Delta E}{\mu_{34}} \right) \right] \left(1 + \frac{2\Delta E}{\mu_{34} g^2} \right)^{1/2} + \right. \\
& \left. + 2 B_1 \alpha_{21} \left(\frac{\mu_{34}}{\mu_{12}} \right)^{1/2} \mathbf{G}_{34} \cdot \mathbf{g} \left(1 + \frac{2\Delta E}{\mu_{34} g^2} \right) \right\} \times \\
& \times \exp\left[-\eta_{34} \left(\mathbf{G}_{34} + \gamma_{34} \mathbf{g} - \mathbf{u} \right)^2 \right] \exp(-\beta_{34} g^2) d\mathbf{G}_{34} d\mathbf{g} \\
- n_1 n_2 & \left(\frac{m_1}{2\pi T_1} \right)^{3/2} \left(\frac{m_2}{2\pi T_2} \right)^{3/2} \frac{1}{2} m_1 B_0 \times \\
& \iint \left(\mathbf{G}_{12} + \alpha_{21} \mathbf{g} \right)^2 U \left(g^2 - \frac{2\Delta E}{\mu_{12}} \right) \\
& \times \exp\left[-\eta_{12} \left(\mathbf{G}_{12} + \gamma_{12} \mathbf{g} - \mathbf{u} \right)^2 \right] \exp(-\beta_{12} g^2) d\mathbf{G}_{12} d\mathbf{g}
\end{aligned}
\tag{3.42}
$$

and again patient and careful calculations allow an explicit result in terms of incomplete gamma functions. Analogous steps are in order for S_3 (and similarly for S_4)

$$
\begin{aligned}
S_3 = n_1 n_2 \left(\frac{m_1}{2\pi T_1}\right)^{3/2} \left(\frac{m_2}{2\pi T_2}\right)^{3/2} \frac{1}{2} m_3 \times \\
\times \iint \left\{ B_0 \left[G_{12}^2 + \alpha_{43}^2 \frac{\mu_{12}}{\mu_{34}} \left(g^2 - \frac{2\Delta E}{\mu_{12}} \right) \right] + \right. \\
\left. + 2 B_1 \alpha_{43} \left(\frac{\mu_{12}}{\mu_{34}}\right)^{1/2} \mathbf{G}_{12} \cdot \mathbf{g} \left(1 - \frac{2\Delta E}{\mu_{12} g^2}\right)^{1/2} \right\} \\
\times U \left(g^2 - \frac{2\Delta E}{\mu_{12}} \right) \exp\left[-\eta_{12} \left(\mathbf{G}_{12} + \gamma_{12} \mathbf{g} - \mathbf{u} \right)^2 \right] \exp(-\beta_{12} g^2) d\mathbf{G}_{12} d\mathbf{g} \\
- \left(\frac{\mu_{12}}{\mu_{34}}\right)^{3/2} n_3 n_4 \left(\frac{m_3}{2\pi T_3}\right)^{3/2} \left(\frac{m_4}{2\pi T_4}\right)^{3/2} \frac{1}{2} m_3 B_0 \times \\
\iint \left(\mathbf{G}_{34} + \alpha_{43} \mathbf{g} \right)^2 \left(1 + \frac{2\Delta E}{\mu_{34} g^2} \right)^{1/2} \\
\times \exp\left[-\eta_{34} \left(\mathbf{G}_{34} + \gamma_{34} \mathbf{g} - \mathbf{u} \right)^2 \right] \exp(-\beta_{34} g^2) d\mathbf{G}_{34} d\mathbf{g} .
\end{aligned}
\tag{3.43}
$$

It is possible to summarize all the exchange rates in the energy equations in a single expression involving stoichiometric coefficients

$$
\begin{aligned}
S_i = & \frac{1}{\sqrt{\pi}} m_i B_0 \left\{ \left(\frac{\mu_{ij}}{\mu_{hk}}\right)^{\frac{3(1+\Lambda_i)}{4}} n_h n_k \exp\left(\frac{(\lambda_i + 1)\Delta E}{2(\alpha_{kh} T_h + \alpha_{hk} T_k)} \right) \left[\left(\frac{3 T_h T_k}{m_k T_h + m_h T_k} \right. \right. \right. \\
& \left. - (1 - \lambda_i) \frac{\mu_{ij}}{m_i^2} \Delta E - (1 + \lambda_i) \mu_{hk} \left(\frac{T_k - T_h}{m_k T_h + m_h T_k} \right)^2 \Delta E + u^2 \right) \Gamma\left(\frac{3}{2}, \frac{\Delta E}{\alpha_{kh} T_h + \alpha_{hk} T_k} \right) \\
& + 2 \left(\alpha_{kh} T_h + \alpha_{hk} T_k \right) \left[\mu_{hk} \left(\frac{T_k - T_h}{m_k T_h + m_h T_k} \right)^2 + \frac{\mu_{ij}}{m_i^2} \right] \Gamma\left(\frac{5}{2}, \frac{\Delta E}{\alpha_{kh} T_h + \alpha_{hk} T_k} \right) \Bigg] \\
& - \left(\frac{\mu_{hk}}{\mu_{ij}}\right)^{\frac{3(1-\lambda_i)}{4}} n_i n_j \exp\left(\frac{(1 - \lambda_i)\Delta E}{2(\alpha_{ji} T_i + \alpha_{ij} T_j)} \right) \times \\
& \times \left[\left(\frac{3 T_i T_j}{m_j T_i + m_i T_j} - (1 - \lambda_i) \mu_{ij} \left[\frac{(m_i + m_j) T_i}{m_j T_i + m_i T_j} \right]^2 \Delta E + u^2 \right) \Gamma\left(\frac{3}{2}, \frac{\Delta E}{\alpha_{ji} T_i + \alpha_{ij} T_j} \right) \right. \\
& \left. \left. + 2 \mu_{ij} \left(\alpha_{ji} T_i + \alpha_{ij} T_j \right) \left[\frac{(m_i + m_j) T_i}{m_j T_i + m_i T_j} \right]^2 \Gamma\left(\frac{5}{2}, \frac{\Delta E}{\alpha_{ji} T_i + \alpha_{ij} T_j} \right) \right] \right\} \\
& - 2 \left(\frac{\mu_{ij}}{\mu_{hk}}\right)^{\frac{1+3\lambda_i}{4}} \alpha_{ij} \alpha_{ji} n_h n_k B_1 \exp\left(\frac{(\lambda_i - 1)\Delta E}{2(\alpha_{kh} T_h + \alpha_{hk} T_k)} \right) \times \\
& \times \left(\frac{3}{2} + \frac{\Delta E}{\alpha_{kh} T_h + \alpha_{hk} T_k} \right) (T_k - T_h) .
\end{aligned}
\tag{3.44}
$$

Because of the total energy conservation in each reactive encounter, we get

$$S_1 + S_2 + S_3 + S_4 = -Q_1 \Delta E \tag{3.45}$$

3.4 Polyatomic gases

In this section we try to extend the previous model for inert monoatomic gases to polyatomic ones as proposed in [16].

Let us start from the kinetic model for internal state transitions [39] in which each species s, $s = 1, \ldots, Q$, is endowed with a discrete internal structure of N energy levels to mimic non-translational degrees of freedom. The $Q \times N$ components are labeled according to a single index and ordered in such a way that the $s-$th species can be regarded as the equivalence class of the indices i which are congruent to s modulo Q. We denote with E_i the energy of the state i and they are monotonically increasing with their index in the frame of each species. Let us denote by ΔE_{ij}^{hk} the net increase of internal energy

$$\Delta E_{ij}^{hk} = E_h + E_k - E_i - E_j \tag{3.46}$$

related to the general binary interaction

$$(i, j) \rightleftharpoons (h, k) \tag{3.47}$$

where $i, j, h, k = 1, \ldots, QN$.

The evolution of the distribution functions is governed by a set of Boltzmann-like equations

$$\frac{\partial f_i}{\partial t} + \mathbf{v} \cdot \nabla_{\mathbf{x}} f_i = J_i[\mathbf{f}] = \sum_{(j,h,k) \in D_i'} \iint K_i^{ijhk}[\mathbf{f}](\mathbf{v}, \mathbf{w}, \hat{n}') d\mathbf{w} d\hat{n}', \quad 1 \leq i \leq QN \tag{3.48}$$

with the collision operator

$$\begin{aligned} K_i^{ijhk}[\mathbf{f}]\left(\mathbf{v}, \mathbf{w}, \hat{n}'\right) &= \Theta\left(g^2 - \delta_{ij}^{hk}\right) B_{ij}^{hk}\left(g, \hat{n} \cdot \hat{n}'\right) \\ &\times \left[\left(\frac{\mu_{ij}}{\mu_{hk}}\right)^3 f_h\left(\mathbf{v}_{ij}^{hk}\right) f_k\left(\mathbf{w}_{ij}^{hk}\right) - f_i(\mathbf{v}) f_j(\mathbf{w})\right] \end{aligned} \tag{3.49}$$

where $(\mathbf{v},\mathbf{w})$ indicate pre-collision velocities, $g=|\mathbf{v}-\mathbf{w}|$ is the relative velocity with $\hat{n}=(\mathbf{v}-\mathbf{w})/g$, and the post-collision velocities $(\mathbf{v}_{ij}^{hk},\mathbf{w}_{ij}^{hk})$ are related to the pre- ones by

$$\begin{cases} \mathbf{v}_{ij}^{hk} &= \alpha_{ij}\mathbf{v}+\alpha_{ji}\mathbf{w}+\alpha_{kh}\,g_{ij}^{hk}\hat{n}' \\ \\ \mathbf{w}_{ij}^{hk} &= \alpha_{ij}\mathbf{v}+\alpha_{ji}\mathbf{w}-\alpha_{hk}\,g_{ij}^{hk}\hat{n}' \end{cases} \tag{3.50}$$

where $g_{ij}^{hk}=\left[\dfrac{\mu_{ij}}{\mu_{hk}}(g^2-\delta_{ij}^{hk})\right]^{1/2}$. The unit step function Θ introduces a threshold for the collision strictly related to the activation energy ΔE_{ij}^{hk} by means of $\delta_{ij}^{hk}=2\Delta E_{ij}^{hk}/\mu_{ij}$.

The set D_i is made up by all triplets (j,h,k) with $h\equiv i$ and $k\equiv j$ and it can be split in two subsets

$$\begin{aligned} D_i^{fast} &= \{(j,h,k)\in D_i, i\equiv j\equiv h\equiv k\} \\ D_i^{slow} &= \{(j,h,k)\in D_i, i\not\equiv j, h\equiv i, k\equiv j\} = D_i\setminus D_i^{fast} \end{aligned} \tag{3.51}$$

characterizing fast phenomenon within each species and slow process which takes account of interactions between different components. Moreover, it is possible to subdivide the set D_i^{fast} in two subsets: the first for the elastic collisions (when $h=i$ and $k=j$) and the second (when $h\neq i$ and $k\neq j$) for the inelastic ones which provide for a change of internal energy level. For this problem equilibrium configurations are Maxwellian-type functions sharing a common value for velocities and temperatures

$$\begin{aligned} f_i^M(\mathbf{v}) &= n_i\left(\frac{m_s}{2\pi T}\right)^{3/2}\exp\left[-\frac{m_s}{2T}(\mathbf{v}-\mathbf{u})^2\right] \;\; \forall i\equiv s,\, s=1,\dots,Q \\ n_i &= \frac{N_s}{Z_s(T)}\exp\left(-\frac{E_i-E_s}{T}\right) \qquad , \qquad Z_s(T)=\sum_{i\equiv s}\exp\left(-\frac{E_i-E_s}{T}\right) \end{aligned} \tag{3.52}$$

where Z_s is the partition function. A strict entropy inequality for relaxation to equilibrium can also be established in terms of the classical H–functional

$$H=\sum_{s=1}^{Q}\sum_{i\equiv s}\int f_i\log f_i\,d\mathbf{v} \tag{3.53}$$

As done in the basic model, we are interested in a two-scale collision process. For this reason we modify the previous system of kinetic equations as follows

$$\frac{\partial f_i}{\partial t} + \mathbf{v} \cdot \nabla_{\mathbf{x}} f_i = \frac{1}{\varepsilon} J_i^{fast}[\mathbf{f}] + J_i^{slow}[\mathbf{f}] \tag{3.54}$$

where

$$\begin{aligned} J_i^{fast}[\mathbf{f}] &= \sum_{(j,h,k) \in D_i^{fast}} \iint K_i^{ijhk}[\mathbf{f}](\mathbf{v}, \mathbf{w}, \hat{n}') d\mathbf{w} d\hat{n}', \quad 1 \leq i \leq QN \\ J_i^{slow}[\mathbf{f}] &= \sum_{(j,h,k) \in D_i^{slow}} \iint K_i^{ijhk}[\mathbf{f}](\mathbf{v}, \mathbf{w}, \hat{n}') d\mathbf{w} d\hat{n}', \quad 1 \leq i \leq QN \end{aligned} \tag{3.55}$$

As seen before, we can deduce a macroscopic description by the hydrodynamic limit when $\varepsilon \to 0$ and by a suitable closure.

The first step is determining the collision invariants for the dominant part of the collision operator which turns out to be suitable linear combinations of mass, momentum and total energy of each species s

$$\varphi_i(\mathbf{v}) = a_s + \mathbf{b}_s \cdot m_s \mathbf{v} + c_s \left(\frac{1}{2} m_s v^2 + E_i \right) \quad \forall i \equiv s, \quad \forall s = 1, \ldots, Q \tag{3.56}$$

where a_s, $\mathbf{b}_s$ and c_s are free parameters and hence collision invariants constitute a space of dimension $5Q$.

Also local collision equilibria for the dominant operator have a crucial role; they are Maxwellian-type functions depending on species macroscopic fields and they are given by

$$M_i(\mathbf{v}) = \frac{N_s}{Z_s(T_s)} \left(\frac{m_s}{2\pi T_s} \right)^{3/2} \exp \left[-\frac{m_s}{2T_s} (\mathbf{v} - \mathbf{u}_s)^2 - \frac{E_i - E_s}{T_s} \right] \tag{3.57}$$

$\forall i \equiv s$ and $\forall s = 1, \ldots, Q$.

Now we are ready to formulate the weak form of the Boltzmann-type equations by using as test functions the usual basis for the space of collision invariants; for each fixed $s = 1, \ldots, Q$ we consider the three following options

$$\mathbf{b}_s = \mathbf{0}, c_s = 0 \qquad ; \qquad a_s = c_s = 0 \qquad ; \qquad a_s = 0, \mathbf{b}_s = \mathbf{0} \tag{3.58}$$

Therefore one has

$$\begin{aligned}
&\frac{\partial N_s}{\partial t} + \nabla_{\mathbf{x}} \cdot (N_s \mathbf{u}_s) = 0 \\
&\frac{\partial}{\partial t}(\rho_s \mathbf{u}_s) + \nabla_{\mathbf{x}} \cdot \sum_{i \equiv s} (\rho_i \mathbf{u}_i \otimes \mathbf{u}_i + \mathbf{P}_i) = \mathbf{R}_s \\
&\frac{\partial}{\partial t}\left[\sum_{i \equiv s}\left(\frac{1}{2}\rho_i u_i^2 + \frac{3}{2} n_i T_i + E_i n_i\right)\right] \\
&\qquad + \nabla_{\mathbf{x}} \cdot \left\{\sum_{i \equiv s}\left[\left(\frac{1}{2}\rho_i u_i^2 + \frac{3}{2} n_i T_i + E_i n_i\right)\mathbf{u}_i + \mathbf{P}_i \cdot \mathbf{u}_i + \mathbf{q}_i\right]\right\} = S_s
\end{aligned} \tag{3.59}$$

where momentum and energy exchange rates are given by

$$\begin{aligned}
\mathbf{R}_s = \sum_{r \neq s} \sum_{i,h \equiv s} \sum_{j,k \equiv r} \iiint m_s \left(\mathbf{v}_{ij}^{hk} - \mathbf{v}\right) \\
\times B_{ij}^{hk}\left(g, \hat{n} \cdot \hat{n}'\right) \Theta\left(g^2 - \delta_{ij}^{hk}\right) f_i(\mathbf{v}) f_j(\mathbf{w}) d\mathbf{v} d\mathbf{w} d\hat{n}'
\end{aligned} \tag{3.60}$$

and

$$\begin{aligned}
S_s = \sum_{r \neq s} \sum_{i,h \equiv s} \sum_{j,k \equiv r} \iiint \left\{\frac{1}{2} m_s \left[(v_{ij}^{hk})^2 - v^2\right] + E_h - E_i\right\} \\
\times B_{ij}^{hk}\left(g, \hat{n} \cdot \hat{n}'\right) \Theta\left(g^2 - \delta_{ij}^{hk}\right) f_i(\mathbf{v}) f_j(\mathbf{w}) d\mathbf{v} d\mathbf{w} d\hat{n}'
\end{aligned} \tag{3.61}$$

The lowest order hydrodynamic closure is obtained by replacing the distribution functions with the fast collision equilibria in all moments and integrals. As concerns moments, one has

$$\begin{aligned}
&\sum_{i \equiv s} \rho_i \mathbf{u}_i \otimes \mathbf{u}_i = \rho_s \mathbf{u}_s \otimes \mathbf{u}_s \;,\; \sum_{i \equiv s} \mathbf{P}_i = N_s T_s \mathbf{I} \;,\; \sum_{i \equiv s} \mathbf{P}_i \cdot \mathbf{u}_i = N_s T_s \mathbf{u}_s \;,\; \mathbf{q}_i = \mathbf{0} \\
&\qquad \sum_{i \equiv s} E_i n_i = N_s \bar{E}_s(T_s) \;,\; \sum_{i \equiv s} E_i n_i \mathbf{u}_i = N_s \bar{E}_s(T_s)\, \mathbf{u}_s
\end{aligned} \tag{3.62}$$

where

$$\bar{E}_s(T_s) = \frac{1}{Z_s(T_s)} \sum_{i \equiv s} E_i \exp\left(-\frac{E_i - E_s}{\kappa T_s}\right) \tag{3.63}$$

represents an equilibrium average of the energy states within the species s and accounts for the correction to the energy law for the s-th molecules due to the non-translational degrees of freedom.

Euler equations for the present model of a polyatomic gas mixture read then as

$$\begin{aligned}
&\frac{\partial N_s}{\partial t}+\nabla_{\mathbf{x}}\cdot\left(N_s\mathbf{u}_s\right)=0\\
&\frac{\partial}{\partial t}\left(\rho_s\mathbf{u}_s\right)+\nabla_{\mathbf{x}}\cdot\left(\rho_s\mathbf{u}_s\otimes\mathbf{u}_s\right)+\nabla\left(N_sT_s\right)=\mathbf{R}_s\\
&\frac{\partial}{\partial t}\left(\frac{1}{2}\rho_s u_s^2+\frac{3}{2}N_sT_s+N_s\bar{E}_s\left(T_s\right)\right)+\\
&\qquad\qquad+\nabla_{\mathbf{x}}\cdot\left[\left(\frac{1}{2}\rho_s u_s^2+\frac{5}{2}N_sT_s+N_s\bar{E}_s\left(T_s\right)\right)\mathbf{u}_s\right]=S_s
\end{aligned}\tag{3.64}$$

and now source terms are known functions of the macroscopic fields

$$\begin{aligned}
\mathbf{R}_{sr} &= -\mu_{sr}\sum_{i,h\equiv s}\sum_{j,k\equiv r}\iiint\left(\mathbf{g}-\sqrt{g^2-\delta_{ij}^{hk}}\hat{n}'\right)\\
&\qquad\times\Theta\left(g^2-\delta_{ij}^{hk}\right)B_{ij}^{hk}\left(g,\hat{n}\cdot\hat{n}'\right)f_i^M(\mathbf{v})f_j^M(\mathbf{w})d\mathbf{v}d\mathbf{w}d\hat{n}'\\
S_{sr} &= -\mu_{sr}\sum_{i,h\equiv s}\sum_{j,k\equiv r}\iiint\left[\mathbf{G}_{sr}\cdot\left(\mathbf{g}-\sqrt{g^2-\delta_{ij}^{hk}}\hat{n}'\right)+\frac{1}{2}\alpha_{rs}\delta_{ij}^{hk}-\frac{E_h-E_i}{\mu_{sr}}\right]\\
&\qquad\times\Theta\left(g^2-\delta_{ij}^{hk}\right)B_{ij}^{hk}\left(g,\hat{n}\cdot\hat{n}'\right)f_i^M(\mathbf{v})f_j^M(\mathbf{w})d\mathbf{v}d\mathbf{w}d\hat{n}'
\end{aligned}\tag{3.65}$$

where $\mathbf{G}_{sr}=\alpha_{sr}\mathbf{v}+\alpha_{rs}\mathbf{w}$ is the center of mass velocity.
Integrations with respect to the unit vector $\hat{n}'\in S^2$ may be computed separately leading to the angular moments of the collision kernel

$$B_{ij}^{hk(\ell)}\left(g\right)=\int_{S^2}\left(\hat{n}\cdot\hat{n}'\right)^{\ell}B_{ij}^{hk}\left(g,\hat{n}\cdot\hat{n}'\right)d\hat{n}'\qquad\qquad\ell=0,1\tag{3.66}$$

Other integrations can be performed in an easier way by a suitable change of variables which involves the center of mass velocity $\mathbf{G}_{sr}$ and the relative velocity $g\hat{n}$ and by noticing that the product of Maxwellians can be cast as

$$\begin{aligned}
&M_i(\mathbf{v})M_j(\mathbf{w})=\\
&=\frac{N_s}{Z_s\left(T_s\right)}\frac{N_r}{Z_r\left(T_r\right)}\left(\frac{m_s}{2\pi T_s}\right)^{\frac{3}{2}}\left(\frac{m_r}{2\pi T_r}\right)^{\frac{3}{2}}\exp\left(-\frac{E_i-E_s}{T_s}-\frac{E_j-E_r}{T_r}\right)\times\\
&\times\exp\left[-\eta_{sr}\left(\mathbf{G}_{sr}+\gamma_{sr}\mathbf{g}-\delta_{sr}\right)^2\right]\exp\left\{-\beta_{sr}\left[\mathbf{g}-\left(\mathbf{u}_s-\mathbf{u}_r\right)\right]^2\right\}
\end{aligned}\tag{3.67}$$

where

$$\begin{aligned} \beta_{sr} &= \left(\frac{2T_s}{m_s}+\frac{2T_r}{m_r}\right)^{-1}, \gamma_{sr} = \frac{\mu_{sr}}{\eta_{sr}}\left(\frac{1}{2T_s}-\frac{1}{2T_r}\right) \\ \delta_{sr} &= \frac{1}{\eta_{sr}}\left(\frac{m_s}{2T_s}\mathbf{u}_s+\frac{m_r}{2T_r}\mathbf{u}_r\right), \eta_{sr} = \frac{m_s}{2T_s}+\frac{m_r}{2T_r} \end{aligned} \tag{3.68}$$

This allows to push further analytical manipulations leaving only a final one-dimensional integral with respect to g which depends on the form of the collision kernel; more precisely, one has

$$\mathbf{R}_s = \sum_{r\equiv s}\mathbf{R}_{sr} = \sum_{r\equiv s} R_{sr}\frac{\mathbf{u}_s-\mathbf{u}_r}{\|\mathbf{u}_s-\mathbf{u}_r\|} \tag{3.69}$$

where

$$\begin{aligned} R_{sr} = {} & \frac{\mu_{sr}}{2\sqrt{\pi}}\frac{1}{\beta_{sr}^{1/2}|\mathbf{u}_s-\mathbf{u}_r|^2}\frac{N_s}{Z_s(T_s)}\frac{N_r}{Z_r(T_r)}\times \\ & \times\sum_{i,h\equiv s}\sum_{j,k\equiv r}\exp\left(-\frac{E_i-E_s}{T_s}-\frac{E_j-E_r}{T_r}\right)\int_0^\infty\Theta\left(g^2-\delta_{ij}^{hk}\right)\bar{B}_{ij}^{hk}(g)\times \\ & \times\Big\{(2\beta_{sr}|\mathbf{u}_s-\mathbf{u}_r|g-1)\exp\left[-\beta_{sr}\left(g-|\mathbf{u}_s-\mathbf{u}_r|\right)^2\right]+ \\ & +(2\beta_{sr}|\mathbf{u}_s-\mathbf{u}_r|g+1)\exp\left[-\beta_{sr}\left(g+|\mathbf{u}_s-\mathbf{u}_r|\right)^2\right]\Big\}gdg \end{aligned} \tag{3.70}$$

We can rewrite the source term as follows

$$\begin{aligned} R_{sr} = {} & \frac{\mu_{sr}}{2\sqrt{\pi}}\frac{1}{\beta_{sr}^{3/2}|\mathbf{u}_s-\mathbf{u}_r|^2}\frac{N_s}{Z_s(T_s)}\frac{N_r}{Z_r(T_r)}\times \\ & \times\sum_{i,h\equiv s}\sum_{j,k\equiv r}\exp\left(-\frac{E_i-E_s}{T_s}-\frac{E_j-E_r}{T_r}\right)X_{ij}^{hk}\left(|\mathbf{u}_s-\mathbf{u}_r|,\beta_{sr}\right) \end{aligned} \tag{3.71}$$

where we have set $\Delta_{sr} = \beta_{sr}^{1/2}|\mathbf{u}_s-\mathbf{u}_r|$

$$\beta_{sr} = \left(\frac{2T_s}{m_s}+\frac{2T_r}{m_r}\right)^{-1} \tag{3.72}$$

and

$$X_{ij}^{hk} = \int_0^{\infty} \Theta\left(x^2 - \beta_{sr}\delta_{ij}^{hk}\right) \bar{B}_{ij}^{hk}(\beta_{sr}^{-1/2}x) \times \\ \times \left\{ (2\Delta_{sr}x - 1)\exp\left[-(x-\Delta_{sr})^2\right] + (2\Delta_{sr}x + 1)\exp\left[-(x+\Delta_{sr})^2\right] \right\} x dx \tag{3.73}$$

Analogously the energy exchange rate can be written as

$$S_s = \sum_{r \equiv s} S_{sr} \tag{3.74}$$

where

$$S_{sr} = \delta_{sr} \cdot \hat{\mathbf{R}}_{sr} + \frac{1}{\sqrt{\pi}} \frac{1}{\Delta_{sr}} \frac{N_s}{Z_s(T_s)} \frac{N_r}{Z_r(T_r)} \times \\ \times \sum_{i,h \equiv s} \sum_{j,k \equiv r} \exp\left(-\frac{E_i - E_s}{T_s} - \frac{E_j - E_r}{T_r} \right) Y_{ij}^{hk}\left(|\mathbf{u}_s - \mathbf{u}_r|, \beta_{sr}, \gamma_{sr}\right) \tag{3.75}$$

where

$$Y_{ij}^{hk} = \int_0^{\infty} \Theta\left(x^2 - \beta_{sr}\delta_{ij}^{hk}\right) \left\{ \mu_{sr}\gamma_{sr}\beta_{sr}^{-1}x^3 \bar{B}_{ij}^{hk}\left(\beta_{sr}^{-1/2}x\right) + \right. \\ \left. + \left[\alpha_{sr}(E_h - E_i) - \alpha_{rs}(E_k - E_j)\right] x B_{ij}^{hk(0)}\left(\beta_{sr}^{-1/2}x\right) \right\} \times \\ \times \left\{ \exp\left[-(x-\Delta_{sr})^2\right] - \exp\left[-(x+\Delta_{sr})^2\right] \right\} dx \tag{3.76}$$

and

$$\eta_{sr} = \frac{m_s}{2T_s} + \frac{m_r}{2T_r}, \; \gamma_{sr} = \frac{\mu_{sr}}{\eta_{sr}}\left(\frac{1}{2T_s} - \frac{1}{2T_r}\right), \; \delta_{sr} = \frac{1}{\eta_{sr}}\left(\frac{m_s}{2T_s}\mathbf{u}_s + \frac{m_r}{2T_r}\mathbf{u}_r\right) \tag{3.77}$$

We hope to find a closed analytical form of the source terms for a simple model of the collision kernel.

If we consider a Maxwell molecule type of interaction for a given collision, hence we have

$$\bar{B}_{ij}^{hk}(g) = \kappa_{ij}^{hk} = \text{constant} \tag{3.78}$$

and after some cumbersome manipulations one gets

$$X_{ij}^{hk} = 2\sqrt{\pi}\kappa_{ij}^{hk} \left\{ \Delta_{sr}^3 \mathscr{F}_1(\beta_{sr}, \Delta_{sr}) - \left(\Delta_{sr}^2 - \frac{1}{2}\right) \mathscr{F}_2(\beta_{sr}, \Delta_{sr}) + \right. \\ \left. + \Delta_{sr}\sqrt{\beta_{sr}\delta_{ij}^{hk}}\, \mathscr{F}_3(\beta_{sr}, \Delta_{sr}) \right\} \tag{3.79}$$

for $\delta_{ij}^{hk} > 0$, where

$$\begin{aligned}
\mathscr{F}_1(\beta_{sr},\Delta_{sr}) &= 1 - \frac{\operatorname{erf}\left(\sqrt{\beta_{sr}\delta_{ij}^{hk}}+\Delta_{sr}\right)+\operatorname{erf}\left(\sqrt{\beta_{sr}\delta_{ij}^{hk}}-\Delta_{sr}\right)}{2} \\
\mathscr{F}_2(\beta_{sr},\Delta_{sr}) &= \frac{e^{-\left(\sqrt{\beta_{sr}\delta_{ij}^{hk}}+\Delta_{sr}\right)^2}-e^{-\left(\sqrt{\beta_{sr}\delta_{ij}^{hk}}-\Delta_{sr}\right)^2}}{2\sqrt{\pi}} \\
\mathscr{F}_3(\beta_{sr},\Delta_{sr}) &= \frac{e^{-\left(\sqrt{\beta_{sr}\delta_{ij}^{hk}}+\Delta_{sr}\right)^2}-e^{-\left(\sqrt{\beta_{sr}\delta_{ij}^{hk}}-\Delta_{sr}\right)^2}}{2\sqrt{\pi}}
\end{aligned} \tag{3.80}$$

Unfortunately, under the assumption of Maxwell molecules, not all the integrations in $\mathbf{R}_s$ can be done explicitly; in fact not only X_{ij}^{hk} is involved but also its reciprocal X_{hk}^{ij} whose collision kernel is related to the first one by the microreversibility condition

$$\left(1+\frac{\delta_{ij}^{hk}}{g^2}\right)^{1/2} B_{ij}^{hk}(g_{hk}^{ij},\hat{n}\cdot\hat{n}') = B_{hk}^{ij}(g,\hat{\mathbf{n}}\cdot\hat{\mathbf{n}}') \tag{3.81}$$

and then also the integral

$$\begin{aligned}
X_{hk}^{ij} = \kappa_{ij}^{hk}\int_0^\infty \left(x^2+\beta_{sr}\delta_{ij}^{hk}\right)^{1/2}\Big\{ &(2\Delta_{sr}x-1)\exp\left[-(x-\Delta_{sr})^2\right]+ \\
&+(2\Delta_{sr}x+1)\exp\left[-(x+\Delta_{sr})^2\right]\Big\}dx
\end{aligned} \tag{3.82}$$

with $\delta_{ij}^{hk} > 0$ has to be solved; but this seems not amenable to any of the most common elementary or special functions.

Also for the energy exchange rates one can compute explicitly

$$\begin{aligned}
Y_{ij}^{hk} = \kappa_{ij}^{hk}\mu_{sr}\gamma_{sr}\beta_{sr}^{-1}\sqrt{\pi}\Bigg[&\Delta_{sr}\left(\Delta_{sr}^2+\frac{3}{2}\right)\mathscr{F}_1(\beta_{sr},\Delta_{sr}) \\
&+\left(1+\beta_{sr}\delta_{ij}^{hk}+\Delta_{sr}^2\right)\mathscr{F}_2(\beta_{sr},\Delta_{sr})+\sqrt{\beta_{sr}\delta_{ij}^{hk}}\Delta_{sr}\mathscr{F}_3(\beta_{sr},\Delta_{sr})\Bigg] \\
&+\kappa_{ij}^{hk}\left[\alpha_{sr}(E_h-E-i)-\alpha_{rs}(E_k-E_j)\right]\sqrt{\pi}\times \\
&\times\left[\Delta_{sr}\mathscr{F}_1(\beta_{sr},\Delta_{sr})+\mathscr{F}_2(\beta_{sr},\Delta_{sr})\right]
\end{aligned} \tag{3.83}$$

but the microreversibility does not make the reciprocal collision term manageable.

Chapter 4

The steady shock problem for multi-temperature gases

In this chapter we want to test some of the fluid-dynamic models presented in the previous one on a very classical problem like the steady shock waves on a one-dimensional space, in which mass velocities become scalar. The shock problem has been investigated extensively in different frameworks like the extended thermodynamics and many results on the occurrence of smooth solution and discontinuities (the so-called sub-shocks) have been presented [19, 43].
The interesting point is that, actually, the formation of sub-shocks is usually not observed at the kinetic level (see for instance [44, 45] for reactive BGK approaches). This discrepancy with respect to macroscopic models is due to the fact that hydrodynamic descriptions are obtained through proper closure procedures which neglect many dissipative effects.
The steady shock problem is studied identifying the limiting equilibria related by the Rankine-Hugoniot conditions, and investigating the basic features of the evolution equations (that become in this frame a dynamical system of ODEs), with particular emphasis on possible singularities and on eigenvalues of limiting equilibria. We are mainly concentrated in discussing the presence of smooth and discontinuous solutions for varying parameters and on the occurrence of possible relevant bifurcations

versus the Mach number.

4.1 One-velocity and multi-temperature description

In this section we consider a reactive mixture of four monoatomic gases undergoing a bimolecular reversible chemical reaction

$$(1,2) \rightleftharpoons (3,4) \tag{4.1}$$

in which each single component is endowed with an internal energy E_i where $\Delta E = E_3 + E_4 - E_1 - E_2 > 0$.
We have seen before that, starting from a kinetic description in presence of a two-scale collision process, it is possible to deduce a macroscopic model at Euler level for the unknown fields n_i (number densities), u_i (mass velocities) and T_i (temperatures) [17]. As anticipated, there are physical scenarios in which the thermal problem can be separated from the mechanical one or, in other words, the equalization of species velocities is faster than the equalization of temperature; in this regard, Landau showed that this faster mechanical relaxation is true for plasmas [42]. This is the physical regime that will be addressed here, and in this frame the deduced set of Euler-type equations read as

$$\begin{cases} \dfrac{\partial n_i}{\partial t} + \nabla_{\mathbf{x}} \cdot (n_i \mathbf{u}) = Q_i \\ \\ \dfrac{\partial}{\partial t}(\rho \mathbf{u}) + \nabla_{\mathbf{x}} \cdot (\rho \mathbf{u} \otimes \mathbf{u}) + \nabla_{\mathbf{x}}(nT) = 0 \\ \\ \dfrac{\partial}{\partial t}\left(\dfrac{1}{2}\rho_i u^2 + \dfrac{3}{2} n_i T_i\right) + \nabla_{\mathbf{x}} \cdot \left[\left(\dfrac{1}{2}\rho_i u^2 + \dfrac{5}{2} n_i T_i\right)\mathbf{u}\right] = \displaystyle\sum_{j \neq i} S_{ij} + S_i \end{cases} \tag{4.2}$$

where

$$Q_1 = Q_2 = -Q_3 = -Q_4 \qquad , \qquad \sum_{i=1}^{4} \sum_{j \neq i} S_{ij} = 0 \qquad , \qquad \sum_{i=1}^{4} S_i = -Q_1 \Delta E \tag{4.3}$$

and, under the assumption of Maxwell molecules, source terms have a closed analytical form described in (3.39), (3.40) and (3.44).
Starting from the system of equations above and by using relations on source terms, one can obtain some conservation laws which express the preservation of suitable combinations of densities (for example $(1,3)$, $(1,4)$ and $(2,4)$), global momentum and total energy. It is convenient to reformulate the problem by coupling these conservations with balance laws for one of the number densities (for example n_1) and three of the species energies (for example second, third and fourth species). In this way, in the one-dimensional steady shock problem the unknown fields are governed by the following set of ordinary differential equations

$$\begin{aligned}
&\frac{d}{dx}(n_1 u) = Q_1 \\
&\frac{d}{dx}\left[(n_i + n_j)\, u\right] = 0 \qquad\qquad (i,j) = (1,3), (1,4), (2,4) \\
&\frac{d}{dx}\left(\rho u^2 + nT\right) = 0 \\
&\frac{d}{dx}\left(\frac{1}{2}\rho u^3 + \frac{5}{2} nTu + \sum_{i=1}^{4} E_i n_i u\right) = 0 \\
&\frac{d}{dx}\left(\frac{1}{2}\rho_i u^3 + \frac{5}{2} n_i T_i u\right) = \sum_{j\neq i} S_{ij} + S_i \qquad\qquad i = 2,3,4,
\end{aligned} \tag{4.4}$$

with limiting conditions $x \to \pm\infty$ given by equilibrium points, in which of course all species share a common value for temperature $T^{\pm}$ and Mass Action Law is fulfilled

$$T_i^{\pm} = T^{\pm} \qquad i = 1,\ldots,4, \qquad\qquad \frac{\chi_1^{\pm}\chi_2^{\pm}}{\chi_3^{\pm}\chi_4^{\pm}} = \left(\frac{\mu_{12}}{\mu_{34}}\right)^{3/2} \exp\left(\frac{\Delta E}{T^{\pm}}\right) \tag{4.5}$$

where $\chi_i = n_i/n$ indicates the concentration of the $i-$th species. Each state can be expressed in term of density $n^{\pm}$, temperature $T^{\pm}$, two out of the four concentration fractions $\chi_i^{\pm}$, and velocity $u^{\pm}$, which also define the relevant sound speeds and the corresponding Mach numbers via [46]

$$c^{\pm} = \alpha^{\pm}\left(\frac{5 n^{\pm} T^{\pm}}{3\rho^{\pm}}\right)^{1/2} \;,\; (\alpha^{\pm})^2 = \frac{\sum_{i=1}^{4} \frac{1}{\chi_i^{\pm}} + \frac{2}{5}\left(\frac{\Delta E}{T^{\pm}}\right)^2}{\sum_{i=1}^{4} \frac{1}{\chi_i^{\pm}} + \frac{2}{3}\left(\frac{\Delta E}{T^{\pm}}\right)^2} < 1 \;,\; \mathrm{Ma}^{\pm} = \frac{u^{\pm}}{c^{\pm}} \tag{4.6}$$

In order to obtain physical shock solutions, the entropy flux condition imposed by the H-theorem must be fulfilled and this gives some restrictions on the admissible values of upstream Mach number, $\mathrm{Ma}^- > 1$, which is equivalent to impose entropy Lax conditions [47].
Conservation laws in the set of ODEs gives a relation between downstream $(+)$ and upstream $(-)$ parameters (called Rankine-Hugoniot conditions) which can determine the downstream state in terms of the upstream one. A detailed analysis has been presented in [46] and we just recall few features.
In particular one has

$$\chi_i^+ = \chi_i^- + \lambda_i \Delta\chi \qquad i = 1,\dots,4, \qquad \frac{n^+}{n^-} = \frac{\rho^+}{\rho^-} = \frac{u^-}{u^+} \tag{4.7}$$

where $\lambda_1 = \lambda_2 = 1 = -\lambda_3 = -\lambda_4$ and the parameter $\Delta\chi$ is proved to be in a one–to–one relationship with u^- and then with the upstream Mach number, and determines uniquely T^+ via (4.5). Finally

$$\begin{aligned} \frac{n^+}{n^-} &= 2\left(1-\frac{T^-}{T^+}\right) - \frac{\Delta E}{T^+}\Delta\chi + \left\{\left[2\left(1-\frac{T^-}{T^+}\right) - \frac{\Delta E}{T^+}\Delta\chi\right]^2 + \frac{T^-}{T^+}\right\}^{1/2} \\ u^- &= \left(\frac{n^- T^-}{\rho^-}\right)^{1/2} \left[\frac{n^+}{n^-}\,\frac{1-(n^+/n^-)(T^+/T^-)}{1-(n^+/n^-)}\right]^{1/2} \end{aligned} \tag{4.8}$$

Moreover, by using the 5 conservation equations, one can eliminate 5 variables, namely all n_i and T, in terms of u

$$n_i = \frac{n_i^- u^-}{u} - \lambda_i N \qquad T = \frac{\rho^-(u^-)^2 + n^- T^-}{n^- u^-}\,u - \frac{\rho^-}{n^-}\,u^2 \tag{4.9}$$

where

$$N = \frac{1}{\Delta E}\left[2\rho^- u^- u - \frac{5}{2}\left(\rho^-(u^-)^2 + n^- T^-\right) + \left(\frac{1}{2}\rho^-(u^-)^3 + \frac{5}{2}n^- T^- u^-\right)\frac{1}{u}\right] \tag{4.10}$$

In this way, the system of ordinary differential equations reduces to the sub-system of four balance laws which have to be rewritten in terms of the remaining unknowns u, T_2, T_3, T_4.The crucial problem is the first equation which reduces to the form

$$\frac{d}{dx}F(u) = G(u, T_2, T_3, T_4) \qquad \lim_{x\to\pm\infty} u(x) = u^{\pm} \tag{4.11}$$

where G is nothing but Q_1 and $F(u) = n_1 u$ can be rewritten as a polynomial of degree 2 in u

$$F(u) = n_1^- u^- - \frac{1}{\Delta E}\left[2\rho^- u^- u^2 - \frac{5}{2}\left(\rho^-(u^-)^2 + n^- T^-\right)u + \frac{1}{2}\rho^-(u^-)^3 + \frac{5}{2}n^- T^- u^-\right] \tag{4.12}$$

Hence its derivative is linear and it vanishes in

$$u^* = \frac{5}{8}\frac{\rho^-(u^-)^2 + n^- T^-}{\rho^- u^-} \tag{4.13}$$

Hence the vector field of the dynamical system is singular on the hyperplane $u = u^*$, which might or might not interfere with the admissible phase space.
It is easy to check that $0 < u^+ < u^-$; in fact, by using relations (4.7) one can prove that

$$\frac{\Delta E}{T^+} = \log\left(m\frac{\chi_1^+\chi_2^+}{\chi_3^+\chi_4^+}\right) < \log\left(m\frac{\chi_1^-\chi_2^-}{\chi_3^-\chi_4^-}\right) = \frac{\Delta E}{T^-} \implies T^+ > T^- \tag{4.14}$$

where $m = (\mu_{34}/\mu_{12})^{3/2}$. By using (4.8) one has

$$u^- < \left(\frac{n^- T^-}{\rho^-}\frac{n^+}{n^-}\right)^{1/2} \tag{4.15}$$

and hence

$$\frac{u^-}{u^+} = \frac{n^+}{n^-} > \frac{\rho^-(u^-)^2}{n^- T^-} = \frac{5}{3}\left(\alpha^-\right)^2\left(\mathrm{Ma}^-\right)^2 > \frac{5}{3}\left(\alpha^-\right)^2 > 1 \tag{4.16}$$

One can discuss also the collocation of u^* with respect to u^-

$$u^* \gtrless u^- \quad \Longleftrightarrow \quad (u^-)^2 \lessgtr \frac{5n^- T^-}{3\rho^-} \quad \Longleftrightarrow \quad \mathrm{Ma}^- \lessgtr \frac{1}{\alpha^-} \tag{4.17}$$

One can notice that for slightly supersonic flows when upstream Mach number is in the interval $(1, 1/\alpha^-)$ the singularity does not interfere with the phase space, thus the vector field is regular and a smooth solution for the steady shock is allowed. But, as soon as u^- increases and the Mach number exceeds the threshold $1/\alpha^- > 1$, a smooth solution is ruled out, and one has to search for weak solutions, presenting

jump discontinuity.
In order to study weak solutions, one has to look for a piecewise smooth profile in the separate intervals $(-\infty,0)$ and $(0,+\infty)$ (discontinuity at some point x can always be shifted to the origin), satisfying limiting conditions at $\pm\infty$, and whose limits for $x\to 0^-$ and $x\to 0^+$, labelled by m and p superscripts, respectively, fulfil the constraints following from the differential equations themselves. Since the source terms at the right hand side of the energy equations (4.4) are bounded functions, those equations imply continuity of the quantities under the derivative operator across the jump, namely

$$\frac{1}{2}\rho_i^m(u^m)^3+\frac{5}{2}n_i^m T_i^m u^m=\frac{1}{2}\rho_i^p(u^p)^3+\frac{5}{2}n_i^p T_i^p u^p \qquad i=2,3,4. \tag{4.18}$$

This is not true for the velocity field since $F'(u)$ vanishes at $u=u^*$; however, the same technique as before yields the constraint $F(u^m)=F(u^p)$ from which

$$\frac{u^p+u^m}{2}=\frac{5}{8}\frac{\rho^-(u^-)^2+n^-T^-}{\rho^-u^-}=u^* \tag{4.19}$$

This last equation means that the singular value $u=u^*$ exactly represents the midpoint of any admissible jump.
The jump in the velocity profile implies corresponding discontinuities in the gas number density $n=n^-u^-/u$ and in the temperature T; there is instead no jump for the concentrations χ_i, since the single continuity equation (the first of (4.4))may be written as

$$\frac{d\chi_i}{dx}=\frac{\lambda_i}{n^-u^-}Q_1 \tag{4.20}$$

where now the right hand side is a bounded function of x and it leads to $\chi_i^p=\chi_i^m$.
In order to construct smooth and weak solutions, an useful tool is the analysis of the stability of the limiting equilibria which, in this case, can be performed easily with the help of symbolic manipulation.
In all cases that have been investigated (a reference case is illustrated in Fig.4.1), all eigenvalues of the downstream state have negative real part. The same happens for the upstream state as long as $\mathrm{Ma}^->1/\alpha^-$ (weak solution regime) but, as soon as Ma^- descends below this bifurcation value (possible smooth solution), the upstream

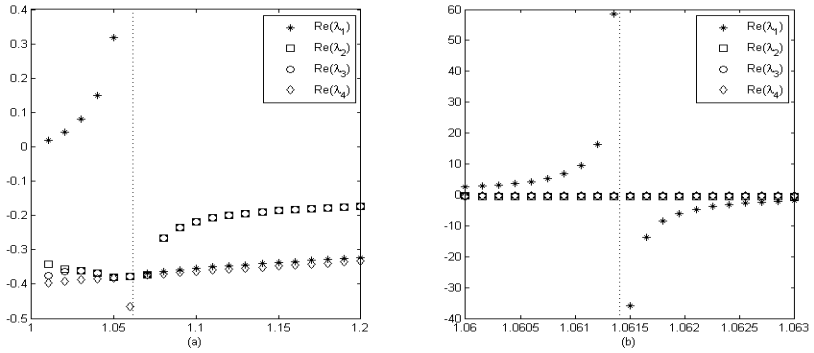

Figure 4.1: Real part of the eigenvalues of the upstream equilibrium versus Mach number on a physical (a) and stretched (b) scale.

Jacobian matrix exhibits one positive eigenvalue, while the other three keep negative real part. In addition, the transition is singular in the sense that an eigenvalue diverges to $-\infty$ when Ma^- approaches the threshold from above, and re–appears from $+\infty$ after the crossing. This suggests the following scenario which will be confirmed by numerical experiments.

- **Case** $\mathrm{Ma}^- < 1/\alpha^-$

In these configurations the upstream equilibrium is a saddle with a one–dimensional unstable manifold and a three–dimensional stable manifold, and the only way to reach it running backwards towards $-\infty$ is to follow the unstable manifold, tangent to the one–dimensional unstable eigenspace. That manifold represents the unique non–constant solution of our shock problem fulfilling the upstream condition, and enters the phase space, where it is attracted by the asymptotically stable downstream equilibrium, providing the sought heteroclinic orbit, and the smooth shock profile.

- **Case** $\mathrm{Ma}^- > 1/\alpha^-$

Now the upstream equilibrium is itself asymptotically stable, and the only admissible solution satisfying the upstream condition is the constant solution, which of course

can not reach the downstream equilibrium for $x \to +\infty$. The only way to do that is through a jump discontinuity, governed by (4.18) and (4.19), where necessarily ρ_i^m, u^m, n_i^m, T_i^m must coincide with ρ_i^-, u^-, n_i^-, T_i^-. A simple calculation yields then the corresponding values reached across the jump

$$\begin{aligned} u^p &= 2u^* - u^- = \frac{\rho^-(u^-)^2 + 5n^-T^-}{4\rho^- u^-} \\ T_i^p &= \frac{n_i^- u^-}{n_i^p u^p} T^- + \frac{1}{5} m_i \left(\frac{n_i^- u^-}{n_i^p u^p} (u^-)^2 - (u^p)^2 \right) \qquad i = 2,3,4 \end{aligned} \tag{4.21}$$

where n_i^p (as well as all other quantities of interest) are determined by u^p. At this point, the state after the jump is a point in the phase space attracted by the asymptotically stable downstream equilibrium, and a smooth trajectory joins it to that state for $x \to +\infty$. This builds up the sought weak shock wave solution, with a jump discontinuity from upstream equilibrium to an intermediate non–equilibrium state, followed by a smooth tail leading that state to the downstream equilibrium.
This scenario does not seem predictable at kinetic level and it seems strictly related to the simple hydrodynamic closure at Euler level.

4.1.1 Numerical simulations

We present some shock profiles resulting from the numerical integrations of the macroscopic differential equations which can be made non-dimensional by rescaling the involved quantities in terms of typical values (indicated by $\tilde{}$). Choosing $\tilde{T} = \Delta E$, and accordingly $\tilde{u} = (\Delta E/\tilde{m})^{1/2}$, the parameter ΔE disappears at all and the dimensionless equations differ from the dimensional ones by the presence of a factor $\tilde{u}/\tilde{B}\tilde{n}L$ in front of space derivatives. In order to obtain a universal set of equations we choose $L = \tilde{u}/\tilde{B}\tilde{n}$. In conclusion, we consider equations (4.4) as dimensionless and with ΔE understood to be unity. In addition, we normalize in such way that

- $u(0) = (u^+ + u^-)/2$ for smooth solutions
- discontinuity is located in $x = 0$ for sub-shocks

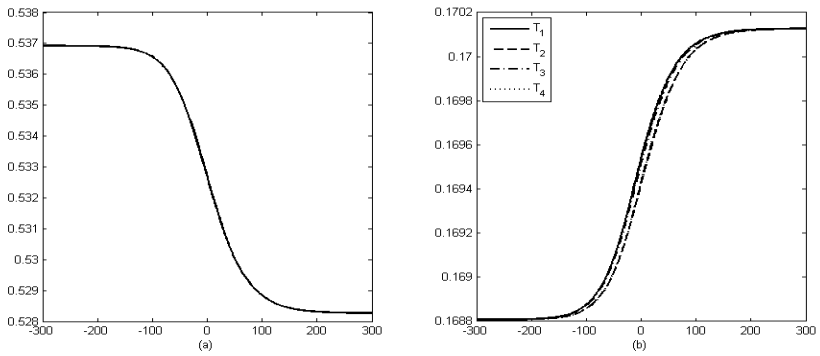

Figure 4.2: Mass velocity (a) and species temperature (b) versus x when $\mathrm{Ma}^- = 1.01$. We are in presence of a slightly supersonic regime and the predicted smooth profiles for the involved quantities are reproduced.

All the simulations have been made up by forward integrations by means of classical Runge-Kutta methods. We consider as reference case the bimolecular reaction

$$H_2O + H \rightleftharpoons OH + H_2 \tag{4.22}$$

for which the (dimensionless) masses result

$$m_1 = 1.8 \quad m_2 = 0.1 \quad m_3 = 1.7 \quad m_4 = 0.2 \tag{4.23}$$

and hence $m_1 + m_2 = m_3 + m_4$. We consider the upstream configuration by fixing $n^- = 1.85$ and the concentration fractions

$$\chi_1^- = 0.4324 \quad \chi_2^- = 0.4865 \quad \chi_3^- = 0.0270 \quad \chi_1^- = 0.0541 \tag{4.24}$$

The Mass Action Law gives $T^- = 0.1688$ and then $\alpha^- = 0.9421$; therefore, the bifurcation value for Mach number is $1/\alpha^- = 1.0614$.
The first choice for Mach number is $\mathrm{Ma}^- = 1.01$, it corresponds to $\Delta\chi = -0.0008$ and it implies $u^- = 0.5369$, $u^+ = 0.5283$ and $T^+ = 0.1701$.
Fig. 4.2 shows the very smooth shock profiles for u and T_i in this slightly supersonic

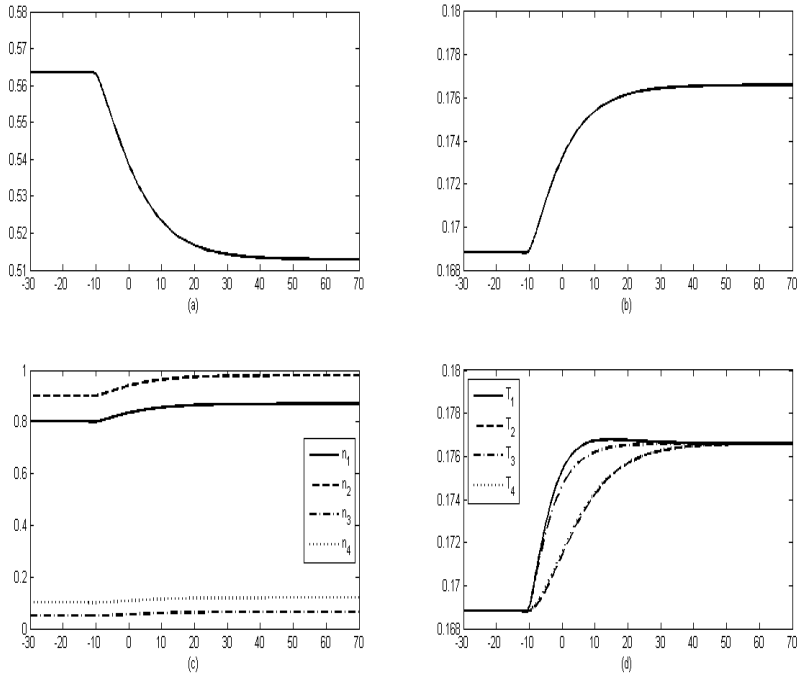

Figure 4.3: Mass velocity (a), global temperature (b), number densities (c) and species temperature (d) versus x when $\mathrm{Ma}^- = 1.06$. The chosen value for Mach number is close to the bifurcation one but still in the 'smooth' region.

scenario. The solution has been found numerically starting from a close neighborhood in phase space of the upstream equilibrium, choosing an initial point in the direction of its one–dimensional unstable eigenspace (we recall that upstream state is a saddle); in this way, the phase trajectory leaves the neighborhood along the unstable manifold, and moves, for $x \to +\infty$, to the downstream equilibrium, which is always asymptotically stable.

We increase Mach number choosing a value very close to the bifurcation one but still in the smooth region: $\mathrm{Ma}^- = 1.06$. In this case $\Delta\chi = -0.0046$, $u^- = 0.5635$,

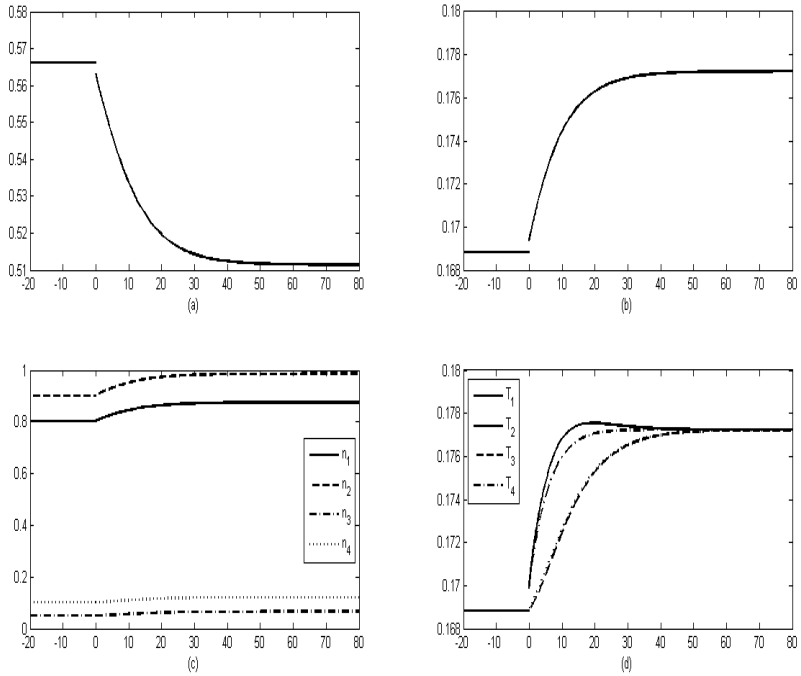

Figure 4.4: Mass velocity (a), global temperature (b), number densities (c) and species temperature (d) versus x when $\mathrm{Ma}^- = 1.065$. The chosen Mach number is still close to the bifurcation value but it is greater than it. A jump discontinuity appears and it involves mass velocity and temperatures.

$u^+ = 0.5128$ and $T^+ = 0.1766$. The profiles in Fig.4.3 are of the same type as in the previous case; they are still smooth but they present a much sharper edge corresponding to higher values of derivatives. This is explained by the presence of a much higher positive eigenvalue which makes detachment from the upstream equilibrium much faster. Moreover, one notice possible occurrence of overshooting in some species temperatures.

Now we increase further the Mach number passing through the threshold. We con-

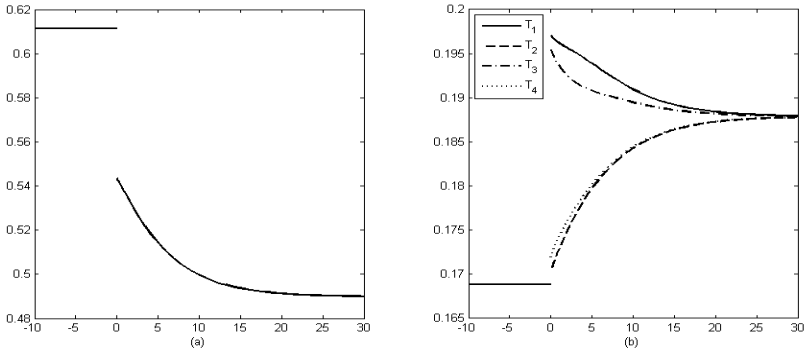

Figure 4.5: Mass velocity (a) and species temperature (b) versus x when $\mathrm{Ma}^- = 1.15$. A higher value of Mach number corresponds to a wider and more evident discontinuity.

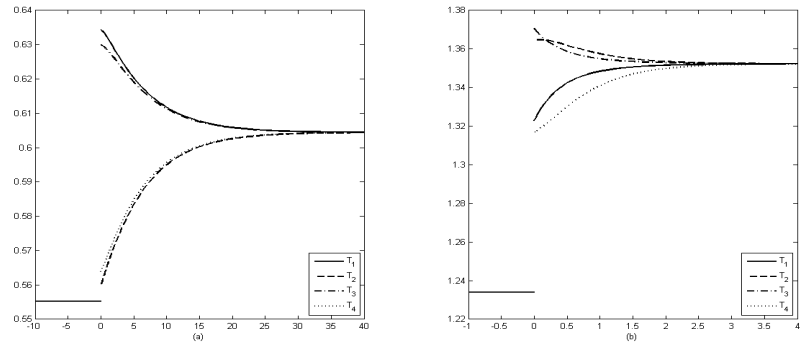

Figure 4.6: Species temperature versus x for a different upstream configuration (a) and for a different chemical reaction (b) for fixed Mach number $\mathrm{Ma}^- = 1.1$.

sider a value for Mach number close to the bifurcation one but greater than it: $\mathrm{Ma}^- = 1.065$, from which $\Delta\chi = -0.0050$, $u^- = 0.5662$, $u^+ = 0.5114$ and $T^+ = 0.1772$. In this case, singularity enters the phase space and a jump appears; this discontinuity can be seen as a development of the previous sharp edge (see Fig4.4).

The last case concerns the choice of Mach number $\mathrm{Ma}^- = 1.15$ for which the jump discontinuity enlarges, overshooting effects are more evident and a much larger spread among species appears across the shock front (see Fig.4.5).
Similar trends can be reproduced also for different upstream configurations or for different chemical reactions. In figure 4.6(a) trends of species temperatures are shown for a different upstream equilibrium

$$\chi_1^- = 0.25 \quad , \quad \chi_2^- = 0.35 \quad , \quad \chi_3^- = 0.25 \quad , \quad \chi_4^- = 0.15 \tag{4.25}$$

which implies a different critical value for upstream Mach number ($1/\alpha^- = 1.0227$). In fig. 4.6(b) also the chemical reaction is changed and we consider the following one

$$NO + CO_2 \rightleftharpoons NO_2 + CO \tag{4.26}$$

whose relevant masses are $m_1 = 3$, $m_2 = 4.4$, $m_3 = 4.6$ and $m_4 = 2.8$. In this last case critical upstream Mach number decreases further ($1/\alpha^- = 1.0049$) and hence $\mathrm{Ma}^- = 1.1$ becomes comparatively higher which explains the larger jump discontinuity. Moreover, now masses are more balanced; this implies larger exchange rates and then a faster relaxation to downstream equilibrium.

4.2 Multi-velocity and multi-temperature binary inert mixture

In this section we want to investigate the steady shock problem for a non-reactive gas mixture in which hydrodynamic variables are densities, velocities and temperatures of each species. This application can seem simpler than the previous one because of the absence of non-conservative processes (the chemical reaction) but the presence of different velocities provides several interesting phenomena even in a mixture of only two components. Results are in agreement with those presented in the framework of extended thermodynamics [48] and smooth solutions as well as sub-shocks of different kind can be discussed. The generalization of this (multi-velocity and multi-temperature) analysis to an higher number of (inert and reactive) gases seems very

cumbersome, and it will be matter of future research.
The basic multi-velocity and multi-temperature model proposed in the previous chapter is the starting point; in the steady version macroscopic fields are governed by the following set of ordinary differential equation

$$\begin{aligned}
\frac{d}{dx}\left(n_1 u_1\right) &= 0 \\
\frac{d}{dx}\left(n_2 u_2\right) &= 0 \\
\frac{d}{dx}\left[\rho_1 \left(u_1\right)^2 + n_1 T_1\right] &= R_{12} \\
\frac{d}{dx}\left[\rho_2 \left(u_2\right)^2 + n_2 T_2\right] &= -R_{12} \\
\frac{d}{dx}\left[\frac{1}{2}\rho_1 \left(u_1\right)^3 + \frac{5}{2} n_1 T_1 u_1\right] &= S_{12} \\
\frac{d}{dx}\left[\frac{1}{2}\rho_2 \left(u_2\right)^3 + \frac{5}{2} n_2 T_2 u_2\right] &= -S_{12}
\end{aligned} \tag{4.27}$$

where terms R_{12} and S_{12} are provided by (3.13) and (3.14).
As before, the shock solution must join two limiting equilibrium states at $\pm\infty$ characterized by a common value for mass velocities and temperatures

$$u_1^{\pm} = u_2^{\pm} = u^{\pm} \qquad T_1^{\pm} = T_2^{\pm} = T^{\pm} \tag{4.28}$$

Therefore, each equilibrium configuration is totally determined by fixing number densities $n_1^{\pm}$, $n_2^{\pm}$, common velocity $u^{\pm}$ and temperature $T^{\pm}$. These quantities define the relevant sound speeds $c^{\pm}$ and the corresponding Mach number $\mathrm{Ma}^{\pm}$

$$\left(\mathrm{Ma}^{\pm}\right)^2 = \frac{\left(u^{\pm}\right)^2}{\left(c^{\pm}\right)^2} = \frac{3\rho^{\pm}\left(u^{\pm}\right)^2}{5 n^{\pm} T^{\pm}} \tag{4.29}$$

From the set of ODEs (4.27) one can deduce easily four independent conservation laws: the first two equations, the sum of third and fourth equations (reproducing momentum conservation) and the sum of fifth and sixth one (energy conservation). As seen in the previous section, these conservations establish some relations between

upstream (-) and downstream (+) parameters (Rankine-Hugoniot conditions)

$$\begin{aligned} n_s^+ u^+ &= n_s^- u^-, \qquad s = 1,2 \\ \rho^+ \left(u^+\right)^2 + n^+ T^+ &= \rho^- \left(u^-\right)^2 + n^- T^- =: \kappa^A \\ \rho^+ \left(u^+\right)^3 + 5 n^+ T^+ u^+ &= \rho^- \left(u^-\right)^3 + 5 n^- T^- u^- =: \kappa^B \end{aligned} \tag{4.30}$$

whose solution in terms of upstream Mach number is given by

$$\begin{aligned} n_s^+ &= \frac{4\left(\mathrm{Ma}^-\right)^2}{\left(\mathrm{Ma}^-\right)^2 + 3} n_s^-, \ s = 1,2, \qquad u^+ = \frac{\left(\mathrm{Ma}^-\right)^2 + 3}{4\left(\mathrm{Ma}^-\right)^2} u^- \\ T^+ &= \frac{\left(\left(\mathrm{Ma}^-\right)^2 + 3\right)\left(5\left(\mathrm{Ma}^-\right)^2 - 1\right)}{16\left(\mathrm{Ma}^-\right)^2} T^- \end{aligned} \tag{4.31}$$

Moreover, conservation laws are valid for all points of the shock profile; hence, fixing the upstream configuration, the solution must fulfill the constraints

$$\begin{aligned} n_1 u_1 &= n_1^- u^- \\ n_2 u_2 &= n_2^- u^- \\ \rho_1 \left(u_1\right)^2 + n_1 T_1 + \rho_2 \left(u_2\right)^2 + n_2 T_2 &= \rho^- \left(u^-\right)^2 + n^- T^- \\ \rho_1 \left(u_1\right)^3 + 5 n_1 T_1 u_1 + \rho_2 \left(u_2\right)^3 + 5 n_2 T_2 u_2 &= \rho^- \left(u^-\right)^3 + 5 n^- T^- u^- \end{aligned} \tag{4.32}$$

These relations allow to express four of the sixth unknown fields in terms of the remaining two. The first two give

$$n_i = \frac{n_i^- u^-}{u_i} \qquad i = 1,2 \tag{4.33}$$

Third and fourth conservations can be seen as a linear system for temperatures T_1 and T_2. Unfortunately the determinant of this system is proportional to $u_1 - u_2$ and it can vanish if velocities share the same value. It is not possible to impose $u_1 \neq u_2$ because we want to determine an orbit joining two limiting equilibria which are characterized by the equalization of species velocities.

Hence, a different approach is required. Our strategy consists in studying a system of three ordinary differential equations; this means that just three of the four conservations are used to reduce the problem. In addition, we introduce also the new variables

$$\hat{T} = \frac{n_1}{n} T_1 \qquad \text{and} \qquad \theta = T_1 - T_2 \tag{4.34}$$

in place of T_1 and T_2

$$T_1 = \hat{T} + \frac{n_2}{n}\theta \qquad \text{and} \qquad T_2 = \hat{T} - \frac{n_1}{n} \tag{4.35}$$

At this point, we can write n_1, n_2 and $\hat{T}$ in terms of u_1, u_2 and θ by using the first three conservations; in particular one has

$$\hat{T} = \frac{u_1 u_2 \kappa^A}{\left(n_1^- u_2 + n_2^- u_1\right) u^-} - \frac{\left(\rho_1^- u_1 + \rho_2^- u_2\right) u_1 u_2}{n_1^- u_2 + n_2^- u_1} \tag{4.36}$$

where κ^A is a constant defined in (4.30). Skipping some details, one can rewrite the problem in terms of u_1, u_2 and θ as

$$\mathbf{A} \cdot \frac{d\mathbf{y}}{dx} = \mathbf{b} \tag{4.37}$$

where $\mathbf{y} = (u_1, u_2, \theta)^T$, $\mathbf{b} = (R_{12}, S_{12}, -S_{12})^T$, and the matrix $\mathbf{A}$ is

$$\begin{bmatrix} \frac{n_2}{n u_1}\left[\rho_1 (u_1)^2 - n_1 T_1\right] & -\frac{n_1}{n u_2}\left[\rho_2 (u_2)^2 - n_2 T_2\right] & \frac{n_1 n_2}{n} \\ \rho_1 (u_1)^2 - \frac{5}{2}\frac{n_1}{n}\left[\rho_1 (u_1)^2 - n_1 T_1\right] & -\frac{5}{2}\frac{n_1 u_1}{n u_2}\left[\rho_2 (u_2)^2 - n_2 T_2\right] & \frac{5}{2}\frac{n_1 n_2 u_1}{n} \\ -\frac{5}{2}\frac{n_2 u_2}{n u_1}\left[\rho_1 (u_1)^2 - n_1 T_1\right] & \rho_2 (u_2)^2 - \frac{5}{2}\frac{n_2}{n}\left[\rho_2 (u_2)^2 - n_2 T_2\right] & -\frac{5}{2}\frac{n_1 n_2 u_2}{n} \end{bmatrix} \tag{4.38}$$

Its determinant

$$\det(\mathbf{A}) = \frac{1}{4}\frac{n_1 n_2}{n}\left[3\rho_1 (u_1)^2 - 5 n_1 T_1\right]\left[3\rho_2 (u_2)^2 - 5 n_2 T_2\right] \tag{4.39}$$

vanishes in correspondence of $(\mathrm{M}_1)^2 = 1$ or $(\mathrm{M}_2)^2 = 1$, where

$$(\mathrm{M}_s)^2 = 3\rho_s (u_s)^2 / (5 n_s T_s) \tag{4.40}$$

denotes the Mach number we would have if we considered the evolution of s-th species only. In all points in which matrix $\mathbf{A}$ is regular and one can compute its

inverse, it is possible to set, in this way, the system of ODEs in normal form

$$\begin{aligned}\frac{du_s}{dx} &= \frac{5R_{12}u_s - 2S_{12}}{3\rho_s (u_s)^2 - 5n_s T_s}, \qquad s = 1,2 \\ \frac{d\theta}{dx} &= -2\sum_{s=1}^{2} \frac{R_{12}\rho_s (u_s)^3 - S_{12}\left[\rho_s (u_s)^2 - n_s T_s\right]}{n_s u_s \left[3\rho_s (u_s)^2 - 5n_s T_s\right]}\end{aligned} \tag{4.41}$$

One can notice that, by a long computation, a suitable combination of these equations can reproduce correctly the last conservation law i.e that conservation in (4.31) not used in the reduction technique.
It is clear that possible smooth solutions can exist only if denominators

$$\mathscr{D}_s = 3\rho_s (u_s)^2 - 5n_s T_s = 5n_s T_s \left[(\mathrm{M}_s)^2 - 1\right], \qquad s = 1,2 \tag{4.42}$$

do not vanish during the evolution. An analysis of these quantities in the equilibrium configurations can give some indications on the existence or not of smooth profiles; in the limiting states parameters are known and hence a detailed investigation can be presented.
Let us introduce concentration $c = n_1^- / n^-$ and mass ratio $\alpha = m_1/m_2$. We suppose $\alpha < 1$ but analogous considerations are possible also for $\alpha > 1$. One can write

$$(\mathrm{M}_1^-)^2 = \frac{\alpha}{\gamma}\left(\mathrm{Ma}^-\right)^2, \qquad (\mathrm{M}_2^-)^2 = \frac{1}{\gamma}\left(\mathrm{Ma}^-\right)^2, \qquad \gamma = \alpha c + 1 - c \tag{4.43}$$

and, under the assumption $\alpha < 1$, one has that $\mathrm{M}_1^- < \mathrm{M}_2^-$ and $\alpha < \gamma < 1$.
As concerns the downstream equilibrium, it is not difficult to show that Mach numbers are given by

$$(\mathrm{M}_1^+)^2 = \frac{\alpha}{\gamma}\,\frac{(\mathrm{Ma}^-)^2 + 3}{5\,(\mathrm{Ma}^-)^2 - 1} \qquad (\mathrm{M}_2^+)^2 = \frac{1}{\gamma}\,\frac{(\mathrm{Ma}^-)^2 + 3}{5\,(\mathrm{Ma}^-)^2 - 1} \tag{4.44}$$

Once the configuration in the upstream equilibrium is fixed, for $\mathrm{Ma}^- = 1$ we have $(\mathrm{M}_1^-)^2 = (\mathrm{M}_1^+)^2 = \alpha/\gamma$ and $(\mathrm{M}_2^-)^2 = (\mathrm{M}_2^+)^2 = 1/\gamma$; for fixed values of the concentration c, $(\mathrm{M}_1^-)^2$ and $(\mathrm{M}_2^-)^2$ will linearly increase up to $+\infty$, while $(\mathrm{M}_1^+)^2$ and $(\mathrm{M}_2^+)^2$ will decrease, respectively, up to the limiting values $\alpha/(5\gamma)$, $1/(5\gamma)$ for varying Mach

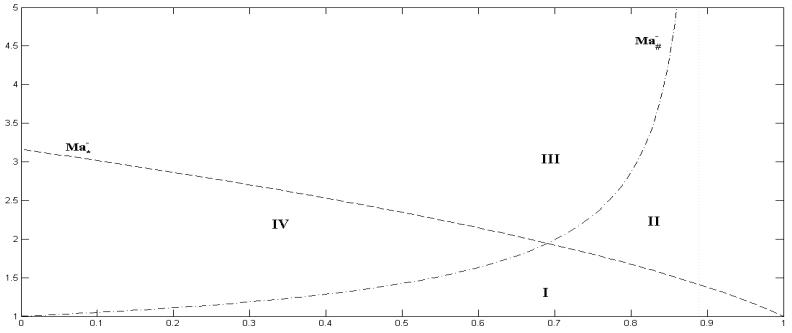

Figure 4.7: Bifurcation values Ma_*^- and $\mathrm{Ma}_\sharp^-$ versus concentration c, for mass ratio $\alpha = 0.1$ ($\bar{c} = 0.\bar{8}$ and $c^* = 0.6905$)

number $(\mathrm{Ma}^-)^2$ from 1 to $+\infty$.
It is easy to see that $\mathscr{D}_1^+ < 0$ and $\mathscr{D}_2^- > 0$ for any $\mathrm{Ma}^- \geq 1$. Existence of a smooth shock wave is then possible only for Mach numbers such that $\mathscr{D}_1^- < 0$ and $\mathscr{D}_2^+ > 0$. It is clear that

- $\mathscr{D}_1^- < 0$ only for $(\mathrm{Ma}^-)^2 < (\mathrm{Ma}_*^-)^2 = \gamma/\alpha$
- as concerns $\mathscr{D}_2^+$
  - if $\gamma < 1/5$ then it is positive for any Ma^-
  - if $\gamma > 1/5$ it is positive only for $(\mathrm{Ma}^-)^2 < (\mathrm{Ma}_\sharp^-)^2 = (\gamma+3)/(5\gamma-1)$

Bifurcation values Ma_*^- and $\mathrm{Ma}_\sharp^-$ are plotted in Fig. 4.7 in a reference case.
It can be checked that

$$\mathrm{Ma}_*^- < \mathrm{Ma}_\sharp^- \quad \Leftrightarrow \quad c > c^* = \frac{1}{10(1-\alpha)}\left[9-\alpha-\sqrt{\alpha^2+62\alpha+1}\right] \tag{4.45}$$

Summing up, we have the following scenarios which will be confirmed by numerical simulations

- if $\alpha > 1/5$, setting $\mathrm{m} = \min\left\{\mathrm{Ma}_*^-, \mathrm{Ma}_\sharp^-\right\}$ and $\bar{\mathrm{m}} = \max\left\{\mathrm{Ma}_*^-, \mathrm{Ma}_\sharp^-\right\}$, a smooth solution is allowed for $1 < \mathrm{Ma}^- < \mathrm{m}$, a solution with one jump is possible for $\mathrm{m} < \mathrm{Ma}^- < \bar{\mathrm{m}}$, while for $\mathrm{Ma}^- > \bar{\mathrm{m}}$ two jumps are required in order to overcome singularities of both denominators $\mathscr{D}_1$ and $\mathscr{D}_2$;

- if $\alpha < 1/5$, this scenario does not change as long as $c < \bar{c} = 4/[5(1-\alpha)]$, whereas for $\bar{c} < c < 1$ a smooth solution is allowed for $1 < \mathrm{Ma}^- < \mathrm{Ma}_*^-$, otherwise we may look only for a weak solution with a jump discontinuity.

As seen in the previous section, discussing stability of equilibria has a crucial role. A numerical investigation of several cases has shown that

- in the upstream configuration (-) one eigenvalue is positive and the other is negative for $\mathrm{Ma}^- < \mathrm{Ma}_*^-$, while they become both negative for $\mathrm{Ma}^- > \mathrm{Ma}_*^-$

- in the downstream state (+) eigenvalues are both negative for $\mathrm{Ma}^- < \mathrm{Ma}_\sharp^-$, when $\mathrm{Ma}_\sharp^-$ exists, while one of them becomes positive for $\mathrm{Ma}^- > \mathrm{Ma}_\sharp^-$

Therefore, the different regions in Fig. 4.7 present the following scenarios

- **Region I:** the downstream equilibrium is asymptotically stable while the upstream one is a saddle with a one-dimensional unstable manifold. The only way to reach the equilibrium at $+\infty$ is following the unstable manifold of the upstream state, getting then attracted by the stable downstream one. This guarantees the presence of smooth shock solutions.

- **Region II:** both equilibria are asymptotically stable, hence no smooth solution can join the two limiting configurations. The only admissible profile satisfying the upstream condition is the constant one and it can reach the downstream state just through a suitable jump discontinuity consistent with conservations.

- **Region III:** the upstream equilibrium is stable while the downstream one is a saddle. The solution starting from the upstream state is again constant, then a jump discontinuity is necessary, but the downstream state can not be reached by a smooth tail; once more it might be possible that the tail undergoes a further

discontinuity leading eventually the solution to the limiting equilibrium by a second tail on its stable manifold.

- **Region IV:** both equilibria are saddle points; no smooth solutions can exist because of the singularities analyzed above. It is possible to find a jump discontinuity in which the solution moves from the unstable manifold of the upstream equilibrium to the stable manifold of the downstream one.

As in the previous case, jump discontinuities seem unpredictable at kinetic level and strictly related to the hydrodynamic closure. Moreover, as far as we know, the occurrence of profiles with two discontinuities is investigated for the first time.
Now we are interested in investigating how the configurations on different sides of a jump are related. If we know the fields on one side of the jump (labelled by superscript $*$), the corresponding ones on the other side, denoted with superscript $\bullet$, are given by

$$\begin{aligned} \rho_1^\bullet \left(u_1^\bullet\right)^2 + n_1^\bullet T_1^\bullet &= k_1^A \\ \rho_1^\bullet \left(u_1^\bullet\right)^3 + 5 n_1^\bullet T_1^\bullet u_1^\bullet &= k_1^B \\ \rho_2^\bullet \left(u_2^\bullet\right)^3 + 5 n_2^\bullet T_2^\bullet u_2^\bullet &= k_2^B \end{aligned} \tag{4.46}$$

where $k_s^A := \rho_s^* \left(u_s^*\right)^2 + n_s^* T_s^*$ and $k_s^B := \rho_s^* \left(u_s^*\right)^3 + 5 n_s^* T_s^* u_s^*$. By simple manipulations, one has that $u_1^\bullet$ must fulfill the algebraic equation

$$4 \rho_1^* u_1^* \left(u_1^\bullet\right)^2 - 5 k_1^A u_1^\bullet + k_1^B = 0 \tag{4.47}$$

with solutions

$$u_1^\bullet = u_1^* , \qquad \text{or} \qquad u_1^\bullet = \frac{\rho_1^* \left(u_1^*\right)^2 + 5 n_1^* T_1^*}{4 \rho_1^* u_1^*} =: \tilde{u}_1 . \tag{4.48}$$

Then, the expressions for temperatures are

$$T_1^\bullet = \frac{k_1^B - k_1^A u_1^\bullet}{4 n_1^* u_1^*} , \qquad T_2^\bullet = \frac{k_2^B - \rho_2^* u_2^* \left(u_2^\bullet\right)^2}{5 n_2^* u_2^*} , \tag{4.49}$$

and finally we get a quadratic equation for $u_2^\bullet$ analogous to (4.47) that has the following roots

$$u_2^\bullet = u_2^* , \qquad \text{or} \qquad u_2^\bullet = \frac{\rho_2^* \left(u_2^*\right)^2 + 5 n_2^* T_2^*}{4 \rho_2^* u_2^*} =: \tilde{u}_2 . \tag{4.50}$$

Four outputs for velocities after the jump are possible

$$(u_1^*, u_2^*) \quad , \quad (u_1^*, \tilde{u}_2) \quad , \quad (\tilde{u}_1, u_2^*) \quad , \quad (\tilde{u}_1, \tilde{u}_2) \tag{4.51}$$

where the first corresponds to continuity and hence it has to be discarded. A discontinuity is necessary to avoid vanishing denominators but occurrence of other, even several, jumps may not be excluded at this point.
Finally, for species undergoing discontinuity it can be noticed that

$$\begin{aligned} \mathscr{D}_s^\bullet &= 3\rho_s^* u_s^* u_s^\bullet - 5\frac{n_s^* u_s^* T_s^\bullet}{u_s^\bullet} = -\frac{1}{u_s^\bullet}\left[3\rho_s^* (u_s^*)^2 - 5n_s^* T_s^*\right]\frac{\rho_s^* (u_s^*)^2 + 5n_s^* T_s^*}{4\rho_s^* u_s^*} \\ &= -\left[3\rho_s^* (u_s^*)^2 - 5n_s^* T_s^*\right] = -\mathscr{D}_s^* , \end{aligned} \tag{4.52}$$

namely the relevant denominator changes sign keeping the same magnitude.

4.2.1 Numerical simulations

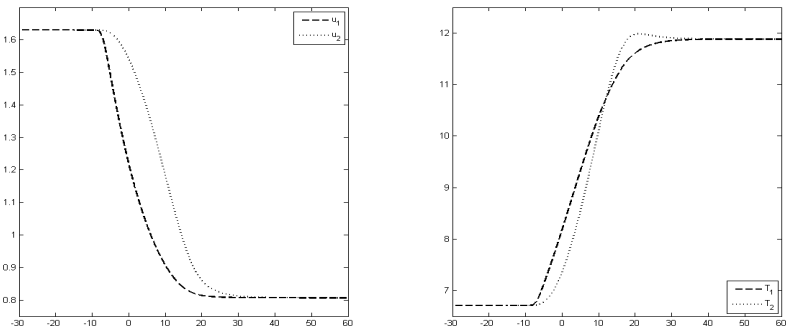

Figure 4.8: Mass velocity (a) and species temperature (b) versus x. In region I smooth profiles for velocities and temperatures can be built up.

In this subsection we shall present some shock profiles resulting from the numerical integration of (4.27) via Runge-Kutta methods. Solutions are normalized in such way that $u_1(0) = (u^+ + u^-)/2$ for smooth profiles, while for solutions with only one

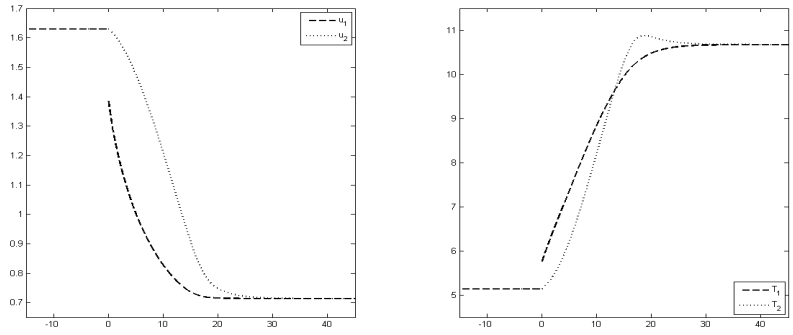

Figure 4.9: Mass velocity (a) and species temperature (b) versus x. In region II a jump occurs and the discontinuity just involves species 1.

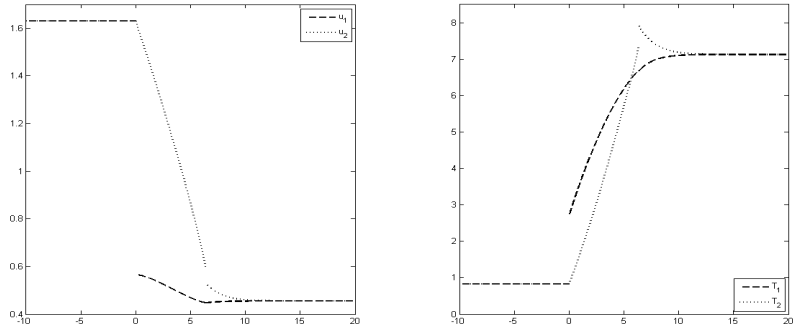

Figure 4.10: Mass velocity (a) and species temperature (b) versus x. In region III two different jump discontinuities occur and they involve separately just one of the two components.

jump, this is located in $x = 0$.
We consider a mixture of Helium and Argon whose dimensionless masses are respectively $m_1 = 4$ and $m_2 = 40$ ($\alpha = 0.1$). We fix the upstream configuration $n_1^- =$

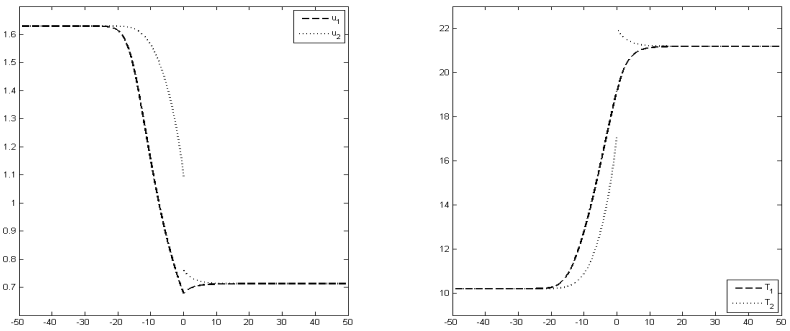

Figure 4.11: Mass velocity (a) and species temperature (b) versus x. In region IV a jump occurs and the discontinuity just involves species 2.

0.753, $n_2^- = 0.247$, $u^- = 1.63$ (thus $n^- = 1$ and $c = 0.753$) while T^- changes for varying upstream Mach number Ma^-. As first case, we consider $\mathrm{Ma}^- = 1.75$ close to the lower bifurcation value ($\mathrm{m} = 1.7593$) but still in the smooth region; we have $T^- = 6.7107$, $n_1^+ = 1.5215$, $n_2^+ = 0.4991$, $u^+ = 0.8067$, $T^+ = 11.8834$ and profiles for mass velocities and temperatures are shown in Fig. 4.8. Trends show a fast detachment from an almost constant profile. One of the two species temperatures overshoots the equilibrium value and this is related to the disparate masses chosen before; moreover there is a point during the evolution in which $T_1 = T_2$ but $u_1 \neq u_2$ and then temperatures split again, reaching then the common value T^+.
Now we increase Ma^- by taking a value in region II ($\mathrm{Ma}^- = 2$, $T^- = 5.1379$, $n_1^+ = 1.7211$, $n_2^+ = 0.5646$, $u^+ = 0.7131$ and $T^+ = 10.6772$). Now both equilibria are asymptotically stable, so the unique solution consistent with the upstream configuration is the constant one with $u_1 = u_2 = u^-$ and $T_1 = T_2 = T^-$.
We recall that $\mathscr{D}_1^- \mathscr{D}_1^+ < 0$ and $\mathscr{D}_2^- \mathscr{D}_2^+ > 0$ and hence the unique possible choice of velocities after the jump is $(u_1^\bullet, u_2^\bullet) = (\tilde{u}_1, u_2^*)$ which changes the sign of $\mathscr{D}_1$ and not of $\mathscr{D}_2$ (and in which u_2 remains continuous) (see Fig. 4.9).
We increase further the upstream Mach number crossing also the second bifurcation value ($\bar{\mathrm{m}} = 2.3309$, $\mathrm{Ma}^- = 5$, $T^- = 0.8221$, $n_1^+ = 2.6893$, $n_2^+ = 0.8821$, $u^+ = 0.4564$,

$T^+ = 7.1355$). In this case $\mathscr{D}_1^- \mathscr{D}_1^+ < 0$ and $\mathscr{D}_2^- \mathscr{D}_2^+ < 0$; again the constant profile is compatible with the upstream configuration. Numerical simulations show that a jump with a discontinuity of both velocities does not enter the stable manifold of the downstream equilibrium and hence a profile with just one jump is not an admissible weak solution for our problem.

We are able to build up a shock solution with two discontinuities (Fig. 4.10). The first one has the same features of the case of the region II, a constant upstream profile, followed by a jump in which $(u_1^\bullet, u_2^\bullet) = (\tilde{u}_1, u_2^*)$; then we consider a tail originating from it; on the other hand, we move backward from $+\infty$ starting tangent to its stable manifold. We can notice that there exists one pair of points, one belonging to the solution after the first jump while the other one to the stable manifold of $+\infty$, that fulfill conservations (4.46). In this way, we build up a second jump consistent with the conservation laws. Finally, one can observe that the first jump changes the sign of $\mathscr{D}_1$ only while the second discontinuity changes the sign of $\mathscr{D}_2$ only.

To investigate shock profiles in region IV, we change upstream configuration and taking a different concentration ($n_1^- = 0.4$, $n_2^- = 0.6$ and $c = 0.4$). We consider $\mathrm{Ma}^- = 2$ which gives $T^- = 10.2025$, $n_1^+ = 0.9143$, $n_2^+ = 1.3714$, $u^+ = 0.7131$, $T^+ = 21.2021$. A weak solution with one jump involving species 2 ($\mathscr{D}_2^- \mathscr{D}_2^+ < 0$) can be computed using on one side the stable downstream manifold (in the backward direction), and on the other side the solution tangent to the upstream unstable manifold (in the forward direction) (Fig. 4.11).

Bibliography

[1] Naldi G., Pareschi L., and Toscani G. (Eds.). *Mathematical Modeling of Collective Behavior in Socio-Economic and Life Sciences. Series: Modelling and Simulation in Science and Technology*. Birkhauser, Norwell, MA, USA, 2010.

[2] Altshuler E., Ramos O., Nuñez Y., Fernandéz J., Batista-Leyva A.J., and Noda C. Symmetry breaking in escaping ants. *The American Naturalist*, 66(6):643–649, 2005.

[3] Bisi M., Spiga G., and Toscani G. Kinetic models of conservative economics with wealth redistribution. *Communications in Mathematical Sciences*, 7(4):901–916, 2009.

[4] Cercignani C. *Rarefied gas dynamics. From basic concepts to actual calculations*. Cambridge University Press, Cambridge, 2000.

[5] Giovangigli V. *Multicomponent flow modeling*. Birkhauser, Boston, 1999.

[6] Cercignani C. and Kremer G. *The relativistic Boltzmann equation: theory and applications*. Birkhauser, Basel, 2002.

[7] Bose T. K. *High temperature gas dynamics*. Springer, Berlin, 2003.

[8] Park C. *Nonequilibrium hypersonic aerothermodynamics*. Wiley, New York, 1990.

[9] D'Orsogna M. R., Chuang Y., Bertozzi A., and Chayes L. Self-propelled particles with soft-core interactions: patterns, stability and collapse. *Physical Review Letters*, 96:104302(1–4), 2006.

[10] Helbing D., Farkas I., and Vicsek T. Simulating dynamical features of escape panic. *Nature*, 407:487–490, 2000.

[11] Piccoli B. and Tosin A. Pedestrian flows in bounded domains with obstacles. *Contin. Mech. Thermodyn.*, 21(2):85–107, 2009.

[12] Pareschi L. and Russo G. An introduction to Monte Carlo methods for the Boltzmann equation. *ESAIM Proceedings*, 10:35–76, 2001.

[13] Ruggeri T. and Simic S. On the hyperbolic sistem of a mixture of Eulerian fluids: a comparison between single- and multi-temperature models. *Mathematical Methods in the Applied Sciences*, 30(7):827–849, 2007.

[14] Ruggeri T. and Lou J. Heat conduction in multi-temperature mixtures of fluids: the role of the average temperature. *Physics Letters A*, 373(34):3052–3055, 2009.

[15] Bisi M., Martalò G., and Spiga G. Multi-temperature Euler hydrodynamics for a reacting gas from a kinetic approach to rarefied mixtures with resonant collisions. *Europhysics Letters*, 95(5):55002(1–6), 2011.

[16] Bisi M., Martalò G., and Spiga G. Multi-temperature hydrodynamic limit from kinetic theory in a mixture of rarefied gases. *Acta Applicandae Mathematicae*, 122(1):37–51, 2012.

[17] Bisi M., Martalò G., and Spiga G. Multi-temperature fluid-dynamic model equations from kinetic theory in a reactive gas: the steady shock problem. *Computer and Mathematics with Applications*, 66(8):1403–1417, 2013.

[18] Bisi M., Martalò G., and Spiga G. Shock wave structure of multi-temperature Euler equations from the kinetic theory for a binary mixture. *Acta Applicandae Mathematicae*, 2014.

[19] Boillat G. and Ruggeri T. On the shock structure problem for hyperbolic system of balance laws and convex entropy. *Continuum Mechanics and Thermodynamics*, 10(5):285–292, 1998.

[20] Albi G. and Pareschi L. Modeling self-organized systems interacting with few individuals: from microscopic to macroscopic dynamics. *Applied Mathematics Letters*, 26(4):397–401, 2013.

[21] Toscani G. Kinetic models of opinion formation. *Communications in Mathematical Sciences*, 4(3):481–496, 2006.

[22] Albi G., Herty M., and Pareschi L. Kinetic description of optimal control problems and applications to opinion consensus. 2014. URL: `http://arxiv.org/abs/1401.7798`.

[23] Albi G., Pareschi L., and Zanella M. Boltzmann type control of opinion consensus through leaders. 2014. URL: `http://arxiv.org/abs/1405.0736`.

[24] Tosin A. From generalized kinetic theory to discrete velocity modeling of vehicular traffic. A stochastic game approach. *Applied Mathematics Letters*, 22(7):1122–1125, 2009.

[25] Fermo L. and Tosin A. A fully-discrete-state kinetic theory approach to modeling vehicular traffic. *SIAM Journal of Applied Mathematics*, 73(4):1533–1556, 2013.

[26] Colombo R.M., Garavello M., and Lècureux-Mercier M. A class of non-local models for pedestrian traffic. *Mathematical Models and Methods in Applied Sciences*, 22(4), 2012.

[27] Colombo R.M. and Lècureux-Mercier M. Nonlocal crowd dynamics models for several populations. *Acta Mathematica Scientia*, 32(1):177–196, 2012.

[28] Bellomo N. *Modeling complex living system - A kinetic theory and stochastic game approach. Series: Modelling and Simulation in Science and Technology*. Birkhauser, Norwell, MA, USA, 2007.

[29] Quarteroni A. *Modellistica numerica per problemi differenziali*. Springer-Verlag, Milano, 2003.

[30] Quarteroni A., Saleri F., and Sacco R. *Matematica numerica*. Springer-Verlag, Milano, 1998.

[31] Bird G. A. *Molecular gas dynamics and the direct simulation of gas flows*. Oxford press, Oxford, MA, USA, 1995.

[32] Bobylev A. V. and Nanbu K. Theory of collision algorithms for gases and plasmas based on the Boltzmann equation and the Landau-Fokker-Planck equation. *Physical Review E*, 61(4):4576–4586, 2000.

[33] Albi G. and Pareschi L. Binary interaction algorithms for the simulation of flocking and swarming dynamics. *Multiscale Modeling and Simulation*, 11(1):1–29, 2013.

[34] LeVeque R. J. *Numerical methods for conservation laws*. Birkhauser, Oxford, MA, USA, 1992.

[35] Kustova E. V. and Nagnibeda E. A. On a correct description of a multi-temperature dissociating $C0_2$ flow. *Chemical Physics*, 231(3):293–310, 2006.

[36] Muller I. and Ruggeri T. *Rational extended thermodynamics*. Springer Verlag, New York, 1998.

[37] Chapman S. and Cowling T. G. *The Mathematical Theory of Non-uniform Gases*. Springer, New York, 1994.

[38] Bisi M., Groppi M., and Spiga G. Kinetic modelling of bimolecular chemical reactions *in* Kinetic methods for nonconservative and reacting systems. *Quaderni di Matematica - Seconda Università di Napoli*, 16:1–143, 2005.

[39] Groppi M. and Spiga G. Kinetic approach to chemical reactions and inelastic transitions in a rarefied gas. *Journal of Mathematical Chemistry*, 26:197–219, 1999.

[40] Groppi M., Spiga G., and Zus F. Euler closure of the Boltzmann equations for resonant bimolecular reactions. *Physics of Fluids*, 18(5):057105(1–8), 2006.

[41] Pavić M. and Simic S. Moment equations for polyatomic gases. *Acta Applicandae Mathematicae (on line first)*, 2014.

[42] Landau L. On the vibrations of the electronic plasmas. *Journal of Physics*, 10(1):25–34, 1946.

[43] Currò C. and Fusco D. Discontinuous travelling wave solutions for a class of dissipative hyperbolic models. *Rendiconti dell'Accademia Nazionale dei Lincei. Matematica e Applicazioni*, 16(1):61–71, 2005.

[44] Groppi M., Aoki K., Spiga G., and Tritsch V. Shock structure analysis in chemically reacting gas mixtures by a relaxation-time kinetic model. *Physics of Fluids*, 20:117103(1–11), 2008.

[45] Groppi M., Rjasanow S., and Spiga G. A kinetic relaxation approach to fast reactive mixtures: shock wave structure. *Journal of Statistical Mechanics*, 9:P10010(1–15), 2009.

[46] Groppi M., Spiga G., and Takata S. The steady shock problem in reactive gas mixtures. *Bulletin of the Institute of Mathematics Academia Sinica (New Series)*, 2(4):935–956, 2007.

[47] Ruggeri T. *Introduzione alla termomeccanica dei continui*. Monduzzi, Bologna, 2007.

[48] Madjarevic D. and Simic S. Shock structure in Helium-Argon mixture - A comparison of hyperbolic multi-temperature model with experiment. *Europhysics Letters*, 102(4):44002(1–6), 2013.